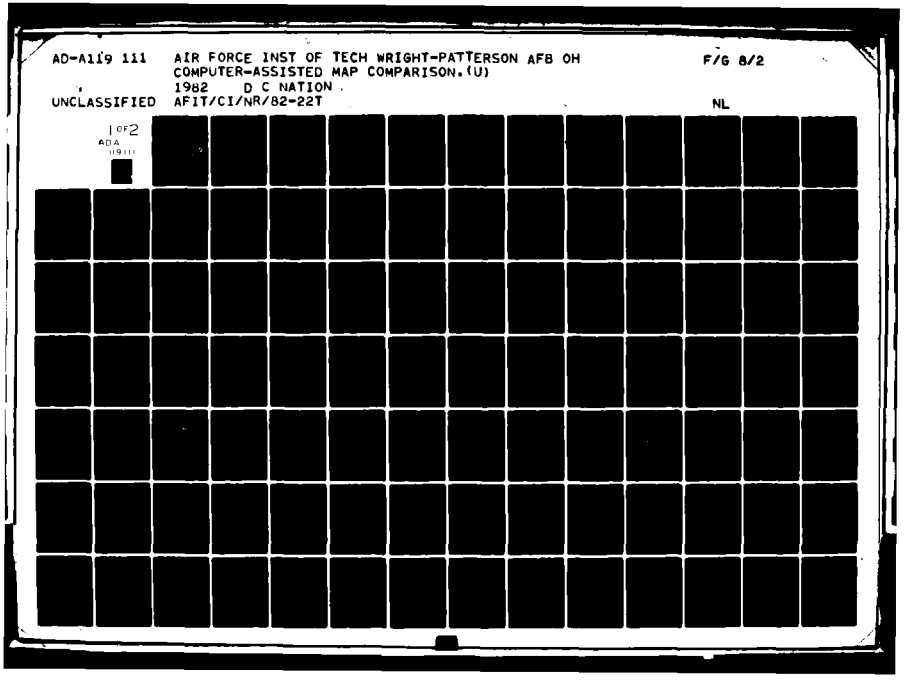
AD-A119 111
AIR FORCE INST OF TECH WRIGHT-PATTERSON AFB OH
COMPUTER-ASSISTED MAP COMPARISON.(U)
F/G 8/2
1982 D C NATION
UNCLASSIFIED
AFIT/CI/NR/82-22T
NL
1 OF 2
ADA
119111

UNCLASS

SECURITY CLASSIFICATION OF THIS PAGE (When Data Entered)

REPORT DOCUMENTATION PAGE

READ INSTRUCTIONS BEFORE COMPLETING FORM

1. REPORT NUMBER: AFIT/CI/NR/82-22T	2. GOVT ACCESSION NO.
3. RECIPIENT'S CATALOG NUMBER	
4. TITLE (and Subtitle): Computer-Assisted MAP Comparison	5. TYPE OF REPORT & PERIOD COVERED: THESIS/DISSERTATION
6. PERFORMING ORG. REPORT NUMBER	
7. AUTHOR(s): Capt Dolf C. Nation	8. CONTRACT OR GRANT NUMBER(s)
9. PERFORMING ORGANIZATION NAME AND ADDRESS: AFIT STUDENT AT: The Ohio State University	10. PROGRAM ELEMENT, PROJECT, TASK AREA & WORK UNIT NUMBERS
11. CONTROLLING OFFICE NAME AND ADDRESS: AFIT/NR, WPAFB OH 45433	12. REPORT DATE: 1982
	13. NUMBER OF PAGES: 148
14. MONITORING AGENCY NAME & ADDRESS(if different from Controlling Office)	15. SECURITY CLASS. (of this report): UNCLASS
	15a. DECLASSIFICATION/DOWNGRADING SCHEDULE

16. DISTRIBUTION STATEMENT (of this Report)

APPROVED FOR PUBLIC RELEASE; DISTRIBUTION UNLIMITED

17. DISTRIBUTION STATEMENT (of the abstract entered in Block 20, if different from Report)

18. SUPPLEMENTARY NOTES

APPROVED FOR PUBLIC RELEASE: IAW AFR 190-17

30 AUG 1982

LYNN E. WOLAVER
Dean for Research and
Professional Development
AFIT, Wright-Patterson AFB OH

19. KEY WORDS (Continue on reverse side if necessary and identify by block number)

20. ABSTRACT (Continue on reverse side if necessary and identify by block number)

ATTACHED

DD FORM 1 JAN 73 1473 EDITION OF 1 NOV 65 IS OBSOLETE

UNCLASS

SECURITY CLASSIFICATION OF THIS PAGE (When Data Entered)

AD A119111

DTIC ELECTE SEP 9 1982 S D H

82 09 07 134

COMPUTER-ASSISTED MAP COMPARISON

A Thesis

Presented in Partial Fulfillment of the Requirements
for the Degree Master of Science
in
The Department of Geodetic Science and Surveying

by

Dolf Claud Nation, B.A.

The Ohio State University
1982

Copyright (c) 1982
by Dolf Claud Nation
All rights reserved.

Approved by

J. C. Loon

Adviser
Department of Geodetic
Science and Surveying

AFIT/CI/NR/82-22T

AFIT RESEARCH ASSESSMENT

The purpose of this questionnaire is to ascertain the value and/or contribution of research accomplished by students or faculty of the Air Force Institute of Technology (ATC). It would be greatly appreciated if you would complete the following questionnaire and return it to:

AFIT/NR
Wright-Patterson AFB OH 45433

RESEARCH TITLE: Computer-Assisted MAP Comparison

AUTHOR: Capt Dolf C. Nation

RESEARCH ASSESSMENT QUESTIONS:

1. Did this research contribute to a current Air Force project?

( ) a. YES ( ) b. NO

2. Do you believe this research topic is significant enough that it would have been researched (or contracted) by your organization or another agency if AFIT had not?

( ) a. YES ( ) b. NO

3. The benefits of AFIT research can often be expressed by the equivalent value that your agency achieved/received by virtue of AFIT performing the research. Can you estimate what this research would have cost if it had been accomplished under contract or if it had been done in-house in terms of manpower and/or dollars?

( ) a. MAN-YEARS _____ ( ) b. $_____

4. Often it is not possible to attach equivalent dollar values to research, although the results of the research may, in fact, be important. Whether or not you were able to establish an equivalent value for this research (3. above), what is your estimate of its significance?

( ) a. HIGHLY SIGNIFICANT ( ) b. SIGNIFICANT ( ) c. SLIGHTLY SIGNIFICANT ( ) d. OF NO SIGNIFICANCE

5. AFIT welcomes any further comments you may have on the above questions, or any additional details concerning the current application, future potential, or other value of this research. Please use the bottom part of this questionnaire for your statement(s).

NAME GRADE POSITION

ORGANIZATION LOCATION

STATEMENT(s):

I hereby declare that I am the sole author of this publication.

I authorize the Ohio State University to lend this publication to other institutions or individuals for the purpose of scholarly research.

Dolf Claud Nation

I further authorize the Ohio State University to reproduce this publication by photocopying or by other means, in total or in part, at the request of other institutions or individuals for the purpose of scholarly research.

Dolf Claud Nation

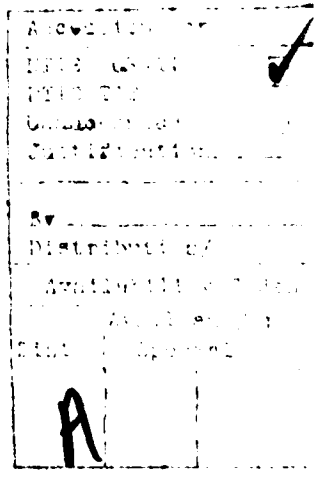

The Ohio State University requires the signatures of all persons using or photocopying this publication. Please sign below, and give address and date.

THESIS ABSTRACT

THE OHIO STATE UNIVERSITY
GRADUATE SCHOOL

NAME: DOLF CLAUD NATION QUARTER/YEAR: SPRING/1982

DEPARTMENT: Department of Geodetic Science and Surveying

TITLE OF THESIS: COMPUTER-ASSISTED MAP COMPARISON

The concept of map comparison is treated in a general manner for thematic, regularly gridded maps. Three methods of map comparison, direct methods, trend surface, and spatial autocorrelation, are investigated. The direct methods and trend surface method are applied to artificial surfaces and subsequently to regularly gridded maps of the pollutant total suspended particulates. A method of forming spatial or two dimensional autocorrelation maps is presented. A strategy based on these methods, is described whereby a large number of regularly gridded maps can be readily compared.

J. C. Loon

Adviser's Signature

ACKNOWLEDGEMENTS

I wish to acknowledge my advisor Dr. Joseph C. Loon for his help in selecting this topic, suggestions, and critical analysis. I also wish to acknowledge Dr. D. P. Hajela, for his valuable insights and comments.

I owe a special thanks to the staff and students of the Department of Geodetic Science and Surveying who have shared their time and ideas with me. In particular, I am indebted to Mr. E. M. Baker for his patient help and good advice.

Finally, I am especially grateful to my wife Cynthia and my daughters Tamara and Vanessa for encouragment and support. Their sacrifices during this project are easily equal to my own.

CONTENTS

LIST OF FIGURES

LIST OF TABLES

Chapter I

INTRODUCTION

1.1 PURPOSE

The purpose of this investigation was to compare some existing methods of map comparison and investigate potentially useful computer-assisted methods of map comparison. The emphasis has been on comparing the different methods and developing a possible strategy for comparing large numbers of potentially similar maps.

There are many reasons for comparing maps and an increasing number of gridded data map sources are becoming available. Geographers have compared maps of many types of human variables such as heat source vs income, spead of infection vs well water source, and many other sets of variables. Geologists compare maps of different subsurface rock units to study tectonic history of an area. In pollution studies, maps of different variables such as terrain, wind patterns, and emissions sources are compared. For this investigation monthly pollution maps will be compared in order to demonstrate possible computer-assisted methods of map comparison.

The analytical skills of a human investigator will not be replaced by a clever program, but helping the investigator focus his attention on potentially important relationships between maps, without having to look at every possible combination of maps, makes the development of computer-assisted methods of map comparison worthwhile. If the geographer, cartographer, or geologist can eliminate or reduce the amount of initial comparisons that require manual efforts, then the investigator is free to concentrate on the potentially important map relationships.

1.2 METHODS OF MAP COMPARISON

In this investigation, three methods of map comparison are discussed and demonstrated. The maps that are compared are thematic, regularly gridded arrays. Computer programs were written to implement the comparison methods. Initial testing and evaluation of the programs was done with artificially generated maps. A final demonstration of the comparison methods was done using pollution data obtained from the Ohio EPA [Ohio EPA, 1979].

Map comparison methods used in this investigation fit into three general catagories: direct methods, trend surface and autocorrelation. general catagories: direct meth-

ods, trend surface and autocorrelation. The direct methods compare the original map, or array members, in a one to one relation with other maps . The direct methods include visual comparison, isopach maps, and direct correlation. The trend surface map comparison techniques fit a bi-variate polynomial to the gridded data sets, using the method of least squares. The estimated parameters of the polynomial fit are compared using the correlation cofficient. The third method uses the autocorrelation of each map to generate a representation of the surface. The autocorrelation of a series or array is computed by comparing the series or array to itself, the exact method that is used to do this will be discussed in chapter five. Autocorrelation can be thought of as the internal relationship of a set of data. A limited autocorrelation function is used to produce a autocorrelation curve for each of the maps. A spatial autocorrelation function is a measure of the internal consistency of a surface (map). The data set has two dimensions, thus the result of calculating the spatial autocorrelation function is an array. A spatial autocorrelation function can be used to form an autocorrelation map for each of the original surfaces.

The direct methods of comparison include the visual comparison of two maps. In order to visually compare the gridded data arrays, one must represent the data in a more human compatible form. The Geodetic Science Plotting Package (GSPP), [SUNKEL,1980], is a plotting package that will produce isarithmic maps from regular gridded arrays. GSPP uses a bi-cubic spline method of interpolation to form isarithmic maps from regularly gridded arrays of data. All isarithmic maps presented in this thesis were formed using GSPP.

1.3 MAPS USED FOR COMPARISON

For the purposes of this investigation, mapped data is regarded as a set of observations ordered with respect to two spatial coordinates. The spatial coordinates are represented with a regular grid structure. The distinction between irregular and regular gridded data can have rather significant numerical consequences. Only regularly gridded data was used. To avoid the problems inherent in the gridding of irregularly distributed data, all discussions with respect to map comparison methods will assume that observed values come from the intersections of a regular grid. The pollution data used came from irregularly located collection sites. The method and theory used to grid the data will be discussed later.

The gridded data map has been referred to as a "numerical map" or a "digital map"[ROBINSON et al.;1978]. It is not a particularly informative map if it is viewed in its most elemental form. It would appear as only a grid of points with real number values printed near the points. Normally, a gridded data set would be presented as an isoline map, that would have been formed by interpolating between the gridded data points to represent isolines.

More specifically, the isarithmic map is a statistical surface. That is, it may represent the volume or surface of data in a mapped area. The isarithmic map is of two general types the isoline and isopleth map. The transition between the isolines, of the isarithmic map, is assumed to be continuous. On the other hand, the isopleth map represents data that can not exist at a point. The statistic represented by the isopleth map occurs inside a boundary of finite extent. The boundaries often used in practice are enumeration districts, townships, counties, etc. Possible statistics used are; average sale price of homes, cattle per acre, deaths per thousand, etc. The isoline and isopleth maps are very different with respect to the nature of the data they are used to represented.

The appearence of the isoline and isopleth maps are quite similar. They both use lines as the mapping symbol. The isopleth map appears very similar to the isoline map. They both represent a statistical surface that is assumed to be continuous, yet the statistic of the isopleth map can't exist at a point because isopleths represent data that is averaged over an area [ROBINSON;1978,p.225].

The map data used in this investigation is of the type that an isarithmic map would be constructed from. The isolines are "threaded" among the gridded data points by an appropriate algorithm. The result is an isarithmic map that is a visual representation of the gridded data. It would be well to emphasize that the techniques used in this investigation assume the data to be in the form of regular gridded values, not stored as isarithms. It is possible to overlook the distiction between an isarithmic map that was formed from gridded data and the gridded data set it was formed from. The gridded data sets are what will be compared.

Because this investigation of map comparison methods is limited to regularly gridded data, it would be a fair question to ask, "where would one obtain data in this special format and what value are the techniques that address only

regular gridded data?". To answer the first part of this question, there are a number of sources of gridded data. The digitizing of existing maps has produced very large data bases of regularly gridded elevation data. These data bases are often referred to as digital terrain models(DTM) or digital elevation models(DEM). The Defence Mapping Agency (DMA) has a very extensive DTM [SAULNIER;1979]. Landsat Imagery is collected directly in the gridded (raster) format and is readly available. Another potentially important source for regularly gridded data is the analytical photogrammetric instrument [HELAVA;1978]. A lesser source, but still an important one, is the collection of geophysical data. Electrical, gravity, and magnetic surveys are often collected on a regular or semi-regular grids. Finally, a potentially large source of gridded data is the transformation of randomly or irregularly distributed data to a regular gridded format.

The second part of the question, "what value are techniques that address only regular gridded data?" is the more interesting aspect of the question. There are a number of uses that have been described for this type of data. One of the primary uses is for navigation. Map Reading is a standard navigation technique where the navigator, from some

vantage point, compares the local terrain with a chart, then orients himself, and finally determines his precise location. The current version of this method replaces the navigator with a computer and radar; the chart is replaced by a DTM. The terrain is scanned by the radar system under computer control and the DTM is compared to the terrain. Until DMA released its DTM to the civilian agencies, research that required a dense DTM was difficult. The DTM has been compared to geological information, pollution, and wind patterns [TESCHE and BERGSTROM ;1978], to name a few. Not only can maps of different types be compared, but gridded data sets that vary temporally can also be studied.

1.4 MANUAL MAP COMPARISON METHODS

Manual methods of map comparison are not efficient enough to handle large amounts of data or maps. In order to compare a large number of surfaces, the investigator must have some method of reviewing the relationship between all possible map combinations. The visual comparison of maps is a useful tool, but the number of comparisons for n maps is:

$$t = 0.5 \ (n+2) \ (n+1) \ ,$$

t : total possible map pairings

n : number of maps to be compared

when all possible combinations are considered. As a preliminary comparison method, the visual method does not appear to be very useful. The other direct method, isopach maps, is also inefficent, because it produces so many difference maps that it is difficult to understand what the relationships are between the original maps.

A computer-assisted method of comparison seems to be necessary for preliminary stages of investigation. Two computer-assisted methods of preliminary comparison are used in this investigation, they are direct comparison of the grid-

ded data sets and comparison of parameters of trend surfaces of data sets. These methods are applied to artifical surfaces. The relationship between the artifical surfaces was known. Once the known surfaces were compared and a "baseline" relationship between the artifical surfaces was formed, the next step was to apply the computer-assisted methods to ata that had an unknown relationship.

The autocorrelation of a surface may also have potential as a map comparison tool. The autocorrelation function of a surface is unique and could be used to represent a map. The comparison between the autocorrelation function of two maps could give an insight into the relation between the gridded data maps. Obviously, autocorrelation will not be practical as a preliminary comparison method, but it should be useful as a secondary method of map comparison.

While the methods of comparison used are not a complete list of every possible technique, they do include a wide range of theory and application. The trend surface method has been used in the past but with much smoother surfaces. To the best of the authors knowledge the spatial autocorrelation function has not been used before, as a map comparison technique. comparison technigue. For the map compari-

son methods that are to be demonstrated the regularly gridded fromat is the most pracitical.

Chapters three, four, and five describe the map comparison methods. Chapter six describes the artifical surfaces that were used to evaluate the computer-assisted methods of map comparison. Additionally, chapter five gives a description of the pollution data maps that are to be compared. Chapter seven presents the results of the map comparison methods applied to the artifical sufaces and the pollution maps. Chapter eight contains a strategy for computer-assisted map comparison using the methods that have been discussed.

Chapter II

REVIEW OF RELATED RESEARCH

Map comparison techniques are used whenever some type of spatial phenomenon is to be investigated. Any discipline that uses spatial data has a need for methods of comparing maps, with the fields of geology and geography notable in this respect. Naturally earth scientists have been leaders in the area. Many of the techniques used in this paper are drawn from these disciplines.

An early compter-assisted method of map comparison was described by Robinson and Bryson [1957]. They used orthogonal polynomials to calculate best fit east west profiles of population density and average rainfall for the state of Nebraska. The parameters of the univariate polynomials were then standarized and a correlation cofficient was calcualted. The study compared a profile from a isopleth map with a profile from an isarithmic map. The resultant correlation cofficient comfrimed the "graphic correlation" that had been observed between population and average rainfall. The next advance in this technique came from the field of geology.

The comparison and contrasting of geological features from one area to another is a fundamental interpretive skill needed by all geologists. A somewhat narrower version of the same skill is the comparison of maps from the same area with different z-values. More specificlly, a geologist may wish to compare maps of "different chemical or mineralogical constituents, different grain size parameters, or structual maps on different geological horizions" [DAVIS, 1973, p.370].

An example of the comparison of structural maps is the now classic paper by Merriam and Sneath [1966]. A structural geological map relates the depths, to the top of a horizon, with some datum, usually sea level. Drill hole data is usually the source of the depth information. For the Merriam and Sneath investigation, the structual maps used were of subsurface beds that extended throughtout Kansas. The structual surfaces that were compared were treated as maps to be compared. The reason for the study was to show that some groups of beds had experienced similar tectonic forces. That is, the characteristics of the surfaces should be similar had they undergone deformation at the same time.

The method of map comparison used, involved the fitting of low order polynomials, by least squares, to randomly se-

lected sites on structual geological maps. Estimated parameters of the polynomials for each surface were used to calculate a correlation coefficient. The correlation coefficient computed in this manner represents the correlation between respective normalized parameter values. By calculating the correlation coefficients for each possible pairing of surfaces, Merriam and Sneath were better able to understand the similarity between the maps.

Both geology and geography use the above technique of comparing estimated parameter values of different trend surfaces [CLIFF, 1975]. Another map comparison technique that is shared by both disciplines is the isopach map method. With this method, the maps that are to be compared are subtracted from one another. The result is a third map that represents the difference between the original surfaces. This is a very common technique [DAVIS, 1973; NORBECK, 1972]. A major shortcoming of this method is the need to interpret the isopach map. That is, the resulting isopach maps don't give an easily quantifiable measure of the similarity between the two initial maps.

Additionally, there are a set of techniques that are found in geology, geography, and geodesy that are quite si-

milar in nature but very different in their applications. These techniques are kriging, autocorrelation, and collocation. They all are used to study the spatial relationship of some variable. In geography, autocorrelation could be used to study the spread of measles infection[CLIFF and ORD, 1981]. The kriging method of geology is used to predict the spatial distribution of ore grades[CLARK, 1979; ROYAL et al., 1980]. In geodesy, point and mean gravity anomalies are the variables predicted with collocation [SUNKEL, 1981]. More specificlly, the correlogram of kriging and the covariance function of collocation have a similar form. These functions are in turn much like the autocorrelation function. They relate a sampled quantity at one location with a similar quantity sampled at a location a distance (d) away. An average value of this relationship is calculated for all samples that are located (d) distance apart. Then a similar calculation is done for distance (2d) and similarly with increasing distances (nd). The relationship used in all three methods is the variation between the samples.

The spatial autocorrelation function of geology [AGTERBERG ,1974] seems to be the most promising method for map comparision. The values of the autocorrelation function have a limited range of $-1<r<1$ where as the variogram as

used in Kriging will have values that are dependent on the variance of the variable used. The theory and use of the autocorrelation function as used in geography is principly associated with ordinal and interval data [CLIFF et al., 1975; CLIFF and ORD, 1978], but the spatial autocorrelation function as in geology and the covariance function of geodesy seem to be the most practical functions for map comparison. They are easily applied to gridded data maps and each surface should have a unique autocorrelation function.

Chapter III

DIRECT METHODS OF MAP COMPARISON

3.1 VISUAL COMPARISON

Possibly the simplest method of map comparison is to form isarithmic maps, from gridded data sets (the maps or surfaces of this investigation) and compare them side by side. This direct method is often done as an initial step prior to other types of investigation or comparisons. A direct comparison has some practical problems, but is worthwhile as a limited use technique.

Ways of comparing two maps visually include examining them side by side, making transparent overlays, or using a light table. A light table was found to be the most practical method for viewing the maps together. For this to work well, the scale of the two maps should be the same, and similar vertical intervals should be used. The following are the most common things to look for with this method.

1. Positive and negative similarity, do the peaks and depressions of the surfaces coincide?

2. Do isolines cross, remain parallel or at least nearly parallel?

3. Does an isoline of a particular value on one map follow the same general pattern as an isoline of the same value on the second map?

Using the visual method has obvious limitations. Comparison of more than a few maps quickly becomes tedious. It is difficult to remain objective when comparing many different map combinations. The map that is on top has a tendency to dominate the comparison. The author has formed different judgments, on the similarity of two different maps, after the maps were reversed and viewed a second time. A map with dense isolines in one area can easily draw attention away from similarities that occur elsewhere in the two maps. This method was applied to the pollution maps and spatial autocorrelation maps. The success of the visual comparison method will be discussed in chapter seven.

The problems inherent in this type of direct comparison are strong arguments for more objective and automated forms

of map comparison. The rest of this chapter will discuss other direct forms of map comparison, direct correlation of points in arrays and isopach maps.

3.2 SIMPLE CORRELATION

With this method, the correlation between two sufaces is developed without regard for sample location. The correlation between z-values at corresponding grid points , on two different maps, is calculated using:

$$r_{jk} = \frac{COV_{jk}}{S_j \; S_k}$$

r_{jk}: correlation cofficient for surfaces j and k

COV_{jk}: covariance between surfaces j and k

S_j : standard deviation of surface j

n: the total number of grid points on the surface

where

$$COV_{jk} = \frac{\sum_{i=1}^{n} x_{ij} \; x_{ik} - \left(\sum_{i=1}^{n} x_{ij} \sum_{i=1}^{n} x_{ik} \; / \; n \right)}{n - 1} \; .$$

Obviously, this method has one serious drawbacks. The fundamental property of a map (spatial location) is almost completely ignored. In a very general way, the relationship between two sufaces is represented, but the spatial information is not considered. The data points are treated as observations without spatial information. The maps are compared as though they were a series of points matched to another series of points.

3.3 ISOPACH METHOD

This method produces a map that represents the differences between two maps. The corresponding locations on two maps are subtracted from each other.

$$I_{jk} = U_{jk} - V_{jk}$$

U_{jk}: the jk th element of map U.

V_{jk}: the jk th element of map V.

I_{jk}: the resultant element of the Isopach Map.

The isopach map that is constructed will show isolines of the differences. This method is by illustrated using maps that are the same except that noise was added to one of the surfaces. The method of adding noise will be discussed in chapter seven. The resultant map is a graphical representation of the noise (see figure 1).

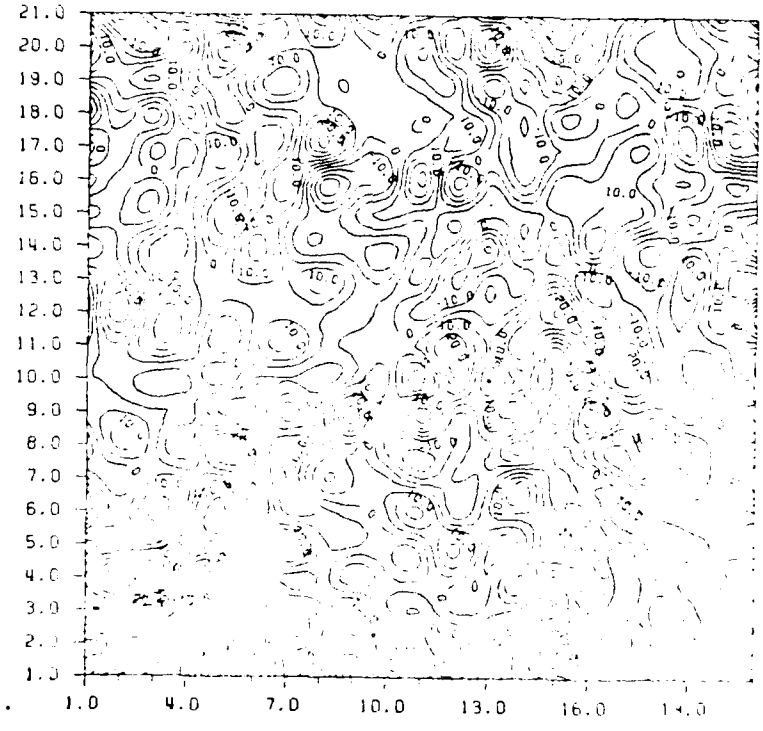

Figure 1: Isopach Map: Noise without Trend

The simplest use of an isopach map in map comparison is to look for some type of trend in the map. That is, to look for structure in the surface. If no structure is apperant as in figure 1, then the difference could be assumed to represent only random variations. The primary advantage of this method is that it is quite simple and gives a quick look at the similarity of two maps. The user should be aware that isopach maps are not unique; similar isopach maps may result from very different surfaces. As Davis [1973] has pointed out an ambiguous cases can arise with profiles that are subtracted from each other. Mathematically correct differences can give the same surface from pairs of surfaces that are very different.

Figure 2 shows two dimensional examples of this problem. These ambiguous cases are more likely to occur when standardized data is used to construct the isopach map.

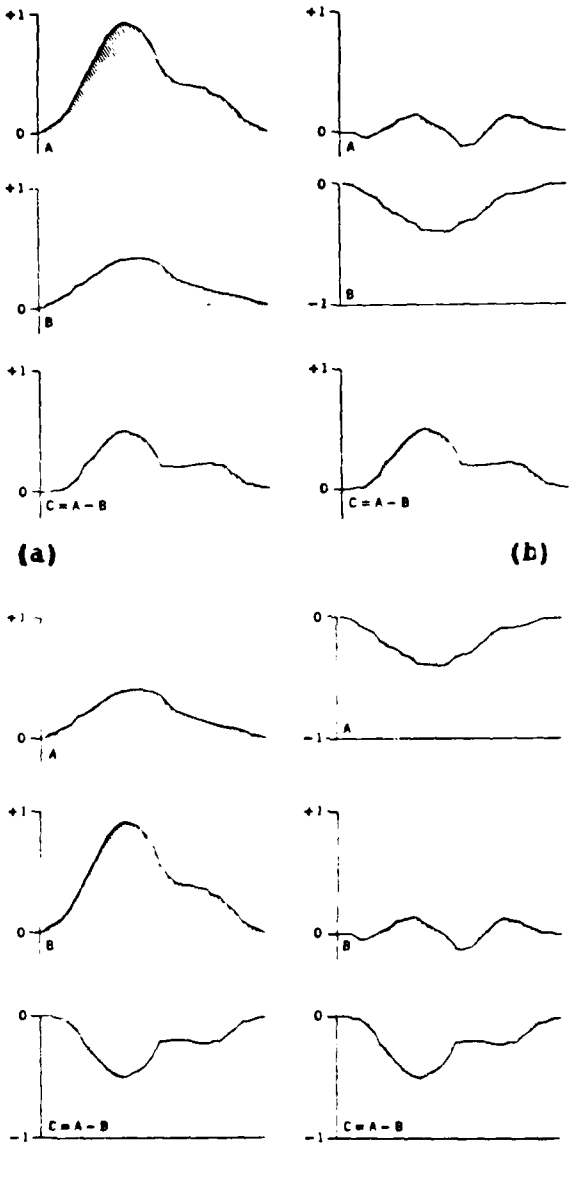

Ambiguous cases with positive and negative profiles a) and b) result in a similar profile, c) and d) result in similar profiles also (after Davis,1973).

Figure 2: Ambiguous cases

Chapter IV

TREND SURFACE METHODS OF MAP COMPARISON

4.1 INTRODUCTION

Trend surface analysis is a method of describing a set of variables that are related spatially. Using multiple regression large, systematic variations of the dependent variable are described. Trend surface methods are usually based on one of two models, the power series polynomial or trigonometric polynomial [PUECKER, 1972, p.26]. The General Linear Model is the unifiying theory for the two trend surface models. The General Linear Model has the form [GRAYBILL and KRUMBEIN, 1965] :

$$Y = \beta_0 + \sum_{i=1}^{k} \beta_i X_i + e$$

The Y and X are observable random variables, β_0 and β_1 are the unknown parameters. The value e is an unobservable or residual ; it represents the difference between the expected and observed Y. It is the value that is to be minim-

ized by the least squares method. The power series polynomial model when used in the general linear model causes the summation term to expand, giving:

$$Y = \beta_0 + \beta_1 X + \beta_2 X^2 + ... + \beta_n X^n + e$$

for the single variable case. Normally the bi-variate case is used for surface fitting. The general form being:

$$Z = \beta_{00} + \beta_{10} X + \beta_{01} Y + \beta_{20} X^2 + \beta_{11} Y X + \beta_{02} Y^2 + ... + \beta_{nn} X^n Y^n + e$$

where X, Y, and Z are the observable variables.

When comparing maps using the trend surface method the estimated parameters of the mathematical model are the important values. By computing the correlation between the parameters of two different maps, a quantitative method of comparison is possible. The correlation between two different sets of parameters is:

$$r_{ik} = \frac{COV\ (B_i, B_k)}{S_i \quad S_k} .$$

B_i : the estimated parameters of surface i.

S_i : the standard deviation of the parameters for surface i.

The correlation coefficient calculated in this manner gives a useful method for comparing different maps. The correlation coefficient has a known range, $-1<r<1$, which aids the comparison. The following discussion will briefly describe the polynomial mathematical models that are used, the method of solution, and some of the numerical considerations associated with fitting a polynomial to regularly gridded data.

4.2 POLYNOMIAL MODELS

The power series polynomial used for trend surfaces is quite flexible and can have many different forms. The number of terms or degree of a polynomial is unlimited. The naming of the polynomial models follows two groupings. The first and most common is where a polynomial is named after its "degree". The degree refers to highest power to which any term is raised. The pattern is illustrated in figure 3. The number of terms (t) in this type polynomial is

$$t = 1/2 \, (n+2) \, (n+1) \, , \; n : \text{degree of polynomial.}$$

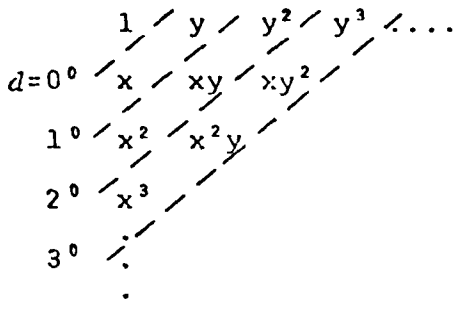

Figure 3: Degree Method of Naming (after Kratky, 1975)

The second naming scheme is the bi-polynomial. It is named by the maximum power of individual terms and not the product of powers [KRATKY ,1975]. Figure 4 shows the pattern that is used in naming bi-polynomials.

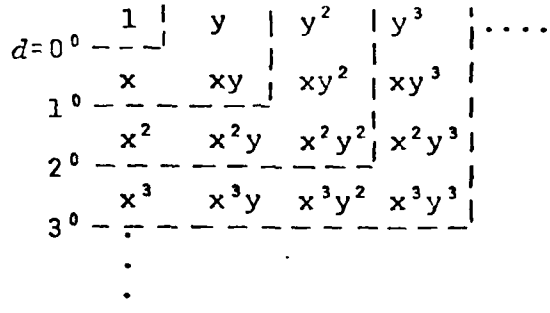

Figure 4: Bi-polynomial Naming Scheme (after Kratky, 1975)

The terms bilinear (d=1), biquadratic (d=2), bicubic etc. are used to describe this type of polynomial. The number of terms is n^2.

Three mathematical models or polynomials were used in this investigation, these were:

1. the cubic polynomial (10 terms)

$$z=\beta o + \beta_1 x + \beta_2 x^2 + \beta_3 x^3 + \beta_4 y + \beta_5 y^2 + \beta_6 y^3 + \beta_7 x^2 y + \beta_8 x y + \beta_9 y^2 x ,$$

2. the bi-cubic (16 terms)

$$z= \beta o + \beta_1 x + \beta_2 x^2 + \beta_3 x^3 + \beta_4 y + \beta_5 y^2 + \beta_6 y^3 + \beta_7 x y + \beta_8 x^2 y + \beta_9 y^2 x + \beta_{10} x^2 y^2 + \beta_{11} x^3 y + \beta_{12} x y^3 + \beta_{13} x^2 y^3 + \beta_{14} x^3 y^2 + \beta_{15} x^3 y^3 ,$$

3. the bi-quartic (25 terms)

$$z= \beta o + \beta_1 x + \beta_2 x^2 + \beta_3 x^3 + \beta_4 y + \beta_5 y^2 + \beta_6 y^3 + \beta_7 x y + \beta_8 x^2 y + \beta_9 y^2 + \beta_{10} x^2 y^2 + \beta_{11} x^3 y + \beta_{12} x y^3 + \beta_{13} x^2 y^3 + \beta_{14} x^3 y^2 + \beta_{15} x^4 + \beta_{16} y^4 + \beta_{17} x^4 y^3 + \beta_{18} x^4 y^2 + \beta_{19} x^4 y + \beta_{20} x^3 y^4 + \beta_{21} x^2 y^4 + \beta_{22} x y^4 + \beta_{23} x^4 y^4 + \beta_{24} x^3 y^3 .$$

4.3 METHOD OF SOLUTION

The least squares method of solution was used, in solving for the parameters of the bi-variate polynomial. Using matrix notation the general form of the solution is [OTOLIA,1967]

$$\beta = (A^tPA)^{-1} A^tPL$$

A: the design matrix

L: vector of observation for the dependent z variable

P: weight matrix

β: vector of parameters of the polynomial model

Using equal weights the above equation reduces to

$$\beta = {}_{c}(A^tA)^{-1}_{c\ c\ n\ n\ 1} A^tL$$

$$\beta = N^{-1}_{cc}\ U_{c1}$$

c: number of parameters in polynomial model

n: number of observations

The last equation is the so called "normal equations". The most difficult task in the solution of the normal equations is computing the inverse of N. This inverse can be rather troublesome to compute explicitly, thus the next section (4.4) will discuss some of the pitfalls associated with the trend surface method.

Two methods were used to evaluate the ability of the polynomial model to fit the gridded data sets. The first was the computation of the <v,v> or sum of squares of the residuals. The second method was the goodness of fit method [MERRIAM AND SNEATH; 1966]:

$$p = 100 \frac{\sum x_t^2 - \left(\sum x_t\right)^2 / n}{\sum x_0^2 - \left(\sum x_0\right)^2 / n} .$$

x_t : the value of the trend surface at location of data point

x_0 : observed data value

n : number of data points

The sum of squares and goodness of fit were calculated with each trend surface computed.

4.4 NUMERICAL CONSIDERATIONS

There are three general sources of error for polynomial trend surface calculations: ill-conditioning of the N matrix, mathematical error, and technical error [UNWIN,1975]. The solution of the normal equations

$$N\beta = U$$
$$\beta = N^{-1} U$$

is the usual source of error in the trend surface method. The parameters must be estimated as accurately as possible if they are to be used to represent the original data when comparing the surfaces.

The conditioning of a matrix is actually a measure of the sensitivity of the matrix to change. If a small change in the original matrix can cause an unusually large change in its inverse matrix, then the original matrix is said to be ill-conditioned. Theoretically, the N matrix should be positive definite, and non-singular [GRAYBILL,1961;UNWIN,1975]. Thus one can assume that an inverse exists, but to know how ill-conditioned the matrix is some tests should be performed.

Four conditioning indicators were used to evaluate the stability of the N matrix. These were; correlation among the parameters, smallness of the determinant, P-number, and the overall range of magnitude of terms in the N matrix. Correlation of the parameters was suggested by Dotila [1975]. The idea here is that dependence among the parameters would suggest some dependence in the columns of the design matrix. The smallness of the determinant and the P-number are tests used by Faddeev and Feddeeva [1963]. A singular matrix has a determinant of zero and can not be inverted, but a matrix that has some dependence can be inverted, although it may be ill-conditioned. A very small determinant suggests that the matrix is almost singular. The P-number is :

$$\text{P-number} = \frac{|\max \lambda_i|}{|\min \lambda_i|}$$

where λ i are the eigenvalues of the N matrix. Faddeev and Faddeeva suggest that a very large P-number could indicate ill-conditioning. The last test is an inspection of the N

matrix to determine if there is a large range in the magnitudes of terms. This is something that is almost unavoidable with the polynomial model, because the higher order terms of the polynomial are the products of variables raised to the 3rd and 4th powers. The best way this author has found to minimize this is to center the gridded data set. That is, put the origin at the center of the grid system.

The "mathematical sources" of error are truncation and roundoff. These are a result of the finite representation of numbers in the computer. An attempt was made, in this research, to avoid or minimize these errors by using double precision computation.

The "technical source" of error that Urwin [URWIN,1975] discusses is the use of an algorithm that is poorly written for the hardware available. This should not be a problem because a proven inversion routine (IMSL: LINV2F) and a very large mainframe computer (Amdahl 470V/6-11) were used.

Before the correlation between the parameters of the surfaces being compared can be caculated, the parameters must be standarized. This is because there is a large range in the values between the high order terms and the low order

terms. The low order terms are large values compared to the high order terms. The corresponding order terms are first grouped then standardized. That is, the ith parameter term of each trend surface is standardized in relation to the ith parameter from all other trend surfaces. If this was not done, the correlation calculation would "amount to estimating the variance of the difference corrected for height..."[MERRIAM and SNEATH,1966]. One other modification of the parameters is necessary before the correlation is calculated, the omission of the first parameter. This is done so that influence of the constants of the surface (data sets) will not be present. The first term β_0 is a constant and represents the intercept of the surface with the z axis. The second (β_1) and higher (β_n) parameters are the ones that contain the surface "character" information, therefore these are the parameters that are compared.

The standardized values are often referred to as "z" scores in statistics. The usual method of standarizing data is as follows:

$$Z_{ik} = \frac{x_{ik} - \bar{x}}{s_x}$$

x_{jk}: data value at grid point jk.

$\bar{x}$: mean value of 'z' values.

s_x : the standard deviation of the surface.

A final consideration is the fact that the parameters are not independent of each other. This can be seen in the correlation matrix of the parameters figure 5. The high order terms of the polynomial are correlated with the first order terms. Because the correlation coefficient is a parameteric statistic, it is assumed that samples (parameters) are independent. The independence of the parameters is established through the use of orthogonal polynomials. A short discussion on the orthogonalization process follows.

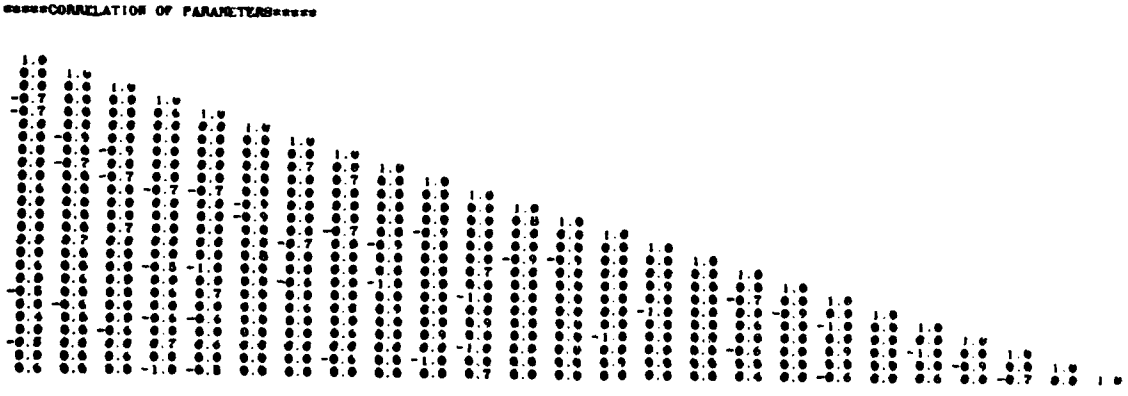

The correlation among pararateters of a nonorthogonalized bi-quartic polynomial (25 terms).

Figure 5: Parameter Correlation

4.5 ORTHOGONALIZATION

The parameter estimates that are generated by the least square solution of the trend surface are not independent. That is there is some correlation between the parameter coefficients in the design matrix and ultimitely the parameters (estimates) themselves. This is because of a lack of complete independence in the columns of the design matrix, A, for

$$A\beta = Z$$

the general model.

A standard method used to transform a non-orthogonal matrix to an orthogonal one is the Gram-Schmidt Process. One can think of the columns of A as a basis for the vector of the dependent variables Z. By applying the Gram-Schmidt Process to the columns of A, the independence of the columns is guaranteed. For example let $< a_1, a_2, a_3, \ldots, a_n >$ be the columns of the design matrix A. Then the set of vectors $< d_1, d_2, d_3, \ldots, d_n >$ are orthogonal when

$$d_1 = a_1,$$

and

$$d_i = a_i - \sum_{k=1}^{i-1} \frac{\langle d_k , a_i \rangle}{\langle d_k , d_k \rangle} d_k \quad , \text{ for } 2 < i < n .$$

This transformation has the added benefit that the inner product of unlike columns will yield zero, thus the N matrix will be a diagonal matrix. While this is not realized completely, because of numerical considerations, the N matrix does come close to being a completely diagonal matrix.

Chapter V

AUTOCORRELATION

5.1 INTRODUCTION

"The most powerful knowledge of a surface is the knowledge of its autocorrelation" [REUCKER;1972]. Autocorrelation as the name suggests is the correlation of something to itself. A good example is the autocorrelation of a waveform, first a copy of the the wave form is superimposed on itself. Then one of the waveforms is shifted a small distance, lag (d), and the waveforms are then compared along their entire common length. The moving waveform is then shifted again so that the total displacement is 2d, the waveforms are then compared again and the process is continued, if desired, until the total displacement is equal to the length of the waveforms. The average degree of similarity between all points a certain distance apart is the value that is calculated with autocorrelation. The autocorrelation of a surface can be used as a representation of the surface. By comparing the autocorrelation functions of the gridded data sets, the original data sets can be compared.

Two comparison methods that use the autocorrelation function method are applied to the gridded data sets. The first method uses a limited autocorrelation function, in which only lags along specific lines are used. In this way, the autocorrelation along cardinal directions is the only consideration. The resultant graphs can be compared visually or a difference curve can be formed. The second method uses the more general two-dimensional spatial autocorrelation function. This function results in a map or gridded data set. By comparing the autocorrelation function (map) of different surfaces, one can compare the original maps or surfaces.

The theory for the autocorrelation function comes from the study of time series. Much of the terminology reflects this origin. The use of times series for spatial analysis is well developed, and there are many good examples available [DAVIS;1973,AGTERBERG;1974]. The logical development for spatial autocorrelation is from a one dimensional analysis to the multi-dimension case. The theory of autocorelation will be introduced using the one dimensional case, following that a discussion of spatial autocorrelation will be presented.

5.2 GENERAL ONE DIMENSIONAL CASE

The following discussion, sections 5.2 and 5.3, relies heavily on the work of Agterberg [1974]. Let $k = -\infty, \ldots 0, 1, \ldots, \infty$ for some random variable x of an ordered series. Autocovariance is defined as :

$$\Gamma_d = E\left[\left(x_k - \mu \right) \left(x_{k+d} - \mu \right) \right].$$

μ : the mean of the ordered series

d : the lag or displacement along the series

The empirical autocovariance function is:

$$C(d) = \frac{1}{n-1} \sum_{k=1}^{n-1} \left(X_k - \bar{X} \right) \left(X_{k+d} - \bar{X} \right)$$

where $\bar{X} = 1/n \sum_{k=1}^{n} X_k$ for $d = 0, 1, 2, \ldots, m$.

n : total number of equally spaced points in the series

The autocorrelation function is:

$$\rho_d = \Gamma_d / \Gamma_o = \Gamma_d / \sigma^2_{|x|} \quad .$$

$\sigma^2_{|x|}$: the variance of the series

The empirical case is [AGTERBERG;1974]:

$$r(d) = C(d) / C(o) \quad .$$

r(d) : autocorrelation of lag (d)

C(d): covariance at lag (d)

C(o): covariance at lag zero (o)

The series X is said to be "weakly" stationary when it has an autocorrelation function that is constant and doesn't depend on location along the series. For a stationary series

r --> 0 as d increases.

When all variables X have the same mean, variance, and autocorrelation function, the series is weak stationary.

A correlogram is a sequence of autocorrelation coefficients, r with d=1,2,...,n. The figure 6 is one possible form of a correlogram.

Figure 6: Sample Correlogram

Before moving to the two dimensional case, some of the important properties of the autocorrelation function will be listed:

1. $r(d) < 1$ for all d
2. $r(0) = 1$
3. $r(d) = r(-d)$

The autocorrelation function has a restricted range because it uses the correlation coefficient to compare the series as it is displaced by different lags. Because of the restricted range of the function it seems to be a good choice for map comparison. The results of the different methods used for map comparison should be easier to compare if the range of the possible results are the same.

5.3 TWO DIMENSIONAL AUTOCORRELATION

The two dimensional case of the autocovariance function can be calculated empirically from [AGTERBERG;1974]:

$$C(r,s) = \frac{1}{(m-r)\ (n-s)} \sum_{i=0}^{m-r-1} \sum_{j=0}^{n-s-1} (X_{ij} - \bar{X}) (X_{i+r,j+s} - \bar{X})$$

and:

$$C(-r,s) = \frac{1}{(m-r)\ (n-s)} \sum_{i=r}^{m-1} \sum_{j=0}^{n-s-1} (X_{ij} - \bar{X}) \quad (X_{i-r,j+s} - X),$$

where the data X is from an (mxn) matrix of regularly gridded data. The r and s variables describe the lag direction and distance. For example, C(2,2) would be the covariance of all points that are seperated by 2 grid units over (east) and 2 units (south) down. The first equation will compute the covariance of all points in the directions 090° - 180°; the second computes the covariance of all lags in the 180° - 270° directions. C(0,0) is the covariance of all points at zero lag distance.

The autocorrelation function is:

$$R(r,s) = C(r,s) / C(0,0) .$$

This result can be used to form an autocorrelation map. This function has been used in a less general form [LOON; 1978]

$$C(d) = \frac{1}{n-d} \sum_{i=1}^{n-d} (X_i)\ (X_{ik}),$$

where: X_i : the normalized residuals at the point

n : the number of points

d : the lag distance.

This is the same as the more general function if the condition $R(r,0)$ and $R(0,s)$ were used and averaged together. That is, only the N/S and E/W lag directions are considered. In calculating this type of limited autocorrelation function, one could be lead to believe that the function was

rather smooth and possibly isotropic. Plotting average profiles results in smooth functions that are similar to figure 7.

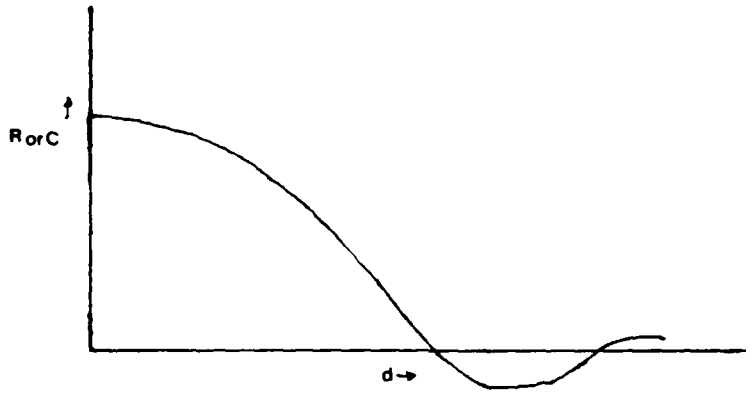

Figure 7: Limited Autocorrelation Function

When a complete autocorrelation function is calculated and averaged to give a profile, the result is rather difficult to interpret. Figure 8 illustrates an autocorrelation function for a complete surface evalutation, without regard for spatial orientation. The function, calculated in its general form, can also be a map where r and s are the coordinates. That is, the independent variables for C(r,s) and C(-r,s) are the coordinates for the autocorrelation function values.

Normally, the calculation is not carried to the largest possible lag. This is because the number of cases for the

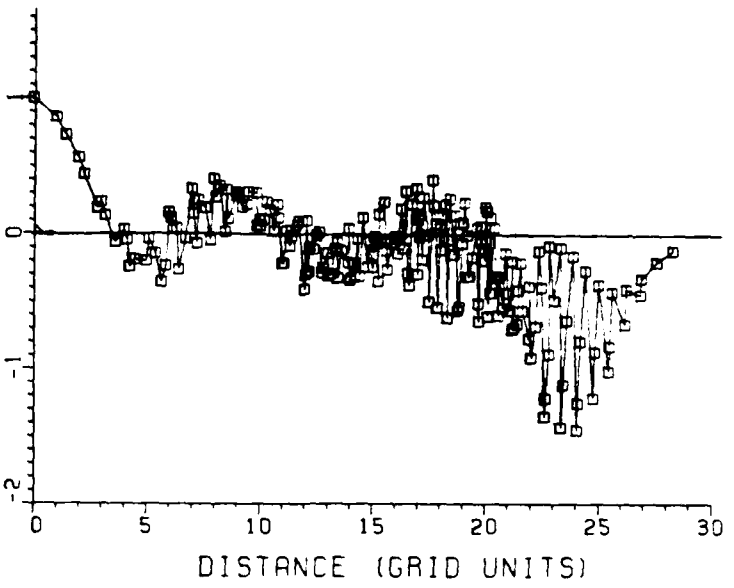

The autocorrelation function for Morrison Surface III, calculated without considering the direction of each lag distance.

Figure 8: Autocorrelation without respect to orientation

larger lags is not statistically significant and the correlation value can exceed one. Figure 8 is an autocorrelation function carried to the largest possible lags; it was calculated on a 21x21 grid. The autocorrelation maps for April, May, and June have correlation isarithms that exceed 1.0. Because it is possible to exceed 1.0, care should be taken

when trying to interpret the autocorrelation for lags that are at or near the map's maximum dimensions. This will be discussed in chapter eight again.

Chapter VI

GRIDDED DATA SURFACES

6.1 INTRODUCTION

The data used for testing and evaluation of direct correlation and trend surface programs came form two artificial surfaces or functions. Once the programs, used for map comparison, were considered tested and operational, pollution data, provided by the Ohio Enviromental Protection Agency (EPA), was evalutated [Ohio EPA, 1979]. Both types of data, artifical and real, were evaluated in a 21x21 gridded format. Smaller grid sizes were possible but 21x21 was chosen because it provided an over-determined system for the least square fitting of the polynomials. The odd size grid was chosen to aid in centering the data sets. Because of the large number of data points (441) in each set a greater degree of freedom was possible when calculating the correlation coefficient for the direct correlation method.

6.2 ARTIFICAL SURFACES

Two artifical surfaces were used for the initial testing and debugging of the map comparison programs. Both gridded data sets were generated by functions described by Morrison [1971]. The simplest surface was generated by the exponential function

$$Z = \exp[-(X^2 + Y^2)].$$

This function, called Surface II by Morrison, was used to generate data values for a 21x21 grid. The z-values were scaled to have a range of 0 - 1000 units. The basic surface was then altered by adding noise. The first alteration added noise sigma=10, the second added sigma=100, and the third sigma=1000. These surfaces thus provided gridded data that was correlated by varying amounts. The generation of noise was done with a random number generator from the Scientific Subroutine Package (SSP). The subroutine, GAUSS, has arguments that require a mean value and a desired standard deviation for the random value returned. The subroutine returns a value that is the sum of the mean and a random value. The surfaces were altered by passing each of the or-

iginal surface data points to GAUSS as a mean value. GAUSS then returned a number that was the sum of the original data value and a random number that had the desired standard deviation. The altered surfaces are shown in figure 9. The original surface is readily visible in figure 9 b, but the original surface is less obvious in figure 9 c. The final alteration with sigma=1000 caused the surface, figure 9 d, to be unrecgonizable with little of the original trend visible.

The second artifical surface was generated from a trigonometric series polynomial. See Morrison [1971] for the exact equation. This complex surface is referred to as Surface III by Morrison [1971], see figure 10 a. This surface was altered also, but instead of adding noise it was smoothed using a nines filter [LOON,1978]. The nines filter used was based on the Gaussian Function, see [LOON;1978,p.142] for a complete discription of the filter used. The resulting gridded data sets are similar enough to show varying correlation between them, (see figure 10b,c,d).

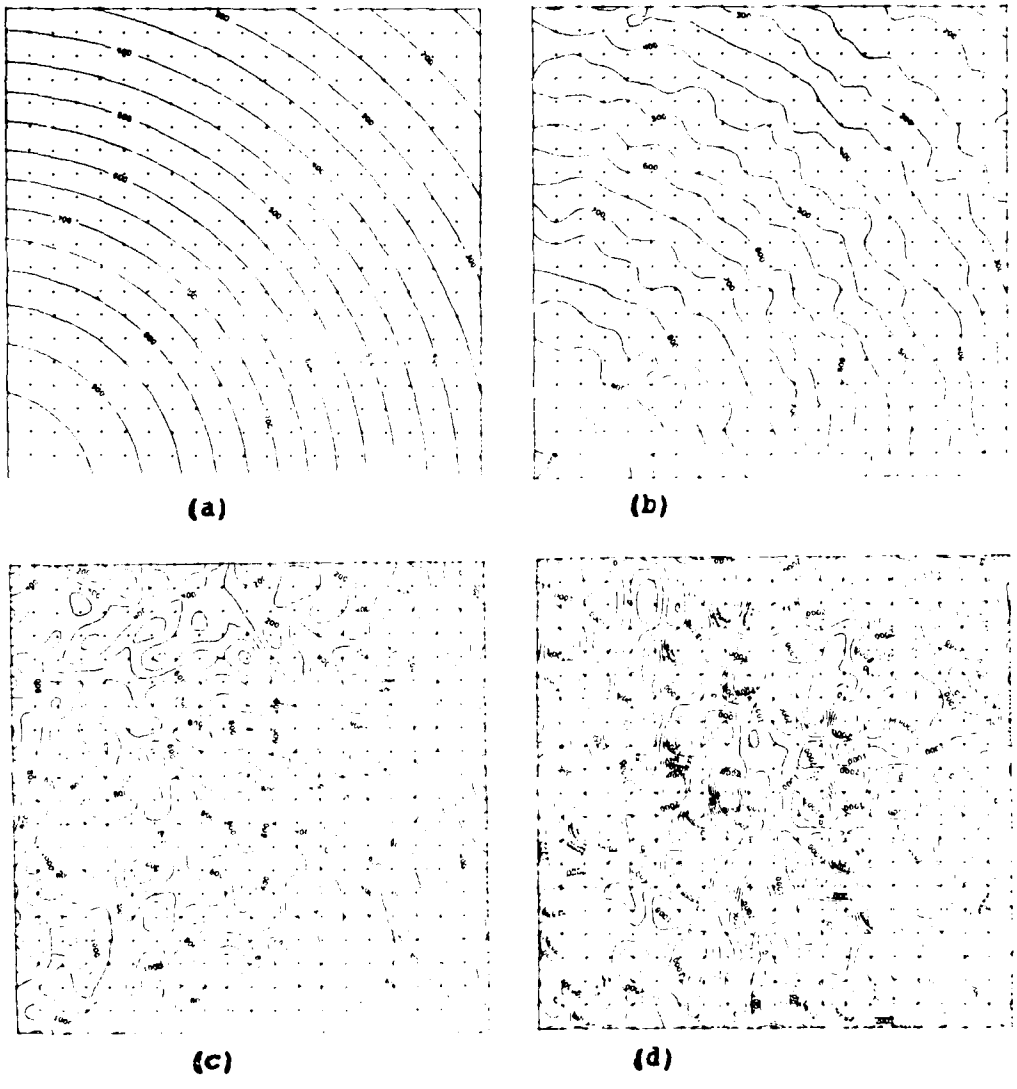

Morrison Surface II altered with noise of different standard deviations, a) original surface, b) sigma=10, c) sigma=100 and d) sigma=1000.

Figure 9: Morrision's Surface II with alterations.

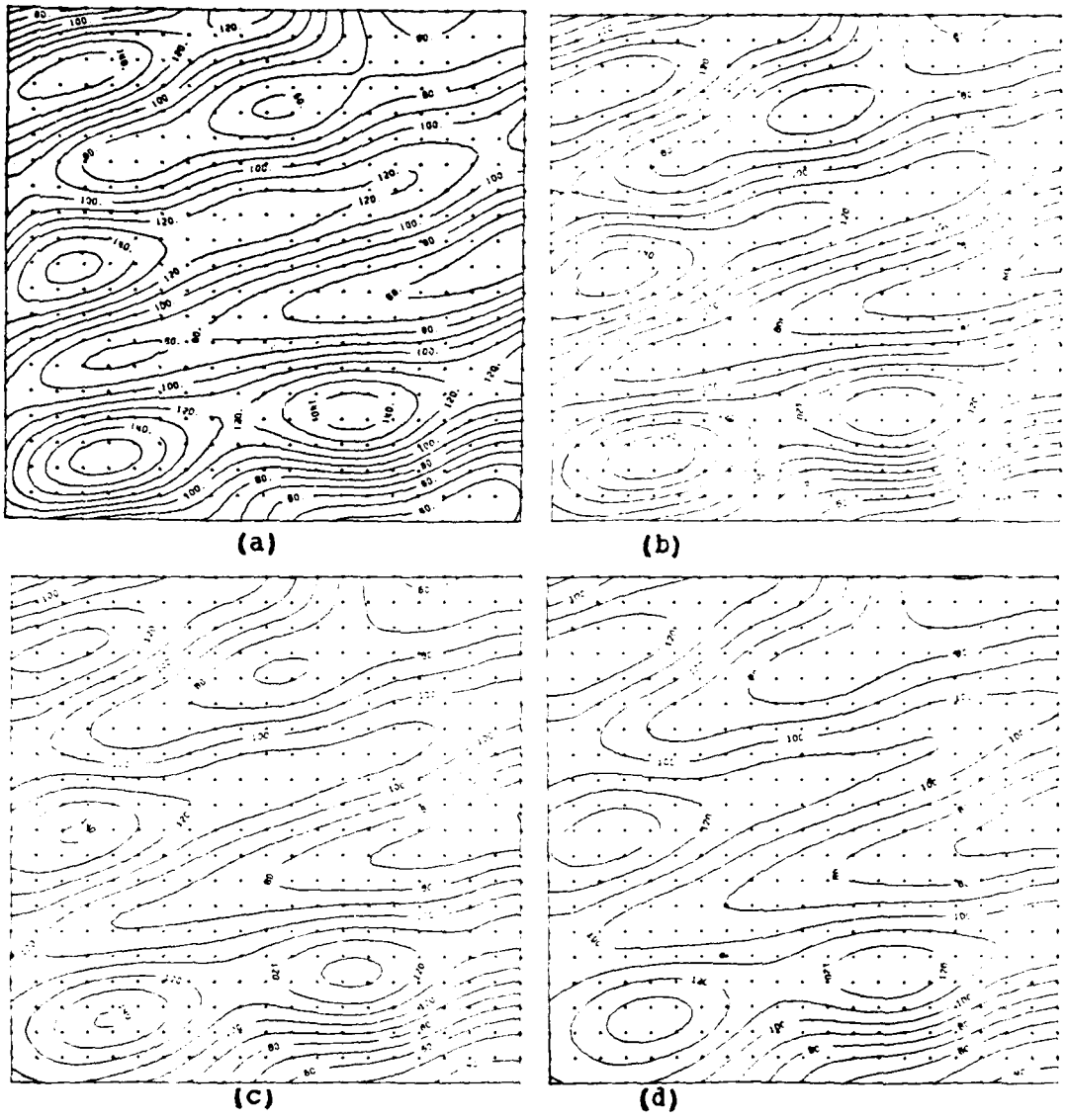

Morrison Surface III with smoothings from a nines filter, a) original surface, b) first smoothing, c) second smoothing, d) third smoothing.

Figure 10: Morrision Surface III with smoothings.

6.3 POLLUTION SURFACES

There are a number of pollutants monitored by the Ohio EPA, Total Suspended Particulates (TSP) is an important one. Substances, both solid and liquid, that are emitted into the air and remain suspended for long periods, are called suspended particulates. Some of the common forms of the suspended particulates are fly ash, process dust, fumes, soot and oil aerosols [Ohio EPA, 1979]. The reason given for monitoring TSP is that in addition to limiting visiblity, it also damages the human respiratory system by interferring with the lung's natural cleaning process.

The sampling of TSP is accomplished by drawing large volumes of air through a preweighed filter for a specific time. The resultant unit is micrograms per cubic liter of air passed through the filter. The normal sampling duration is a twenty-four hour period every six days. The sampling of TSP has been extensive and continuous since the mid 1970's, thus a large amount of data was readily available.

The samples used to construct gridded data maps of TSP are monthly averages for the calendar year 1980. There were a total of 60 continuously operating collection sites in Cuyahoga and surrounding counties for 1980. Approximatly half

of the sites used were located in the City of Cleveland with the balance of the sites in the surrounding counties.

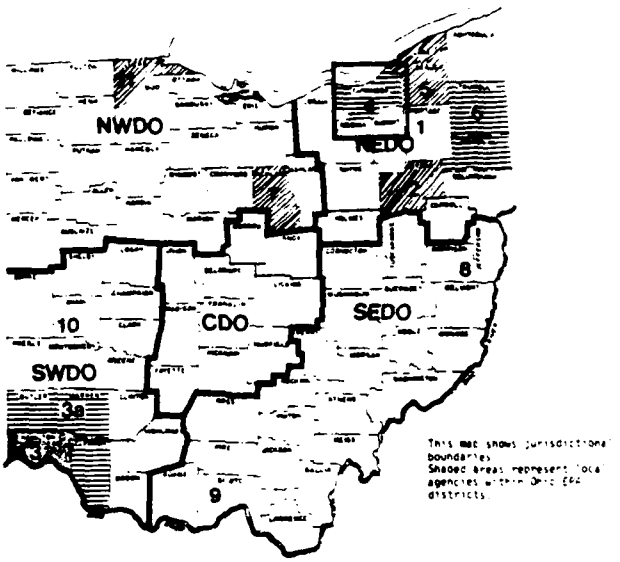

The box with the number four in it is the area containing the collection stations, it corresponds to the area of the map in figure 12.

Figure 11: Location of the EPA monitoring sites used.

The obvious clustering of the data presented a difficult problem when putting the data in a 21x21 grid form. The Geodetic Science Plotting Package (GSPP) was used to grid the data. GSPP uses a weighted average of the nearest neighbors to predict the values of the grid points. For this pollution data, a power of prediction of four was det-

ermined to be the most suitable value to use for the weighting function. For a detail discussion of the weighted average method of prediction see Sunkel [1980].

Using the mean monthly TSP values, for each of the sixty sites, twelve gridded data maps were constructed using the prediction algorithm of GSPP. See appendix A for all twelve monthly maps. The isarithmic maps produced from the gridded data represent continuous surfaces. The concentration of TSP is the unit or statistic of the continuous surface. The drawing of the isarithmns was done with GSPP and figure 12 is an example of one of the monthly maps produced.
It should be clear that the map comparison techniques used are not comparing isarithmic maps, but rather the gridded data sets the isarithmic maps were constructed from.

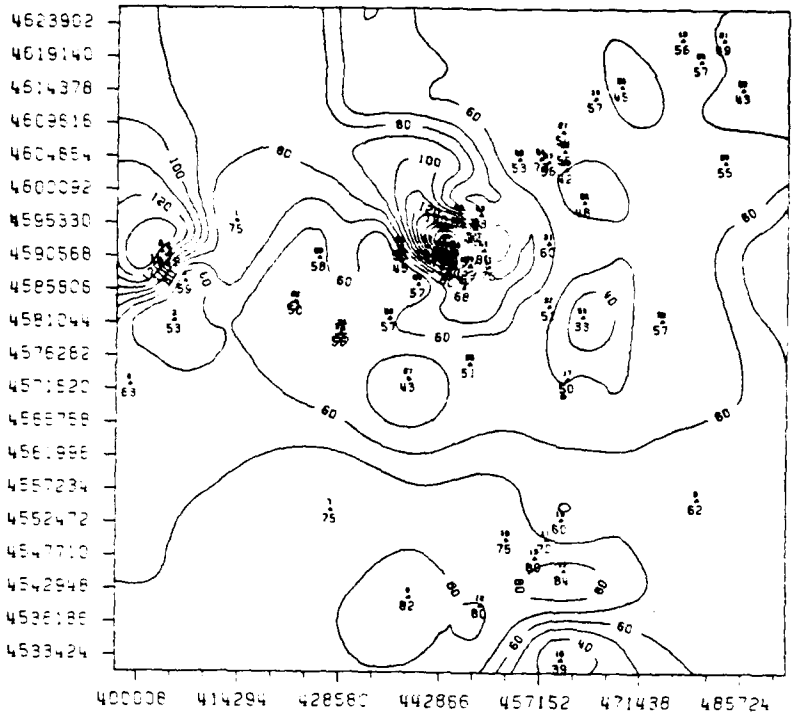

Triangles represented collection stations, values below the triangle are the monthly averages for TSP at the sites during January.

Figure 12: Isarithmic map for January 1980 TSP.

Chapter VII

RESULTS

Two of the three methods of map comparison, direct correlation and trend surface, were applied first to the test surfaces (figures 9,10) and finally to the twelve monthly TSP surfaces (see appendix A). The test maps were expected to be correlated, but the nature of the pollution surfaces was unknown. Comparison of the sequential months was looked at for possible groupings. The relationships between all months was also examined. There were a total of sixty-six possible combinations that the maps could be grouped for comparison. Spatial autocorrelation maps were formed for each of the twelve monthly TSP maps. Some of the methods, notably the differences of the limited autocorrelation functions, were generated only for surfaces that had shown promise of being significantly correlated. A large amount of data and maps were generated by the different comparison methods. For a complete presentation of all the results see the appropriate appendix. Only representative examples have been included in this discussion.

7.1 ARTIFICAL SURFACES

The artifical surfaces, figures 9 and 10, were evaluated by applying the direct methods of visual comparison, isopach map generation, and direct correlation. As would be expected, the artifical surfaces were highly correlated visually. The four variations of the Morrison Surface II were compared by the direct correlation method; the results are in table 1.

TABLE 1

Direct Method of Correlation for Surface II

	standard deviation of noise			
	0.0	1.0	100.0	1000.0
0.0	1.0	--	--	--
10.0	.99	1.0	--	--
100.0	.92	.91	1.0	--
1000.0	.21	.21	.20	1.0

It can be seen in table 1 that the correlation for the surfaces was large. The correlation between the smoothed sur-

faces formed from Morrison Surface III were also high. There were known variations in the surfaces but the correlations indicated little variation between the surfaces. The direct correlation method didn't appear to be sensitive to small changes between the data sets, like the variations caused by adding noise.

The isopach method was applied to the surfaces and difference maps were formed. The result was a set of maps that were similar to figure 1. Figure 1 was formed by subtraction of the unaltered Morrison Surface II from the altered (Sigma=100) Surface II. The result was an ideal random surface, without any trends or "topographic" forms. The only difference between the surfaces was noise so the map (figure 1) has a random character. The other isopach maps formed had a similar appearence with different isoline values.

Next, the trend surface method was applied to the Morrison surfaces. The correlation between the parameters of the Surface II maps is in table 2. Correlation between the original surface and the first two alterations is significant, but there is a negative correlation between the sigma=1000 and the other surfaces. This relationhip among the surface is like the relationship in table 1. The sigma=1000 surface

is much less correlation with the rest of the surfaces. This is because the range of the unaltered surfaces was 1000 and the noise with a standard deviation of 1000 has caused the original surface to be radically altered. See figure 9 for a visual verification of the radical change in the surface.

TABLE 2

Correlation of cubic parameters

	Sigma of Noise			
	0.0	10.0	100.0	1000.0
0.0	1.0	--	--	--
10.0	.99	1.0	--	--
100.0	.79	.76	1.0	--
1000.0	-.96	-.95	-.93	1.0

Correlation between parameters of a cubic polynomial fit to the Morrison Surface II and alterations.

Table 2 was generated by comparing the parameters of a cubic polynomial. The fit of the polynomial was good for all surfaces, see table 3, execpt for the sigma=1000 surface.

TABLE 3

Precentage goodness of fit for Surface II

Sigma of Surface II	Goodness of Fit, %		
	Cubic	Bi-cubic	Bi-quartic
0.0	99.97	100.0	100.0
10.0	99.78	99.78	99.80
100.0	83.91	84.14	84.60
1000.0	6.8	8.94	16.60

Table 4 is the result of using a bi-quartic polynomial with trend surface method. Table 4 shows a drop in correlation between the sigma=0, sigma=10, and sigma=100 surfaces. This is most likely because the bi-quartic polynomial can be made to fit the gridded data sets better than the cubic polynomial. The better fit of the higher order polynomial causes the correlation between the parameters to decease with, an increase in the ability of the polynomial to represent the surface. What seems to be happening was an increase in sensitivity of the trend surface method corresponding to an increase in the ability of polynomial model to fit the gridded data sets. A similar trend was seen with the Morrison Surface III and alterations. The size of the

polynomial used should improve the sensitivity of the method, but the overall relationship between the surfaces remains the same. Pairs of surfaces that are more correlated will remain so regardless of the polynomial model used, this can be seen by comparing the results from the different models.

TABLE 4

Correlation of Bi-Quartic Parameters

	Sigma of Noise			
	0.0	10.0	100.0	1000.0
0.0	1.0	--	--	--
10.0	.89	1.0	--	--
100.0	.79	.69	1.0	--
1000.0	-.94	-.90	-.91	1.0

Correlation of bi-quartic polynomial parameters.

7.2 DIRECT METHODS APPLIED TO TSP MAPS

The direct visual comparison of the TSP isarithmic maps was done with a light table. The similarity between each map was determined as each was overlayed in combination with every other surface. The relation between the temporally related months was examined thoroughly and the remaining relationships were given a more superfical evalution. The sixty-six pairings were tedious and objectivity was difficult to maintain. During the visual comparison, equal weight was given to each of the three points discussed in chapter 3 under the heading of direct visual comparison. An attempt was made to construct a correlation matrix of the pollution maps, but the results were not consistent or objective.

The direct correlation of the gridded data sets without regard for spatial location was accomplished by calculating the correlation coefficient between all twelve gridded data sets. This resulted in a symmetric array of numbers in which the diagonal elements are 1.0, a perfect correlation between each surface and itself. The off diagonal elements of the array are the correlation between the respective months. Figure 13 is the correlation between the monthly TSP maps. The ten highest correlations are underlined. As

can be seen in the array, there are many strong to moderate correlations present. None of the surfaces were zero or negativly correlated. The correlation appeared to be quite strong between the months that are temporally associated. August thru November appeared to have a strong correlation; they were all related with correlations greater than 0.8. The strongest correlations were March/December and May/June. The strong to moderate correlation throughtout the array suggests that all TSP surfaces are similar. Most likely the lack of spatial information could be causing everything to seem to be more correlated than it actually is.

The third method was the differencing method of isopach maps. The TSP maps were used to form sixty-six isopach maps, of which fourteen are in appendix B. The fouteen isopach maps in appendix B include the twelve monthly related isopach maps and three other maps that will be discussed. A notation of Jan/Feb represents the isopach map formed by subtracting the January data points from the February data points. The review of these maps revealed none of the isopach maps to have a structure or appearance similar to figure 1. Almost all of the maps had a peak or depression in the upper center of the map, near the location of the City of Cleveland. No readily apparent map similarities were

	JAN	FEB	MAR	APR	MAY	JUN	JUL	AUG	SEP	OCT	NOV	DEC
JAN	1.00											
FEB	0.53	1.00										
MAR	0.79	0.70	1.00									
APR	0.60	0.54	0.77	1.00								
MAY	0.30	0.19	0.50	0.64	1.00							
JUN	0.44	0.14	0.62	0.69	0.89	1.00						
JUL	0.55	0.33	0.65	0.60	0.78	0.76	1.00					
AUG	0.63	0.36	0.75	0.81	0.70	0.78	0.73	1.00				
SEP	0.83	0.45	0.80	0.74	0.53	0.61	0.72	0.83	1.00			
OCT	0.78	0.63	0.86	0.80	0.49	0.59	0.59	0.85	0.81	1.00		
NOV	0.87	0.65	0.82	0.71	0.40	0.46	0.58	0.69	0.85	0.84	1.00	
DEC	0.75	0.71	0.93	0.74	0.45	0.54	0.67	0.75	0.78	0.82	0.80	1.00

Figure 13: Correlation without regard for spatial location

found in the isopach maps. The sources of the correlation indicated by the direct method were not apparent in the isopach maps. The maps that had strong correlation with the direct method correlation didn't appear significantly different than the maps that had lower correlations. The map of lowest correlation, Feb/Jun, was specifically examined but

it had no special features either. The Apr/Jun isopach map did seem rather flat, which might indicate that the surfaces of April and June were similar, but there was a strong depression near Cleveland on the map, suggesting there were, also some siginificant differences between May and June.

7.3 TREND SURFACE METHOD APPLIED TO TSP MAPS

The monthly gridded data sets of TSP were fitted with three different polynomial models. A cubic, bi-cubic, and a bi-quartic polynomial were used as mathematical models. The design matrix in each case was orthogonalized so that the estimates of the parameters would be independent. The parameters were then standardized by the method described in chapter 4. The resultant standardized parameters for each surface were compared using the correlation coefficient. An array was formed with the resultant correlations, (see figure 14).

The goodness of fit for the higher order polynomials was much better than the lower order polynomials, see table 5. The sum of squares for the residuals <V' V>, decreased also with the larger polynomials. This would seem to indicate that the mathematical model (polynomial) was becoming flexible enough to fit the irregular TSP surfaces. If the sur-

TABLE 5

Percentage Goodness of Fit for TSP Maps

Monthly TSP Map	Goodness of fit, % Cubic	Bi-cubic	Bi-quartic
Jan	40.21	45.00	58.52
Feb	62.98	68.29	75.25
Mar	28.68	32.90	52.43
Apr	27.90	29.56	46.34
May	27.09	28.78	45.75
Jun	28.45	30.26	48.72
Jul	31.60	39.56	57.43
Aug	31.64	34.85	54.41
Sep	35.27	39.26	54.11
Oct	26.26	30.37	47.95
Nov	39.35	46.28	55.21
Dec	39.53	44.92	61.01

faces were smoother the polynomial models would have fitted even better.

The correlation matrix formed gives an indication of the relative similarity between all the compared surfaces. The surfaces that had strong correlation with the direct method showed less correlation when the trend surface method was applied. The correlations of figure 13 are larger than those of the the trend surface methods see figure 14 and ap-

***** CORRELATION BETWEEN MONTHS *****

	JAN	FEB	MAR	APR	MAY	JUN	JUL	AUG	SEP	OCT	NOV	DEC
JAN	1.00											
FEB	-0.24	1.00										
MAR	0.34	-0.20	1.00									
APR	-0.64	0.08	0.05	1.00								
MAY	-0.83	-0.03	-0.35	0.20	1.00							
JUN	-0.40	-0.05	-0.47	0.08	0.72	1.00						
JUL	-0.05	-0.32	-0.37	-0.40	0.30	0.35	1.00					
AUG	-0.23	-0.55	0.08	0.23	-0.05	-0.05	-0.09	1.00				
SEP	0.25	-0.60	0.06	-0.03	-0.27	-0.41	0.13	0.23	1.00			
OCT	-0.02	0.24	0.29	0.20	-0.33	-0.49	-0.66	0.35	-0.18	1.00		
NOV	0.12	0.58	-0.64	-0.27	0.02	0.03	-0.01	-0.52	-0.22	-0.06	1.00	
DEC	0.07	-0.09	0.55	-0.12	-0.55	-0.45	-0.20	0.20	0.06	0.08	-0.38	1.00

Correlation of TSP maps using the trend surface method with a bi-quartic polynomial.

Figure 14: Correlation matrix for bi-quartic model

pendix C. There are negative and near zero correlations where large correlations had appeared with the direct method. The range of correlation values has increased significantly with the trend surface method. The two highest value pairings, May/June and March/December, remained the highest values.

The shift of values between the trend methods of different mathematical models, most likely was a result of the improved fitting of the polynomial to the data. That is, with improved fitting of the model, the comparison of estimated parameters would give a more accurate comparison of the TSP gridded data maps. See Appendic C for the correlation of the TSP sufaces using a cubic and bi-cubic mathematical models. The correlation array for the biquartic model should be the most accurate relation of the three models used, because the bi-quartic model resulted in the best goodness of fit and lowest <v,v> value.

7.4 AUTOCORRELATION METHODS

The autocorrelation function was used to compare gridded data maps in two ways. The first method used a limited autocorrelation function, by which the general spatial autocorrelation function (see section 5.3) was evaluted in only one direction. Autocorrelation in the North/South direction was used to form a series of curves with R(0,s) form of the general autocorrealtion function. An R(0,s) function was calculated for each of the twelve TSP monthly maps. Then sixty-six difference curves were formed, with printer plots, from the monthly curves. The printer plots were checked to see if the surfaces that had showed correlation by a previ-

ous methods would appear different from the rest of the curves. The March and December curves were similar and resulted in a difference curve that was nearly zero. The May and June curves were not as similar as one would expect based on the results of the other methods. Looking at the plots of the monthly curves, in pairs, seemed more useful than looking a the curve differences.

The major problem with the limited autocorrelation method was that by choosing a particular profile to work with, the rest of the autocorrelation information was neglected. Figure 15, shows the profile for the North/South, East/West, Northwest/Southeast, and Northeast/Southwest directions on the autocorrelation map of January. They are different enough that to use one as a representation of the surface, much additonal autocorrelation information would be ignored. Possibly, a potential correlation would be missed this way.

The second method of comparison used the general form of the function. The twelve TSP gridded data sets were evaluated and the autocorrelation map of each TSP surface was formed. The general autocorrelation function would produce only one half of the autocorrelation map, but that was all that was necessary because of the symmetry of the function.

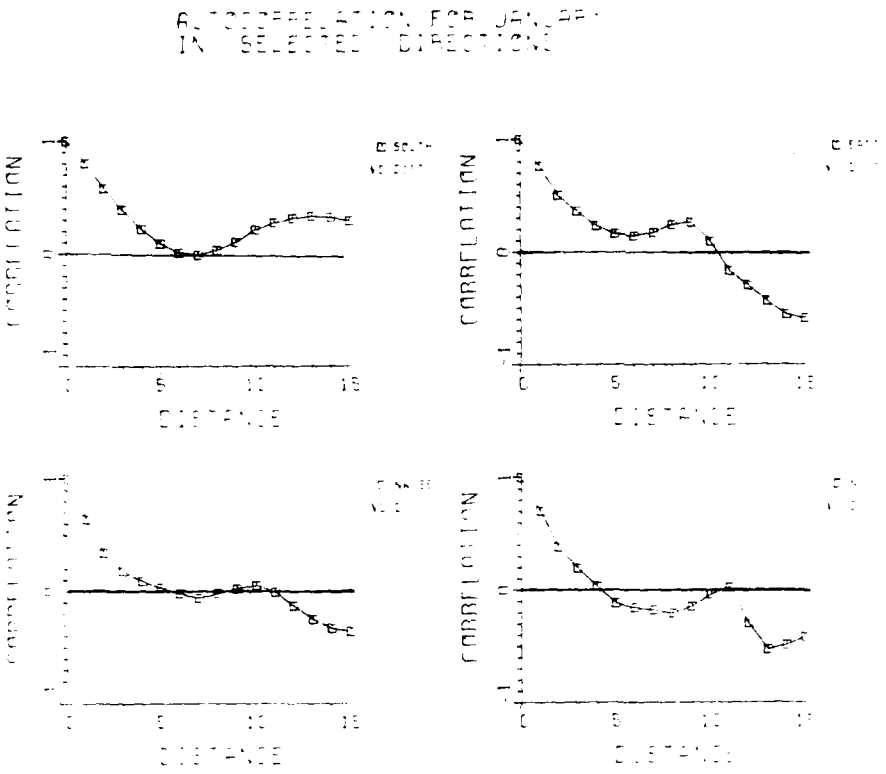

Figure 15: Autocorrelation profiles for January

In order to form an autocorrelation map, (see figure 16), matrices that were generated by the general spatial autocorrelation were put together to form the lower half of the map. The common boundary between these matrices caused the elimenation of one column, thus the two (r x s) arrays formed a single (s x 2r-1) array. That was only one half of total autocorrelation function map. The second half was formed by rotation of the first half by 180 degrees about the east/west axis and 180 degrees about the north/south

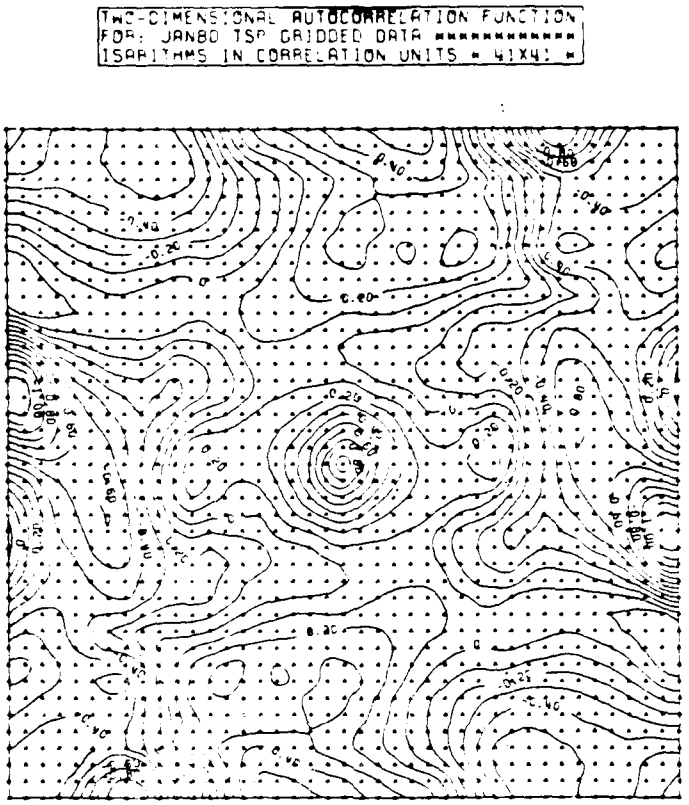

Figure 16: January autocorrelation map.

axis. There will be a common row shared by the upper and lower halves when joined, thus causing a loss of one row in the map. The final map array is (2s)-1 by (2r)-1 , with the northwest quadrant a symmetric image of the southeast quadrant. A similar symmetry was true between the southwest and northeast quadrants. The original TSP maps were (21 x 21) the resultant autocorrealtion maps were (41 x 41).

The symmetry of the map is evident in figure 16. The center of the map, point (21,21), is where a correlation of 1.0 should exist. The direction and distance out from the center yields the autocorrelation for a similar shift and direction on the TSP surface. The boundary areas of the autocorrealtion map are subject to large variations. At times, the correlation value will exceed 1.0 or -1.0,(see figure 16). This is most likely caused by the number of samples available for lag distances near the extremes of the surface. The smaller lags have more samples available, thus the sample is a more accurate representation of the population it is intended to represent.

Because of the large variation near the edge of the autocorrelation map, the values may not be as reliable as the ones near the center of the map. One should use the center 2/3 of the dimension of the map. Figure 8 doesn't have correlation values exceeding 1.0 if the lags less than 2/3 of the surface are used. Inspection of the spatial autocorrelation maps (appendix D) reveal that none of the surfaces have isolines (correlation) greater than 1.0 if only the inter 2/3 of the map is considered. For map comparison, only the center part of the function should be used. By avoiding the large boundary variations, a more accurate comparison

should be possible. To compare these surfaces is somewhat easier than comparing the original TSP gridded data maps because the autocorrealtion surfaces are symmetric. With a large number of surfaces to compare, the problem may still be present that the investigator may have to judge between many possible map combinations.

The form of the autocorrelation function was similar for each map, (see appendix C for all the autocorrelation maps). The center area is peaked, with the value at or near 1.0 and a symmetric cone dropping away on all sides to a value of .5 to .2. A completely isotropic surface would be plotted as concentric contours. The isotropic nature of the TSP surface was lost after 4-5 lags from the center in any direction. This would seem to be a strong indication that the gridded pollution data used in this study is not isotropic.

A visual comparison of the two pairs of strongly correlated months, May/June and March/December, revealed that the autocorrelation maps were also similar. It was also found that May/June/July have very similar autocorrelation maps. To avoid the problem of comparing many different combinations of maps, the trend surface method were applied to the autocorrelation maps. A bi-quartic polynomial was applied

to the 41x41 autocorrelation maps. No significant change in the correlations was observed (see appendix C).

Chapter VIII

CONCLUSION

Three general methods of map comparison have been presented; direct methods, trend surface and autocorrelation. Each method compares the gridded data surface in a different manner and thus will give a different indication of similarity of the maps compared. The relation between maps, if looked at with only one method, may not give the investigator a complete evaluation of the similarity between surfaces. More than one method should be used to evaluate the similarity between surfaces. To investigate a large number of maps, a testing strategy should be used.

An initially quick and inexpensive method of map comparison is the test of correlation without regard to spatial location. The map similarity will be somewhat exaggerated with this test, because the surfaces will appear more correlated than they really are. This happened with the test data and the monthly TSP surfaces. They all showed high correlations. If more investigation is warranted, then the next test could be the trend surface method. If the direct

correlation method reveals very high correlation between the maps, then the direct method may not be sensitive enough to sort out the differences in the set of maps the investigator is using. If the investigator feels that the comparison using the direct method is not seperating the map set sufficiently the trend surface method should be the next method applied.

For this method, a large bi-polynomial should be used if the surface is highly irregular. In the original use of this method by Merriam and Sneath [1966] a cubic polynomial was the largest polynomial used because the surfaces could be fitted well without going to larger polynomials. This investigation required a much larger polynomial to get a reasonable goodness of fit, see table 5. Once a polynomial model is chosen, then the surface can be tested. An orthogonal polynomial should be used to maintain independence among the estimated parameters that are to be tested for correlation, see figure 5. Correlation testing with trend surfaces methods requires considerably more numerical processing than the direct method, but the resultant correlation should give a good indication of the similarity in shape between the surfaces that are compared.

At this point in the testing sequence, there may be strong correlations evident from either the direct method or the trend surface method. By choosing the most promising or interresting relationship from the correlation matrix and then applying the visual method the investigator would avoid studying every single map comparison. The isopach map of the surfaces, that have an indication of strong correlation with direct or trend surface methods, could also be formed and looked at, thus avoiding the construction of many isopach maps.

If the investigator wished a more thorough investigation, the autocorrelation of the surfaces should be the next step to study the similarity of the maps being compared. The calculation of the limited autocorrelation function seems to have a minimal value, because of its inablity to represent non-isotropic surfaces, see figures 13 and 15. The general autocorrelation function map seems to be good method of representing a surface in an unique to facilate the visual comparison of gridded data maps. The calculation of the general spatial autocorrelation function map requires more numerical effort than the trend surface method, but the efforts seem worthwhile. The quickest way to evaluate the correlation between many autocorrelation maps is to use the

trend surface method applied to the autocorrelation maps. An advantage in comparing the autocorrelation maps, over comparing the original data, is the symmetry of the correlation map. Additionally, the better goodness of fit possible with the symmetric surface improves the accuracy of the correlation comparison. Visual comparison is also improved because of the symmetry of the maps, see figure 16. The use of visual comparison is best reserved for the final check of maps that are to be compared. Unless the number of maps to be compared is small the visual method should be used last.

To compare maps by only one of the techniques presented here, may cause the investigator to overlook important similarities or differences that are present. The best strategy for map comparison using the methods outlined in this paper, appears to be the use of a battery of tests that have increasing computational overhead, that the investigator can follow as far as is necessary. It is felt by the author that no one test is going to tell the full story about the similarity between a set of gidded data maps, but in concert with each other the methods can be adequately used to analyze a set of gridded data maps.

Appendix A

ISARITHMIC MAPS OF THE MONTHLY TSP DATA

This appendix contains the isarithmic representation of the gridded data maps of Total Suspended Particulates. The TSP maps are of the monthly averages of the pollutants from sixty monitoring sites in Northern Ohio. The isarithmic maps are formed on a 21 x 21 grid.

JANSO ****** TOTAL SUSPENDED PARTICULATE
PREDICTED (21X21) GRID * UTM COORDINATES
CONTOUR UNITS: MICROGRAMS / CUBIC METER

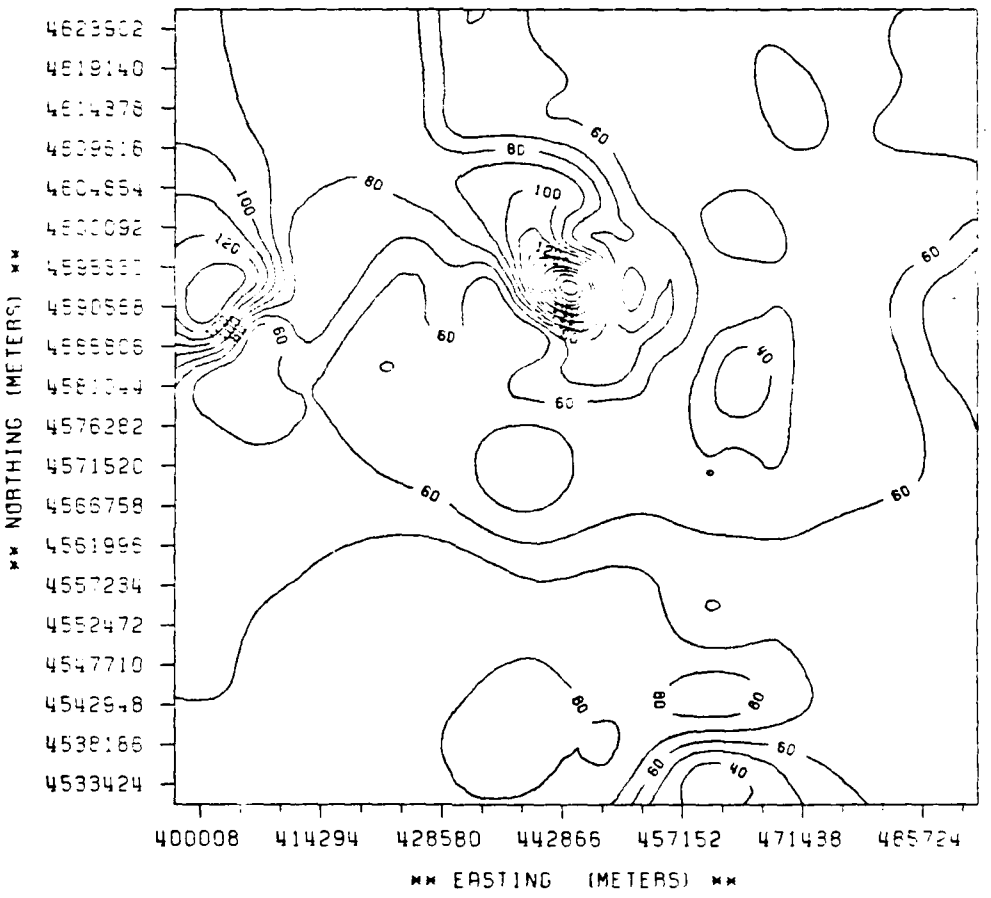

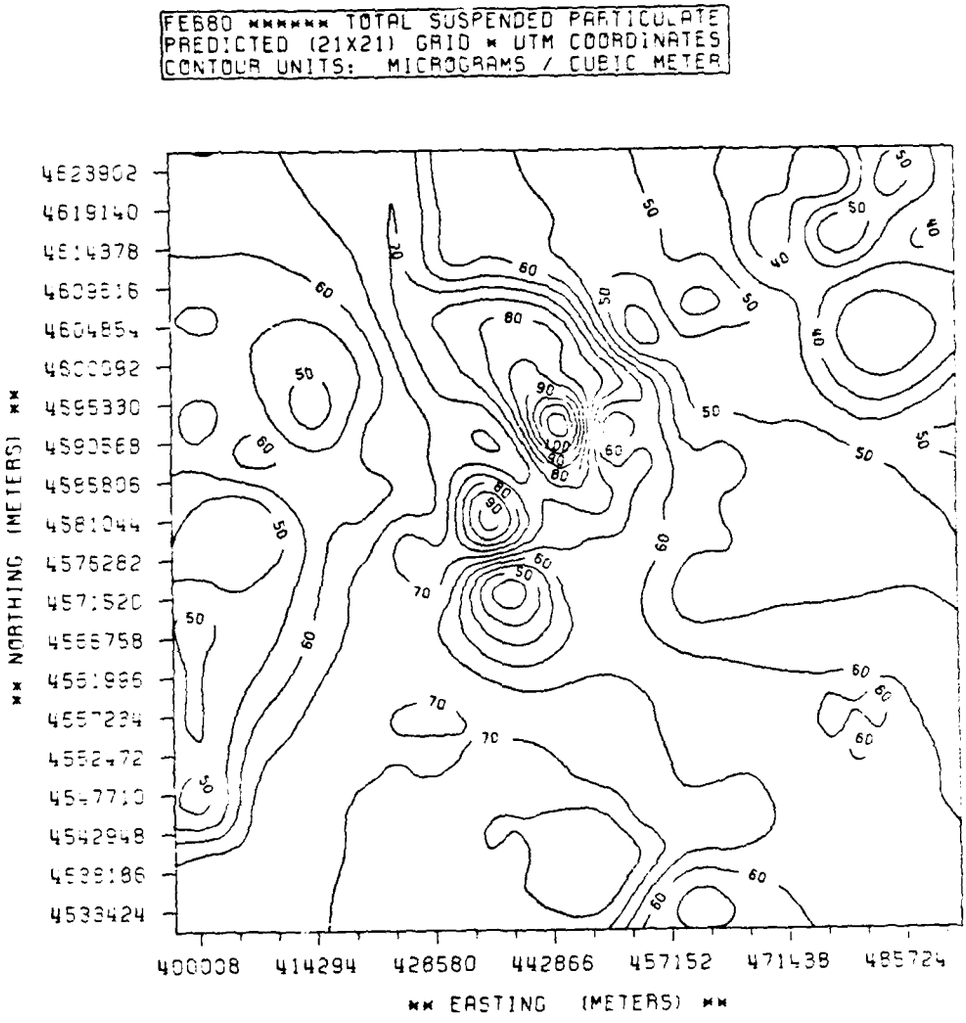
FEB80 ******* TOTAL SUSPENDED PARTICULATE
PREDICTED (21X21) GRID * UTM COORDINATES
CONTOUR UNITS: MICROGRAMS / CUBIC METER
** NORTHING (METERS) **
4623902
4619140
4614378
4609616
4604854
4600092
4595330
4590568
4585806
4581044
4576282
4571520
4566758
4561996
4557234
4552472
4547710
4542948
4538186
4533424
400008
414294
428580
442866
457152
471438
485724
** EASTING (METERS) **

MARBO ****** TOTAL SUSPENDED PARTICULATE
PREDICTED (21X21) GRID * UTM COORDINATES
CONTOUR UNITS: MICROGRAMS / CUBIC METER

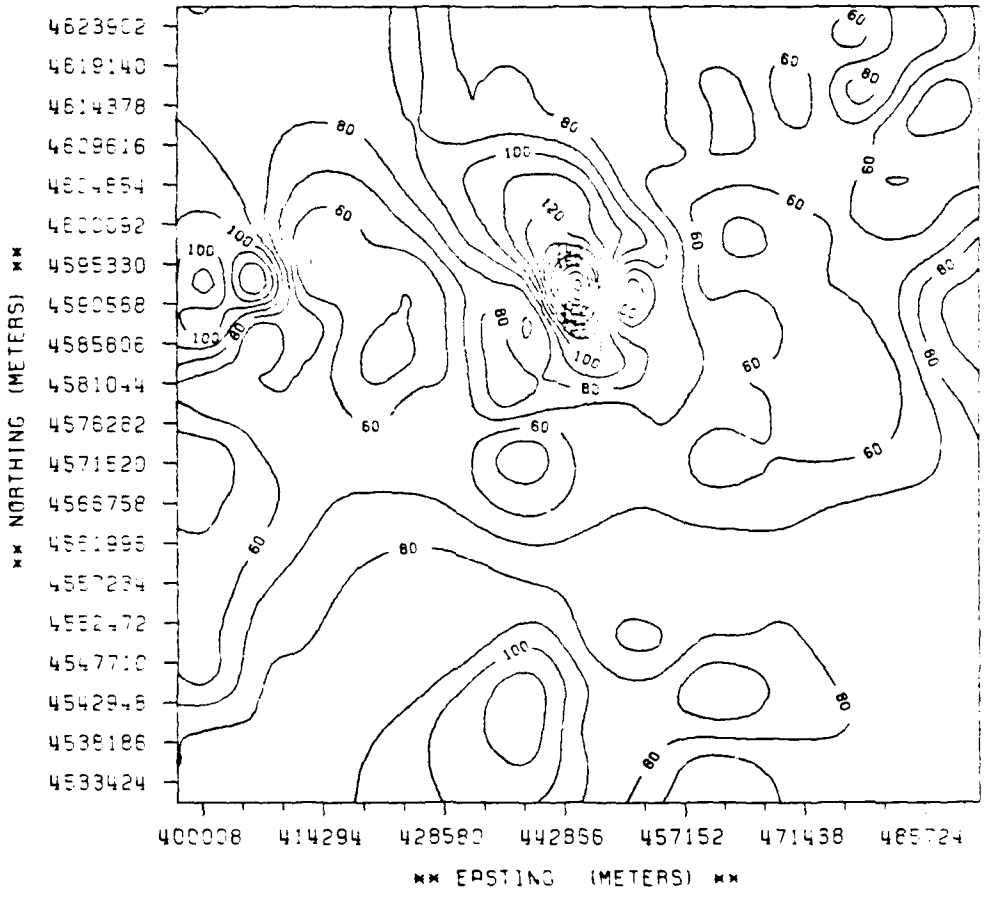

APR80 ****** TOTAL SUSPENDED PARTICULATE
PREDICTED (21X21) GRID * UTM COORDINATES
CONTOUR UNITS: MICROGRAMS / CUBIC METER

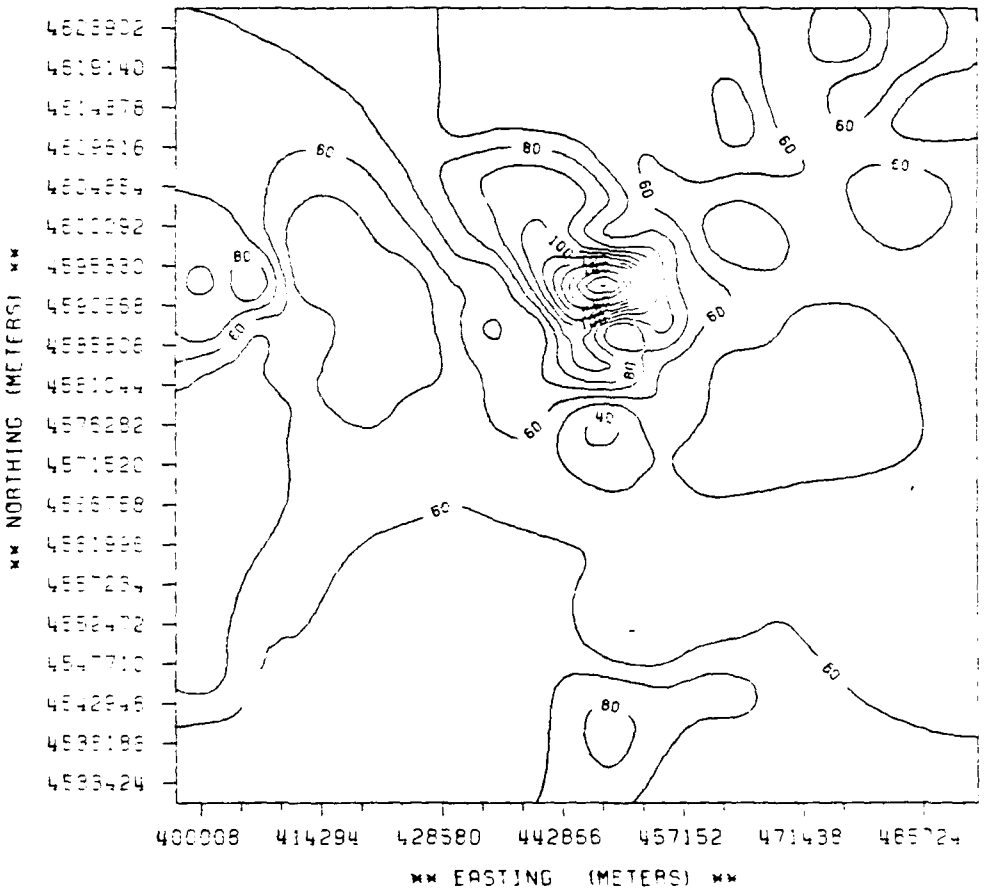

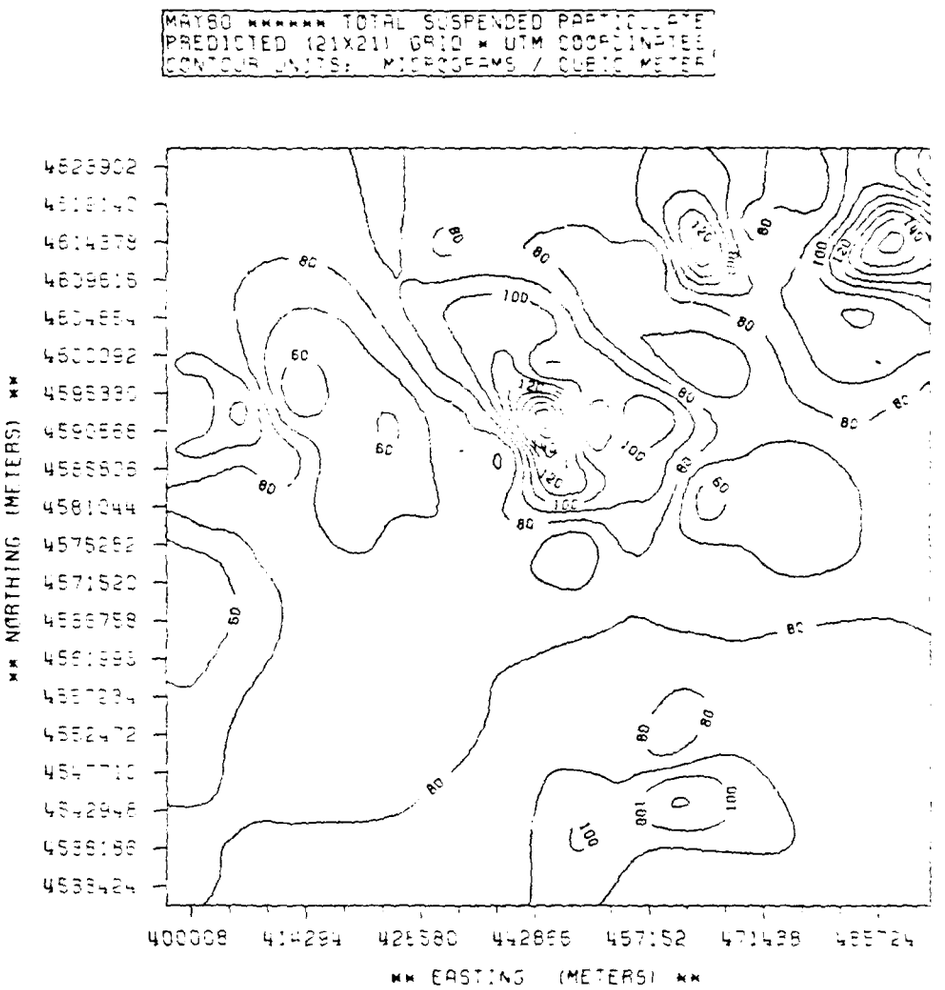
MAY80 ******* TOTAL SUSPENDED PARTICULATE
PREDICTED (21X21) GRID * UTM COORDINATES
CONTOUR UNITS: MICROGRAMS / CUBIC METER
** NORTHING (METERS) **
4626902
4618140
4614378
4609616
4604854
4600092
4595330
4590568
4585806
4581044
4576282
4571520
4566758
4561996
4557234
4552472
4547710
4542948
4538186
4533424
400008
414294
428580
442866
457152
471438
485724
** EASTING (METERS) **

AD-A119 111 AIR FORCE INST OF TECH WRIGHT-PATTERSON AFB OH F/G 8/2
COMPUTER-ASSISTED MAP COMPARISON.(U)
1982 D C NATION
UNCLASSIFIED AFIT/CI/NR/82-22T NL

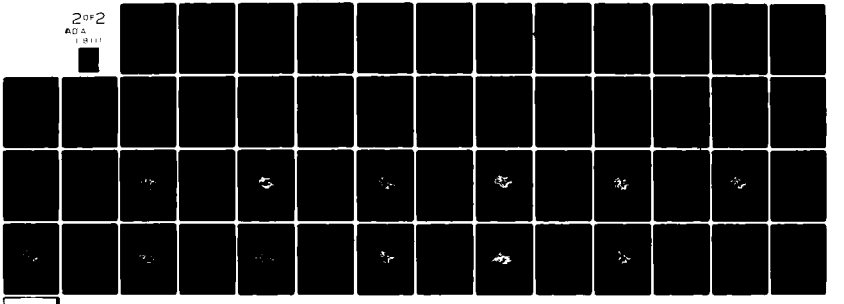

END
DATE FILMED
10-82
DTIC

JUNE80 ****** TOTAL SUSPENDED PARTICULATE
PREDICTED (21X21) GRID ** UTM COORDINATES
CONTOUR UNITS: MICROGRAMS / CUBIC METER

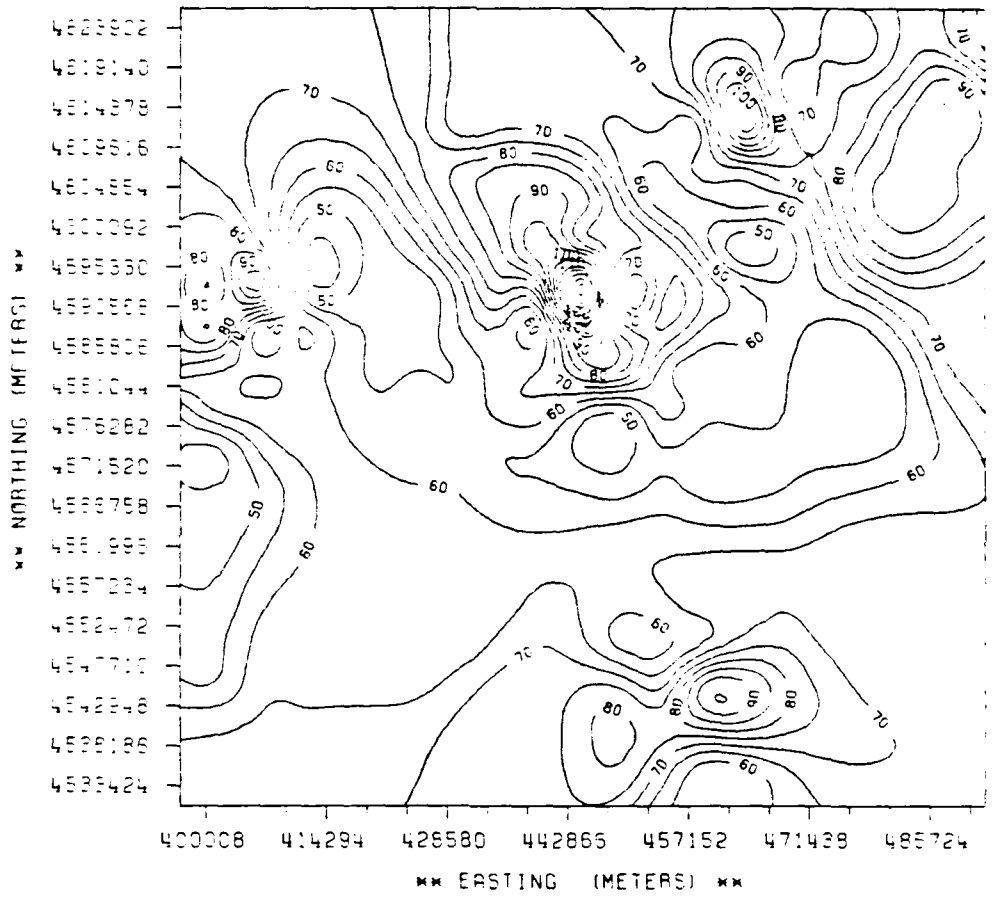

JUL80 ******* TOTAL SUSPENDED PARTICULATE
PREDICTED (21X21) GRID * UTM COORDINATES
CONTOUR UNITS: MICROGRAMS / CUBIC METER

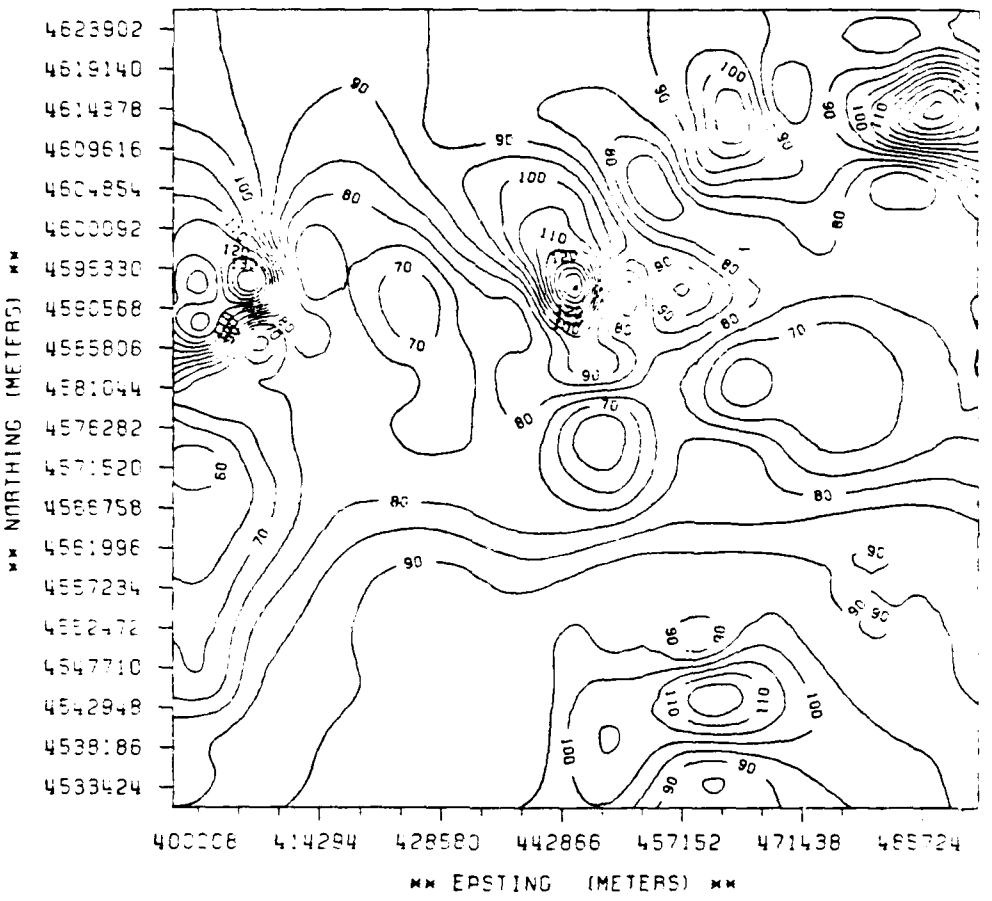

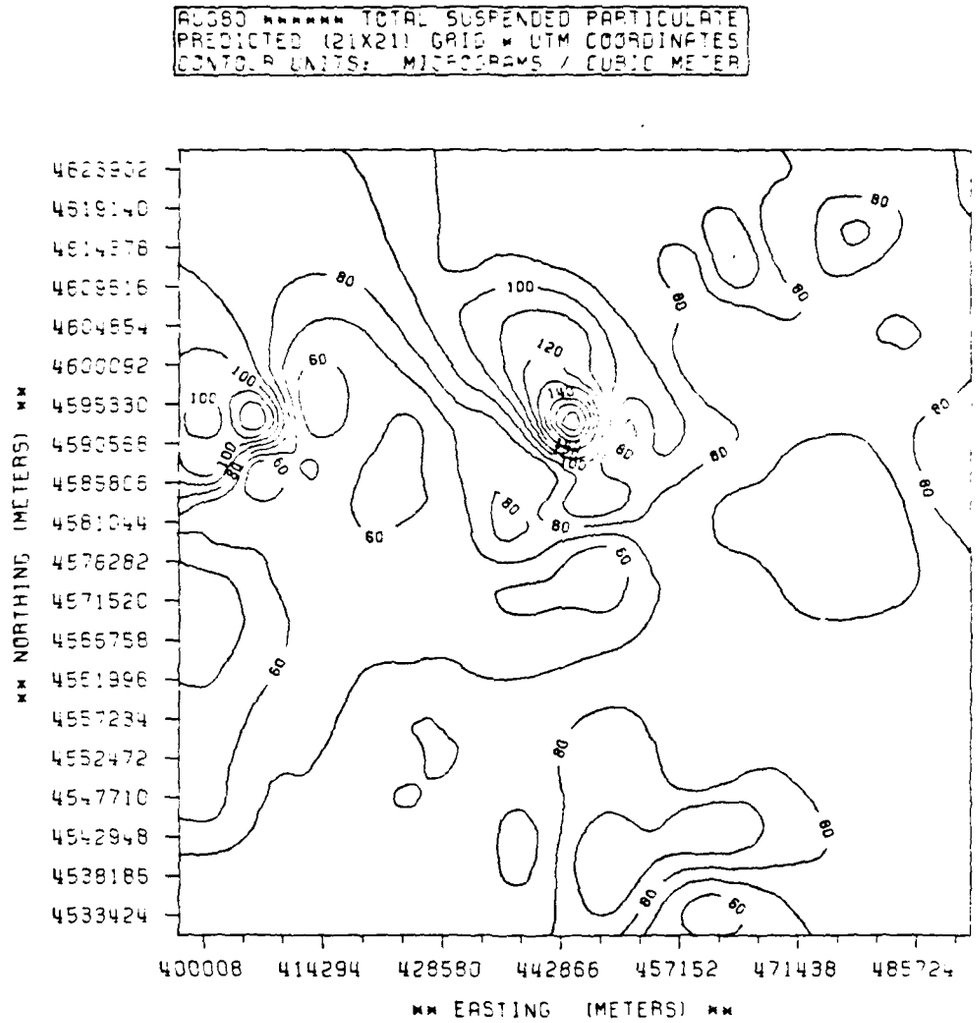
AUSEO ******* TOTAL SUSPENDED PARTICULATE
PREDICTED (21X21) GRID * UTM COORDINATES
CONTOUR UNITS: MICROGRAMS / CUBIC METER
** NORTHING (METERS) **
4623932
4619140
4614348
4609556
4604764
4599972
4595180
4590388
4585596
4580804
4576012
4571220
4566428
4561636
4556844
4552052
4547260
4542468
4537676
4532884
400008
414294
428580
442866
457152
471438
485724
** EASTING (METERS) **

SEP80 ******* TOTAL SUSPENDED PARTICULATE
PREDICTED (21X21) GRID * UTM COORDINATES
CONTOUR UNITS: MICROGRAMS / CUBIC METER

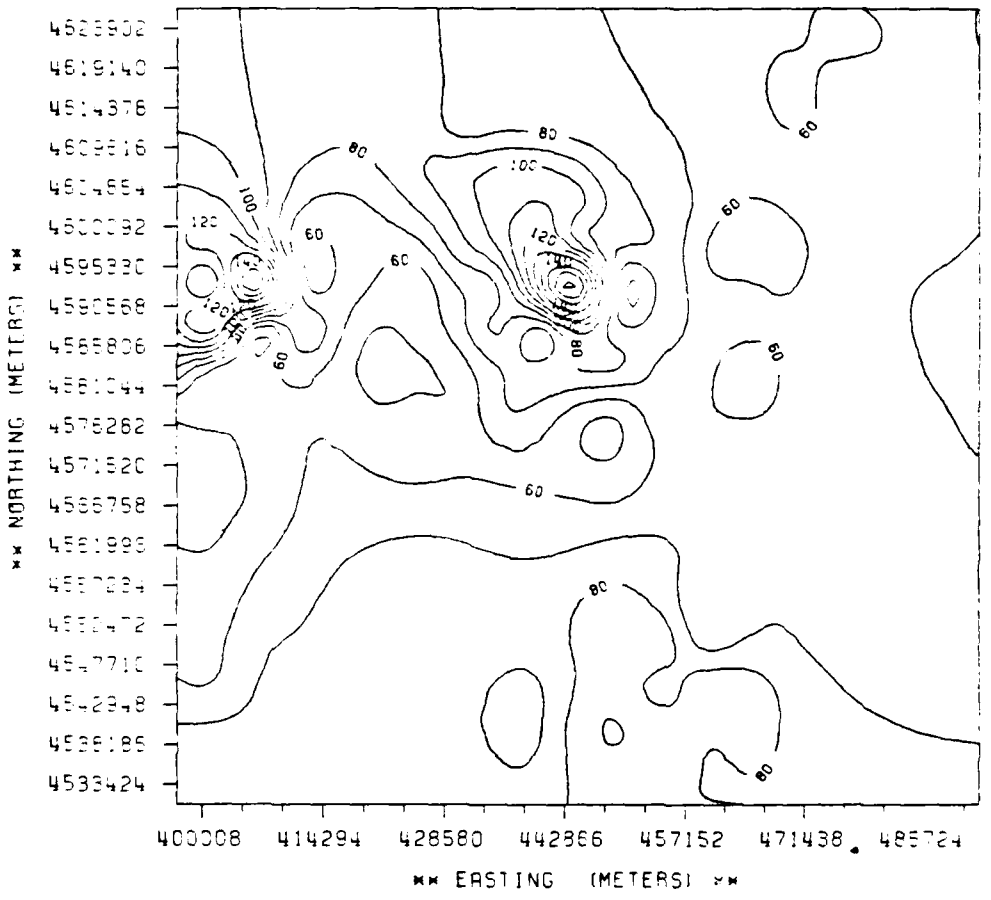

OCT80 ******* TOTAL SUSPENDED PARTICULATE
PREDICTED (21X21) GRID * UTM COORDINATES
CONTOUR UNITS: MICROGRAMS / CUBIC METER

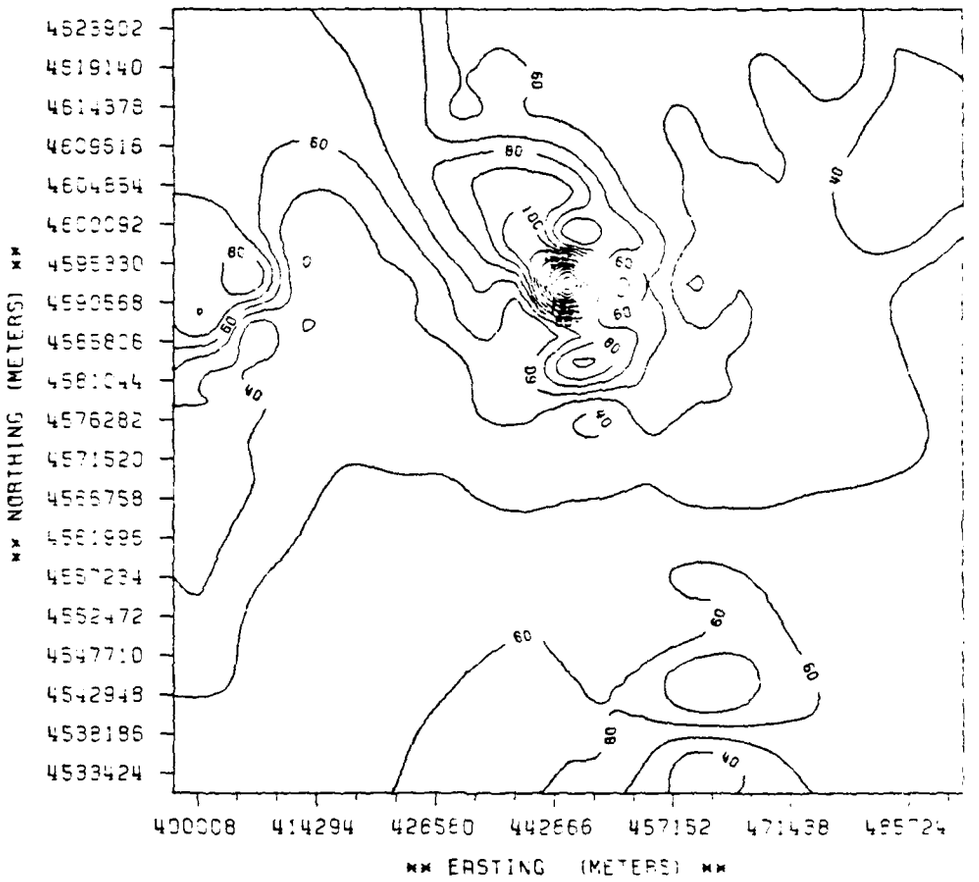

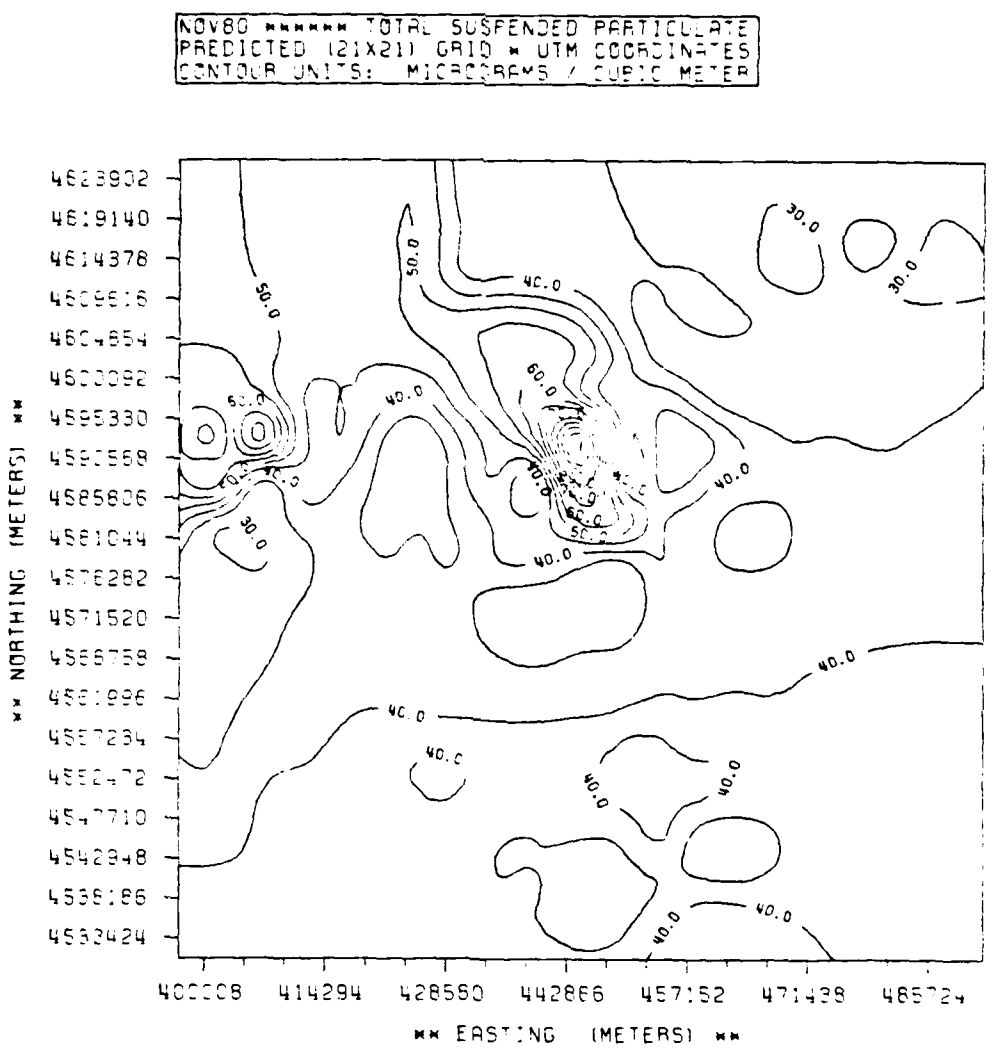
NOV80 ******* TOTAL SUSPENDED PARTICULATE
PREDICTED (21X21) GRID ** UTM COORDINATES
CONTOUR UNITS: MICROGRAMS / CUBIC METER
** NORTHING (METERS) **
4623902
4619140
4614378
4609616
4604854
4600092
4595330
4590568
4585806
4581044
4576282
4571520
4566758
4561996
4557234
4552472
4547710
4542948
4538186
4533424
400008
414294
428580
442866
457152
471438
485724
** EASTING (METERS) **
30.0
40.0
50.0
60.0

DEC80 ****** TOTAL SUSPENDED PARTICULATE
PREDICTED (21X21) GRID * UTM COORDINATES
CONTOUR UNITS: MICROGRAMS / CUBIC METER

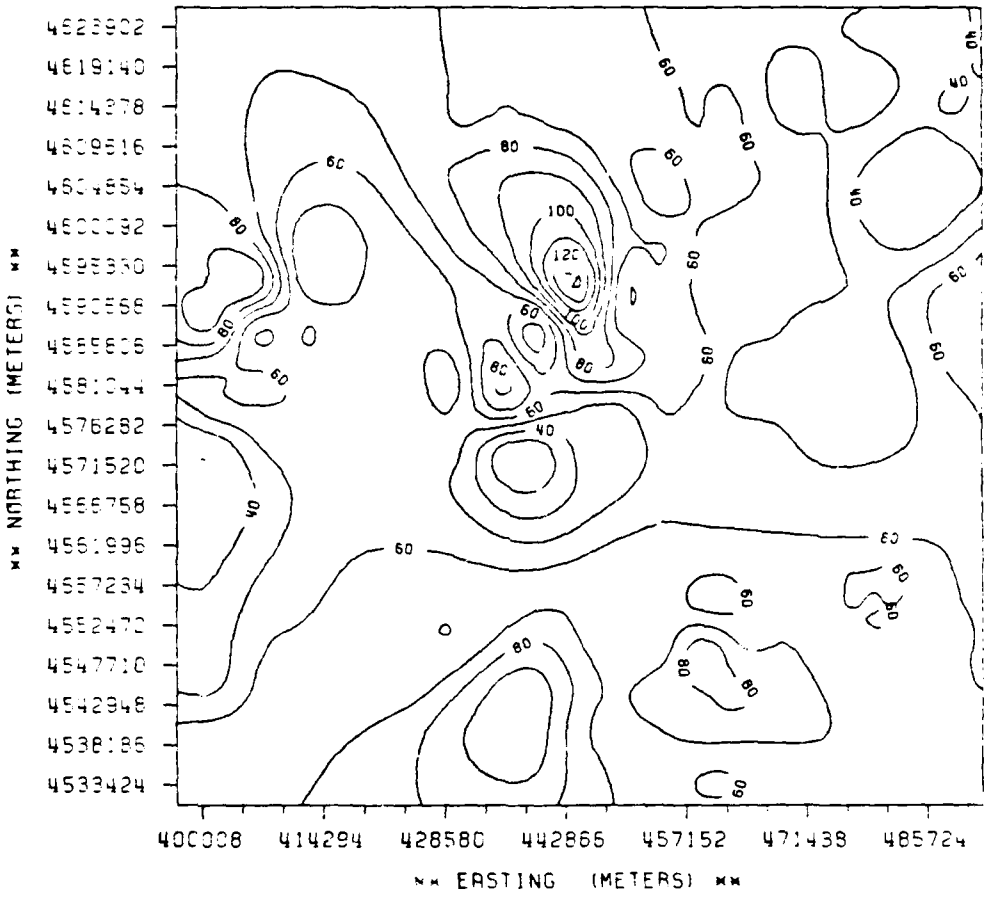

Appendix B

ISOPACH MAPS

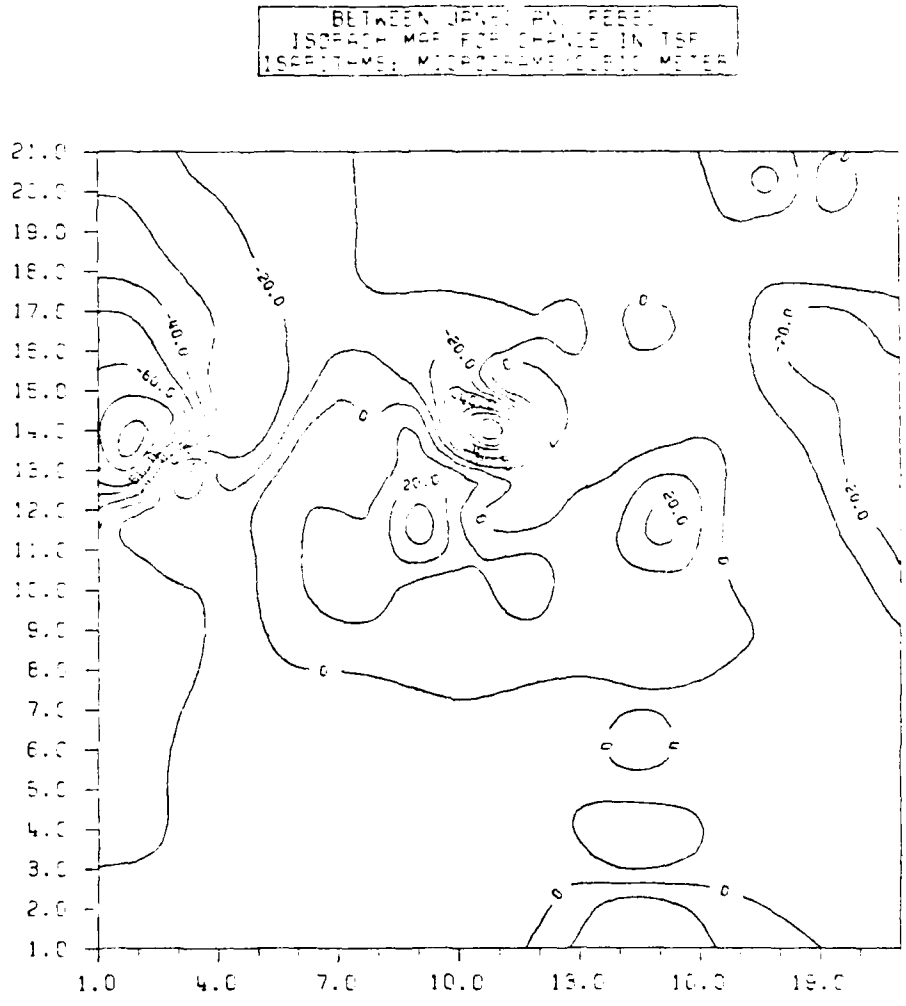
BETWEEN
ISOPACH MAP FOR CHANGE IN TSF
ISOPLETHS: MICROSIEMENS/CUBIC METER
21.0
20.0
19.0
18.0
17.0
16.0
15.0
14.0
13.0
12.0
11.0
10.0
9.0
8.0
7.0
6.0
5.0
4.0
3.0
2.0
1.0
1.0
4.0
7.0
10.0
13.0
16.0
19.0
-20.0
-40.0
-60.0
-20.0
0
-20.0
-20.0
-20.0
0
0
0
0
0
0
0
0

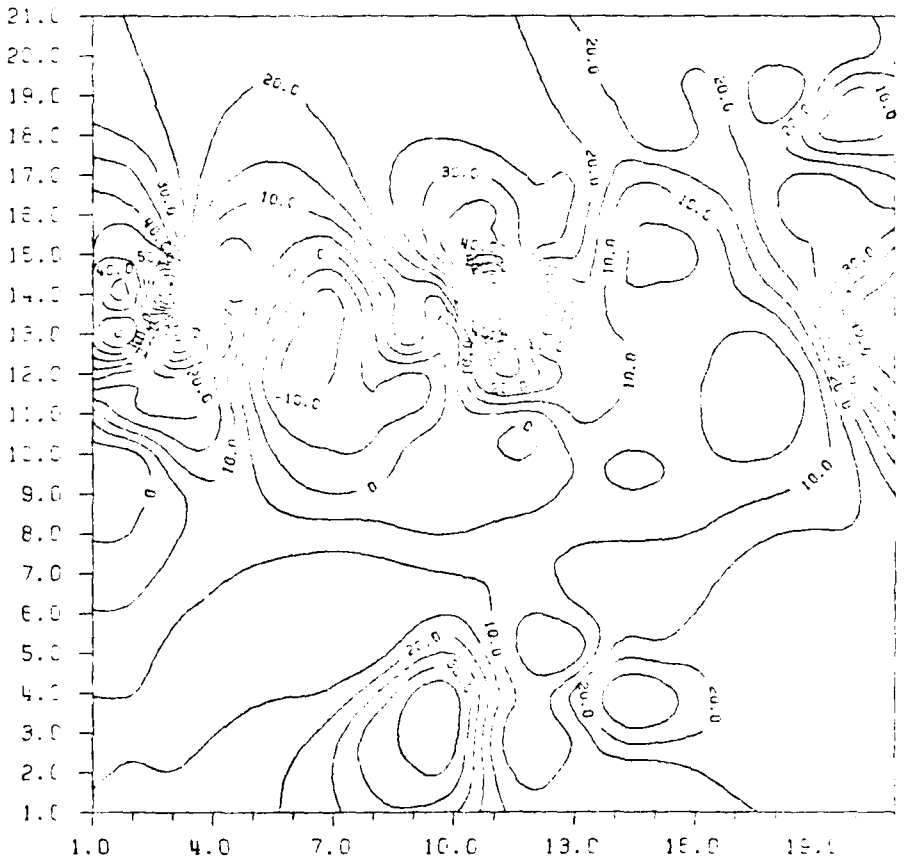
21.0
20.0
19.0
18.0
17.0
16.0
15.0
14.0
13.0
12.0
11.0
10.0
9.0
8.0
7.0
6.0
5.0
4.0
3.0
2.0
1.0
1.0
4.0
7.0
10.0
13.0
16.0
19.0
20.0
10.0
0
-10.0
30.0

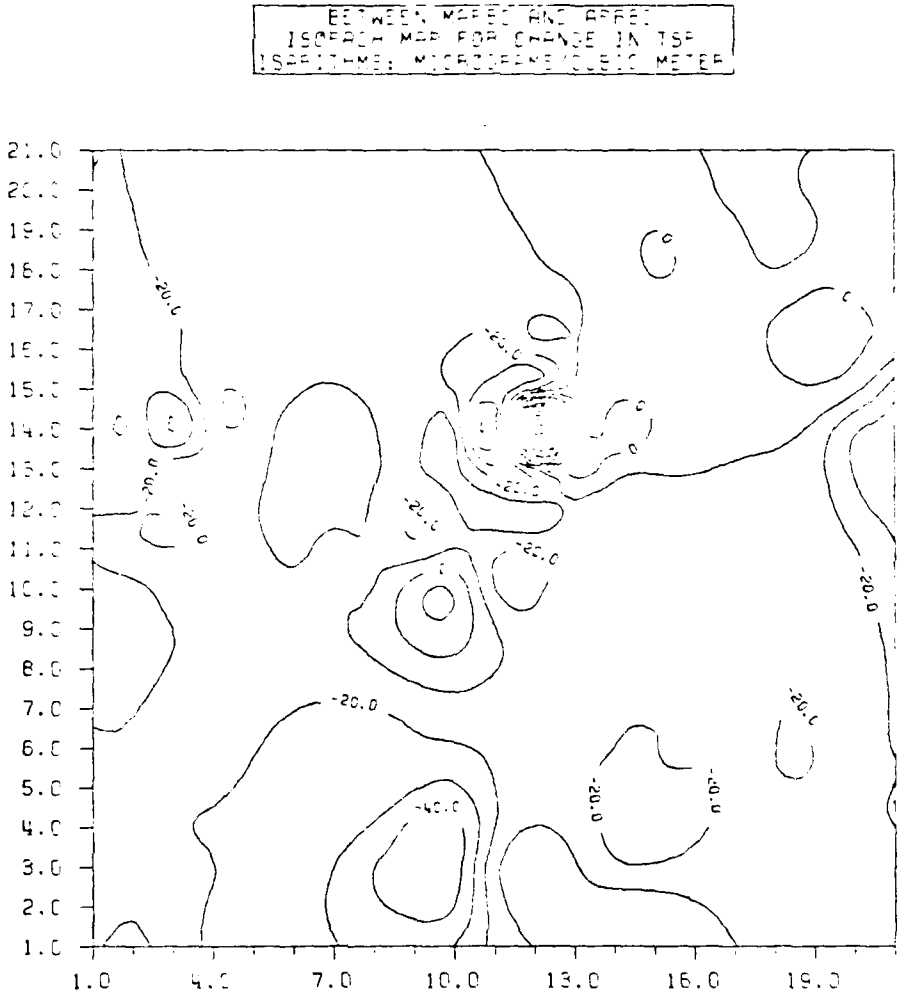
BETWEEN MAPEC AND APPEL
ISOPACH MAP FOR CHANGE IN TSP
ISOPACH INTERVAL: MICROGRAMS/CUBIC METER
21.0
20.0
19.0
18.0
17.0
16.0
15.0
14.0
13.0
12.0
11.0
10.0
9.0
8.0
7.0
6.0
5.0
4.0
3.0
2.0
1.0
1.0
4.0
7.0
10.0
13.0
16.0
19.0
-20.0
0

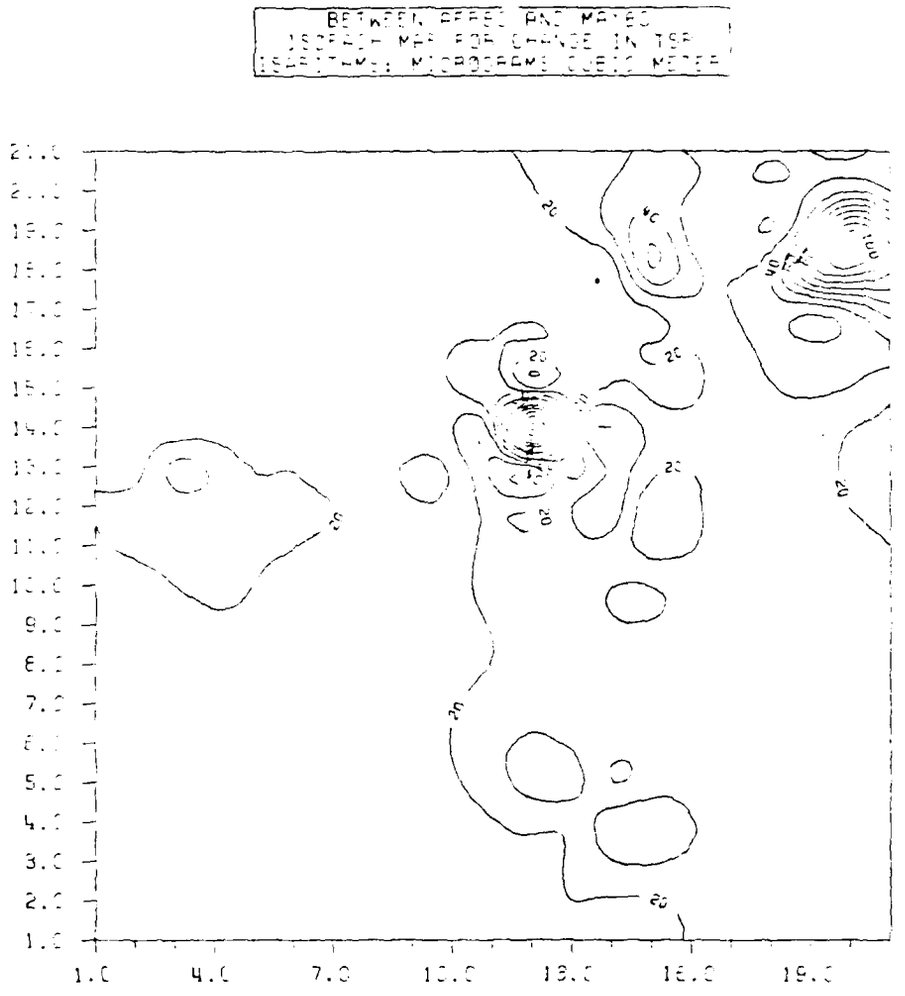
BETWEEN APRIL AND MAY
ISOPLETH MAP FOR CHANGE IN TSP
ISOPLETHS: MICROGRAMS CUBIC METER
1.0
4.0
7.0
10.0
13.0
16.0
19.0

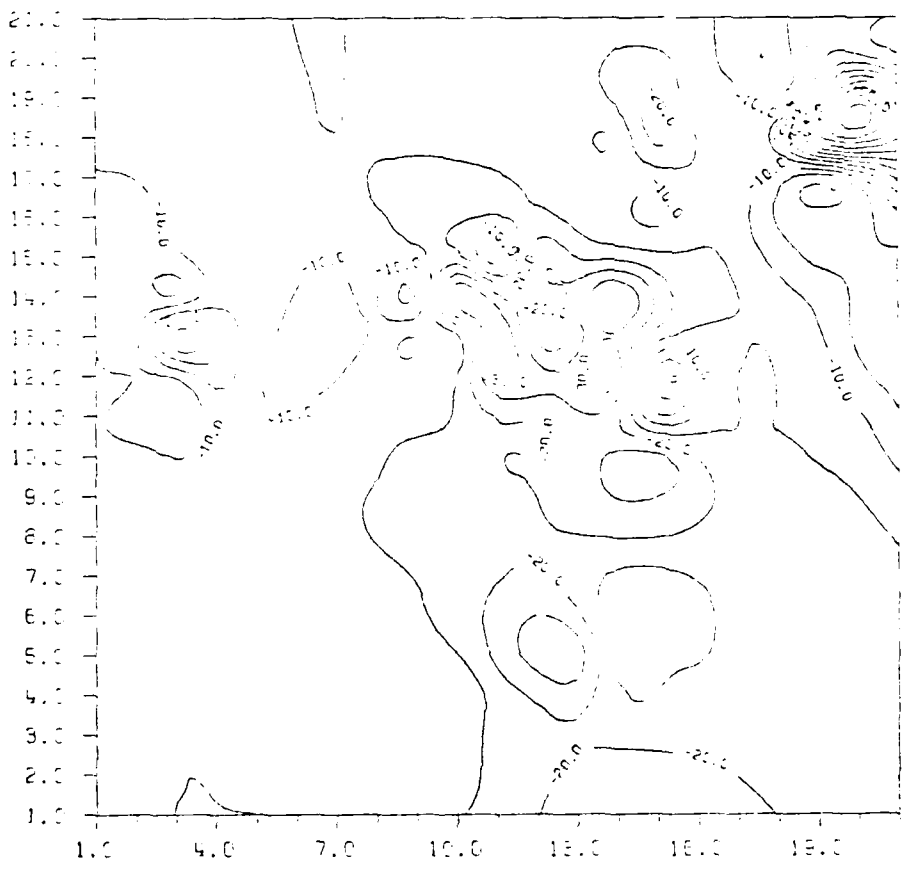

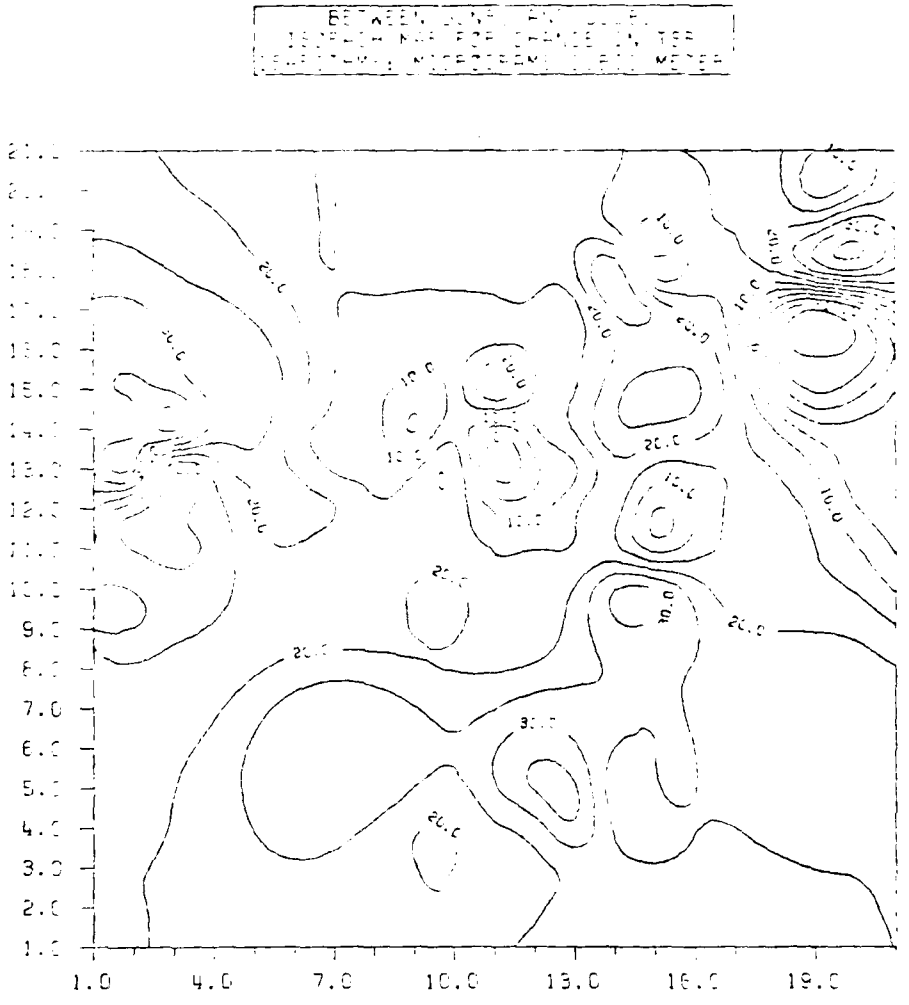
7.0
1.0
4.0
7.0
10.0
13.0
16.0
19.0

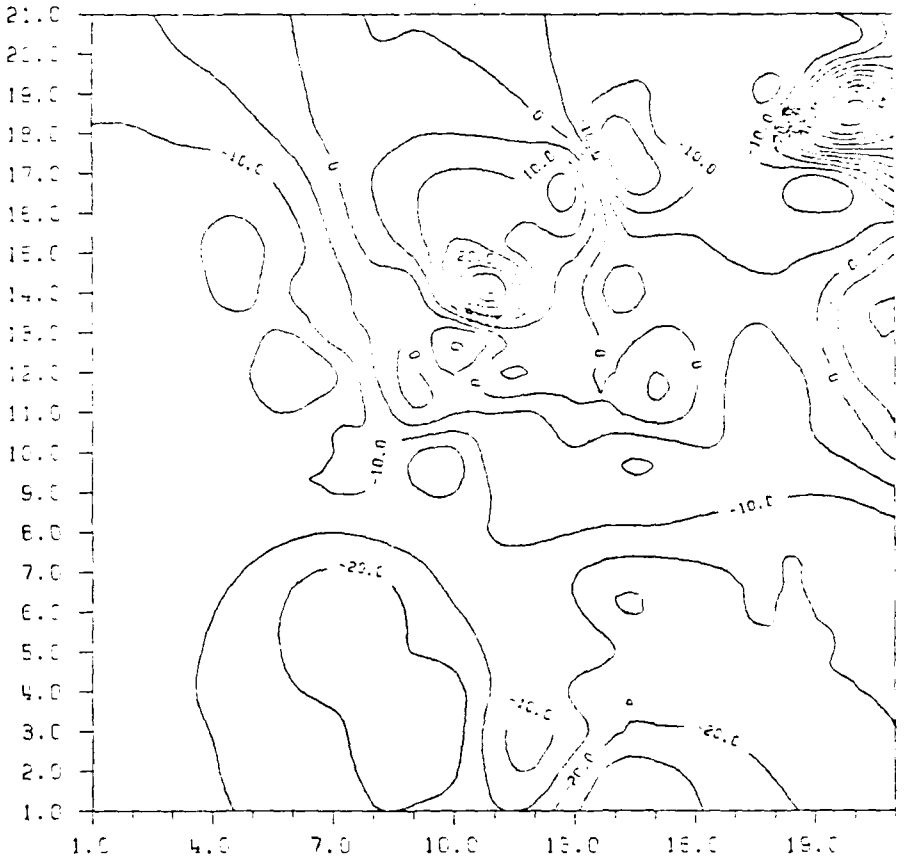
21.0
20.0
19.0
18.0
17.0
16.0
15.0
14.0
13.0
12.0
11.0
10.0
9.0
8.0
7.0
6.0
5.0
4.0
3.0
2.0
1.0
1.0
4.0
7.0
10.0
13.0
16.0
19.0
-10.0
0
-10.0
-10.0
-10.0
-20.0
-20.0
-20.0

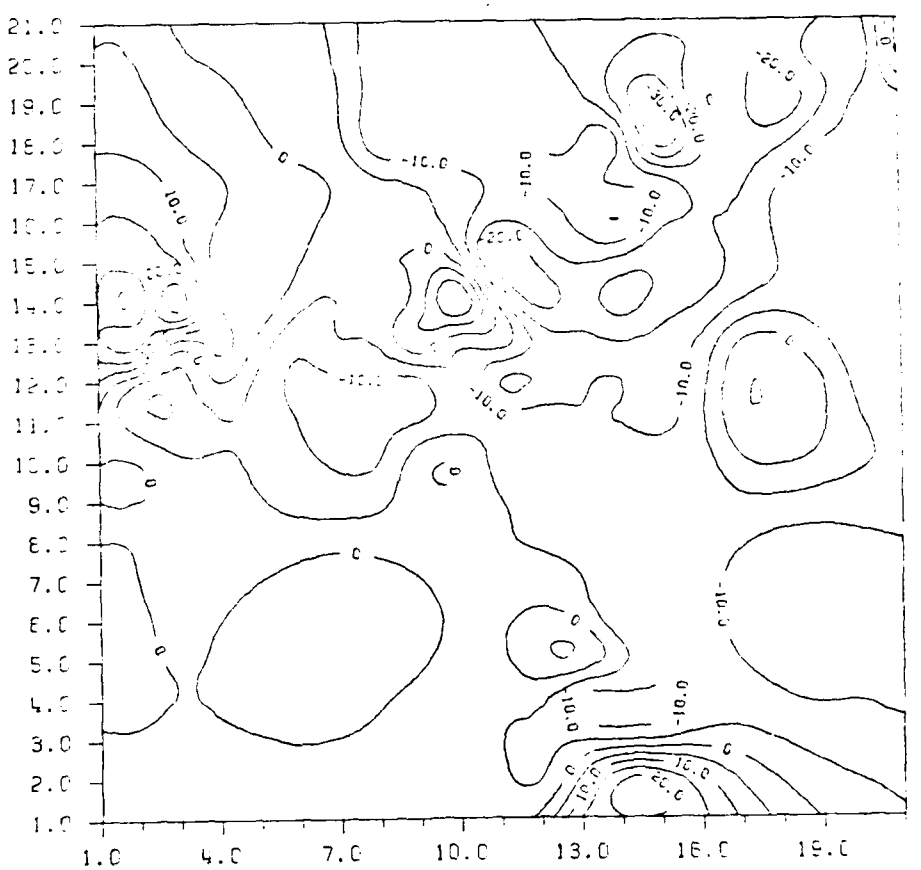
21.0
20.0
19.0
18.0
17.0
16.0
15.0
14.0
13.0
12.0
11.0
10.0
9.0
8.0
7.0
6.0
5.0
4.0
3.0
2.0
1.0
1.0
4.0
7.0
10.0
13.0
16.0
19.0
0
-10.0
10.0
-20.0

BETWEEN SEPT PM OCT
ISOPLETH MAP FOR CHANGE IN TSP
(SCATTERED MICROGRAMS PER METER

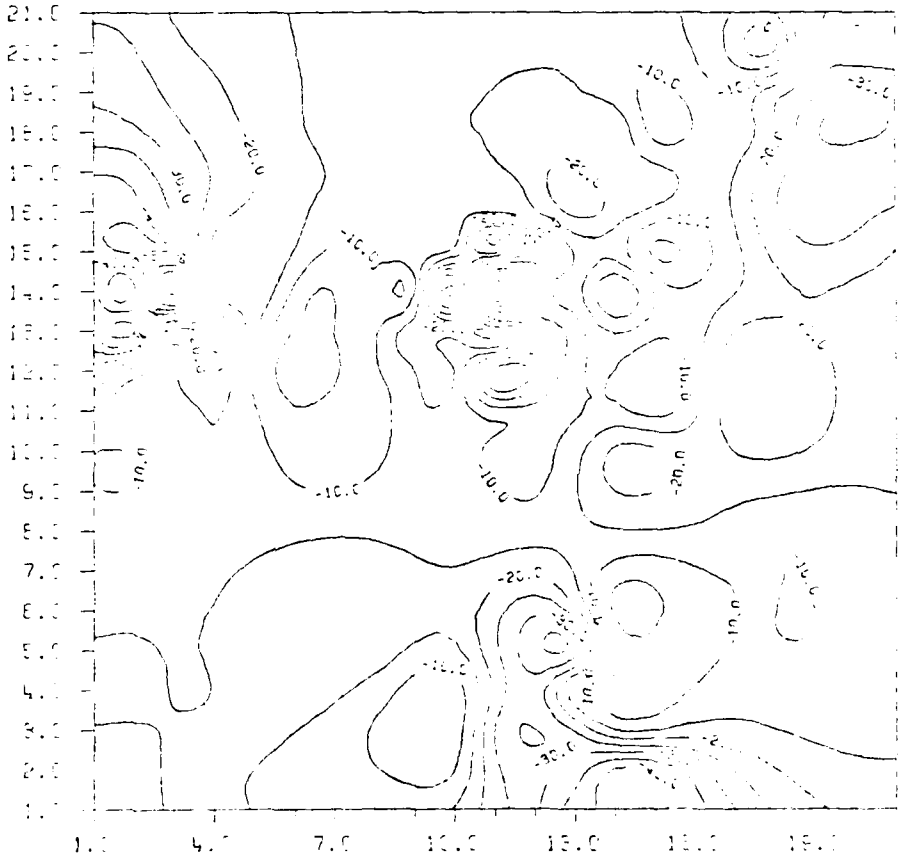

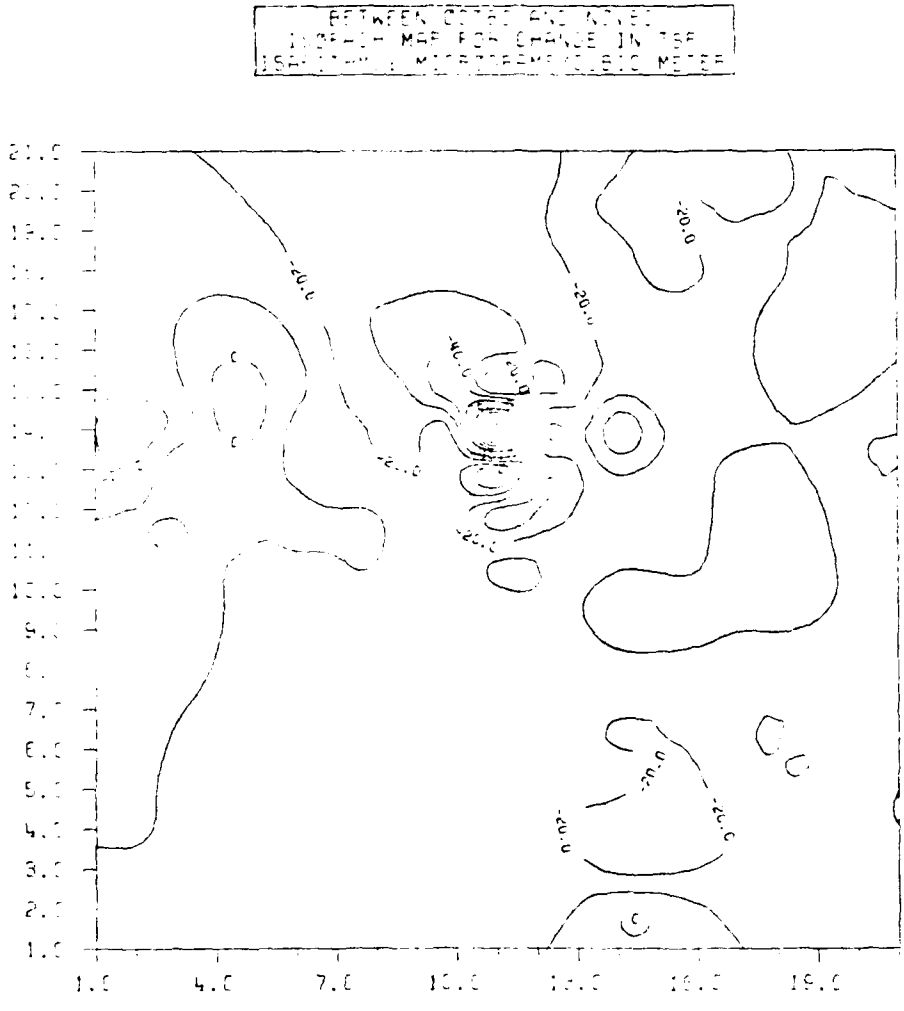
-20.0
-20.0
-20.0
-20.0
-20.0
-20.0
1.0
4.0
7.0
10.0
13.0
16.0
19.0

BETWEEN NOSEC PAT DECRE
ISOPLETH MAP FOR CHANGE IN TSP
ISOPLETHS: MICROGRAMS/CUBIC METER

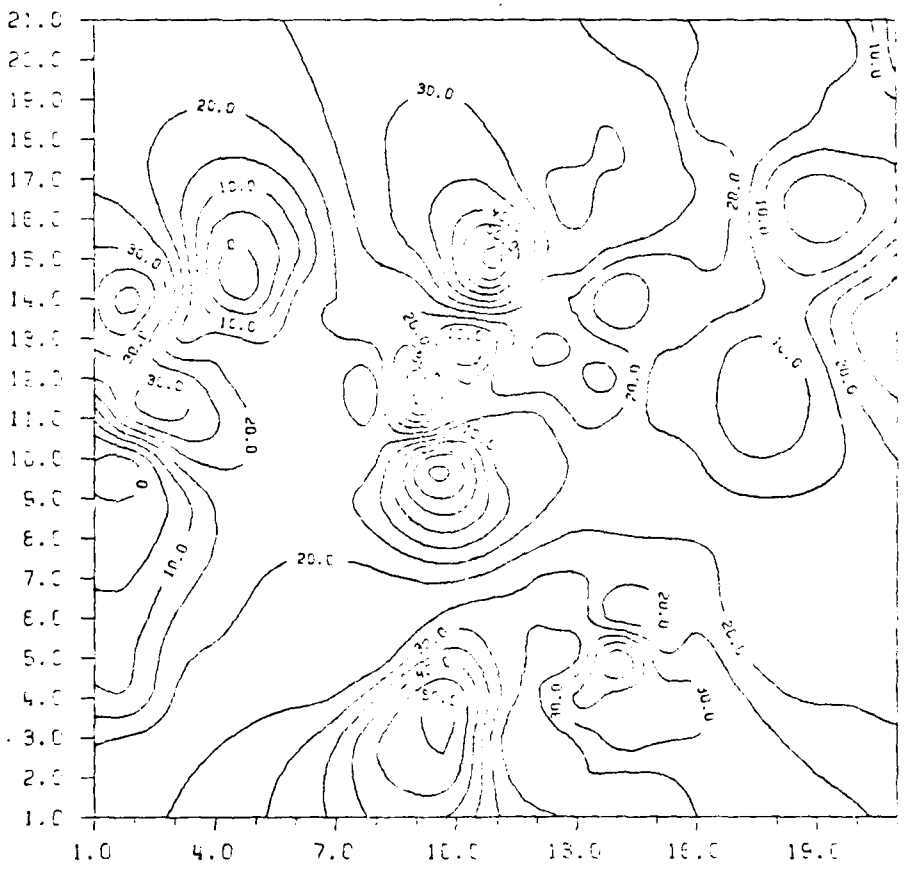

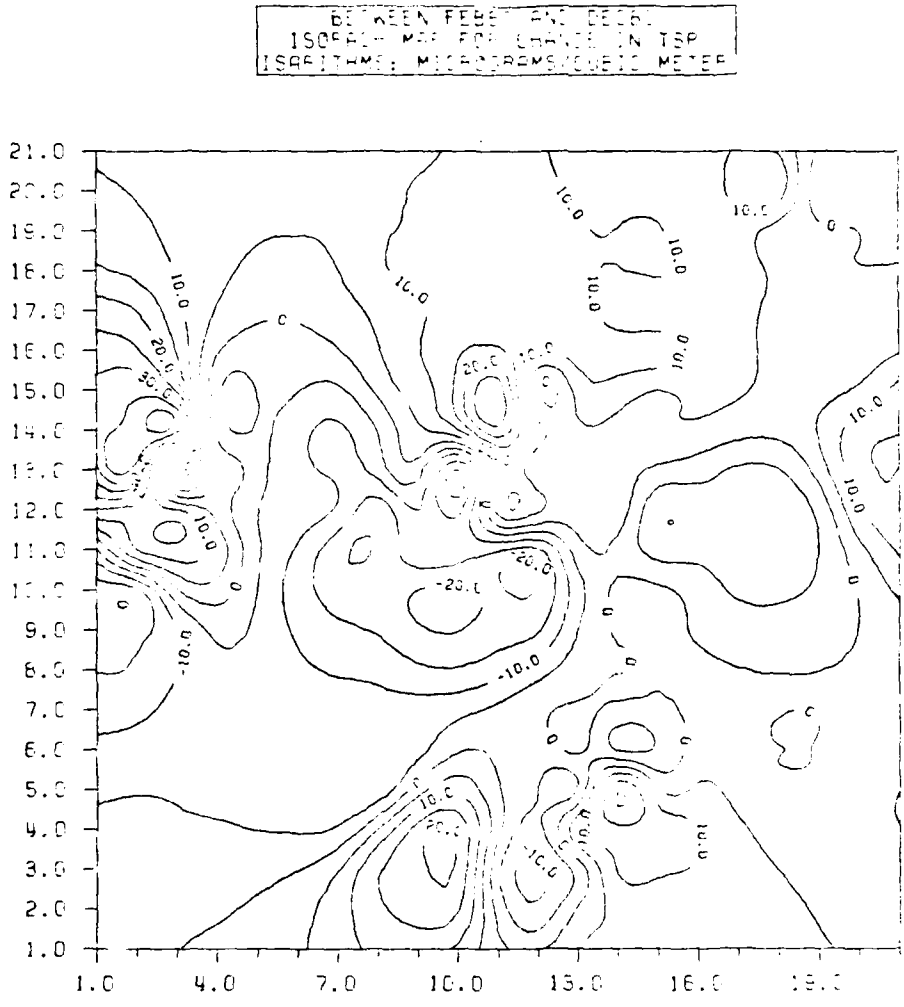
BETWEEN FEBR AND DECBR
ISOPLETH MAP FOR CHANGE IN TSP
ISOPLETHS: MICROGRAMS/CUBIC METER
21.0
20.0
19.0
18.0
17.0
16.0
15.0
14.0
13.0
12.0
11.0
10.0
9.0
8.0
7.0
6.0
5.0
4.0
3.0
2.0
1.0
1.0
4.0
7.0
10.0
13.0
16.0
19.0
10.0
-10.0
0
-20.0

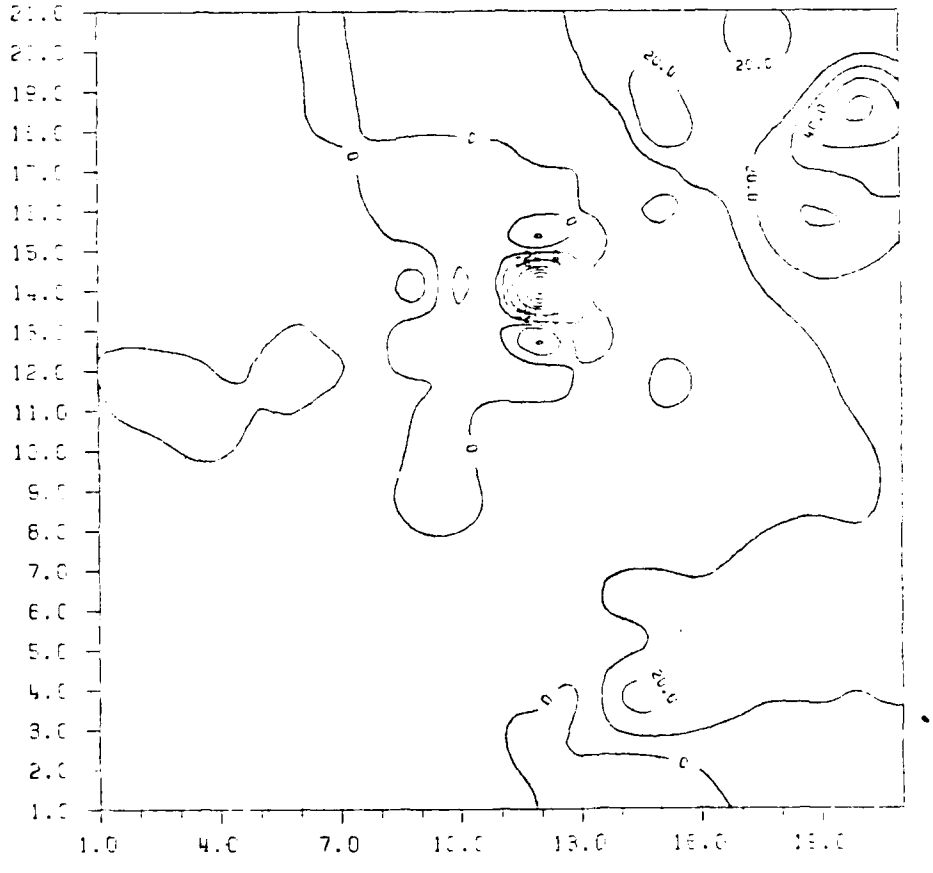
1.0
4.0
7.0
10.0
13.0
16.0
19.0
20.0
0

BETWEEN FEB80 AND JUN80
ISOPLETH MAP FOR CHANGE IN TEF
ISOBITHMS: MICROGRAMS/CUBIC METER

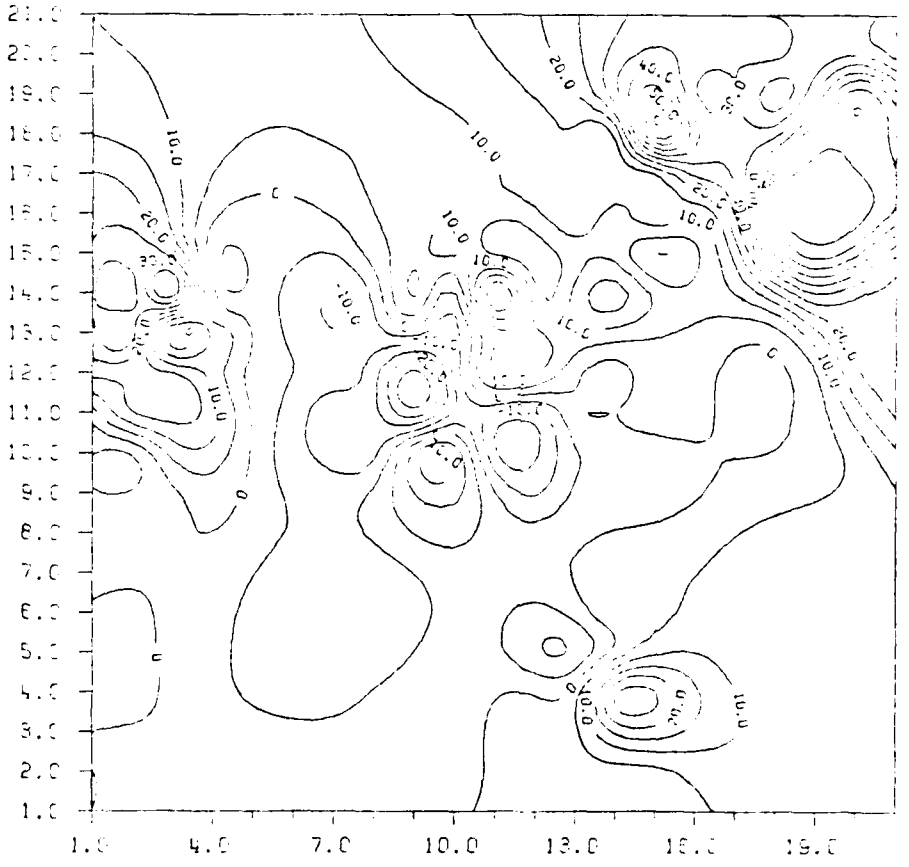

Appendix C

TREND SURFACE PARAMETER CORRELATION RESULTS

The parameters of different size polynomial were used for comparison of the TSP map. A cubic (9 term), bi-cubic(16 term), and bi-quartic (25 term) polynomial were each used as mathematical models for the trend surface method. The results of fitting a cubic and bi-cubic polynomial to the TSP maps and the calculation of the correlation between the parametrs of each of the 12 TSP maps are in this appendix. The result of each comparison is a 12x12 symmetric array with correlation between each possible pairing of the TSP monthly pollution maps. The result of the bi-quartic polynomial are in figure 14. The third table in this appendix is the correlation between the autocorrelation maps that were formed from the twelve TSP maps. The bi-quartic polynomial was used to compare the spatial autocorrelation maps.

	JAN	FEB	MAR	APR	MAY	JUN	JUL	AUG	SEP	OCT	NOV	DEC
JAN	1.00											
FEB	-0.04	1.00										
MAR	0.23	0.38	1.00									
APR	-0.73	-0.15	-0.10	1.00								
MAY	-0.65	-0.41	-0.69	0.47	1.00							
JUN	-0.86	-0.50	-0.63	0.44	0.83	1.00						
JUL	-0.22	-0.29	-0.41	-0.15	0.49	0.14	1.00					
AUG	-0.48	-0.52	-0.84	0.48	0.37	0.46	-0.10	1.00				
SEP	0.41	-0.85	-0.10	-0.21	0.08	0.09	0.28	0.10	1.00			
OCT	-0.28	0.44	-0.00	0.21	-0.45	-0.00	-0.55	0.42	-0.61	1.00		
NOV	0.48	0.87	-0.58	-0.67	-0.26	-0.01	-0.14	-0.15	-0.30	0.28	1.00	
DEC	-0.81	-0.68	0.72	0.28	-0.31	-0.67	0.05	-0.20	0.14	-0.14	-0.79	1.00

Correlation of TSP maps using the cubic polynomial model

	JAN	FEB	MAR	APR	MAY	JUN	JUL	AUG	SEP	OCT	NOV	DEC
JAN	1.00											
FEB	-0.21	1.00										
MAR	0.42	0.06	1.00									
APR	-0.78	0.17	-0.26	1.00								
MAY	-0.65	-0.16	-0.47	0.36	1.00							
JUN	-0.85	-0.28	-0.40	0.14	0.71	1.00						
JUL	-0.09	-0.46	-0.15	-0.25	0.25	0.54	1.00					
AUG	-0.52	-0.49	-0.50	0.22	0.09	0.12	0.05	1.00				
SEP	0.14	-0.60	-0.16	0.05	-0.05	-0.16	0.21	0.14	1.00			
OCT	-0.06	0.57	-0.05	0.04	-0.55	-0.47	-0.64	0.23	-0.43	1.00		
NOV	0.24	0.51	-0.38	-0.17	-0.11	-0.28	-0.49	-0.22	-0.28	0.52	1.00	
DEC	0.29	-0.14	0.77	-0.18	-0.44	-0.44	-0.08	-0.00	0.07	0.06	-0.53	1.00

Correlation of TSP maps with bi-cubic polynomial model

	JAN	FEB	MAR	APR	MAY	JUN	JUL	AUG	SEP	OCT	NOV	DEC
JAN	1.00											
FEB	-0.29	1.00										
MAR	-0.56	0.34	1.00									
APR	-0.86	0.29	0.76	1.00								
MAY	0.28	-0.37	-0.37	-0.28	1.00							
JUN	0.12	-0.34	-0.51	-0.21	0.95	1.00						
JUL	0.44	-0.52	-0.87	-0.69	0.61	0.56	1.00					
AUG	-0.33	-0.13	0.09	0.17	-0.28	-0.05	-0.14	1.00				
SEP	0.48	-0.33	-0.82	-0.65	0.42	0.31	0.79	-0.17	1.00			
OCT	0.34	-0.19	-0.20	-0.32	-0.48	-0.52	0.12	0.29	0.16	1.00		
NOV	-0.07	-0.01	0.17	-0.04	-0.67	-0.70	-0.18	0.01	-0.07	0.41	1.00	
DEC	-0.53	0.88	0.92	0.68	-0.80	-0.76	-0.83	0.17	-0.69	0.02	0.43	1.00

Correlation of Autocorrelation maps using a bi-quartic polynomial

Appendix D

AUTOCORRELATION MAPS

This appendix contains the autocorrelation maps for the twelve monthly TSP surfaces. For each monthly TSP map there is one isarithmic map and one surface representaion. On the isarithmic maps the symmetry of the autocorrelation is readily apperant. The N/W quadrant is symmetric with respect to the S/E quadrant. These maps are produced on a 41 x 41 grid. The small triangles are grid intersections where data values were predicted.

TWO-DIMENSIONAL AUTOCORRELATION FUNCTION
FOR: JAN80 TSP GRIDDED DATA **********
ISARITHMS IN CORRELATION UNITS * 41X41 *

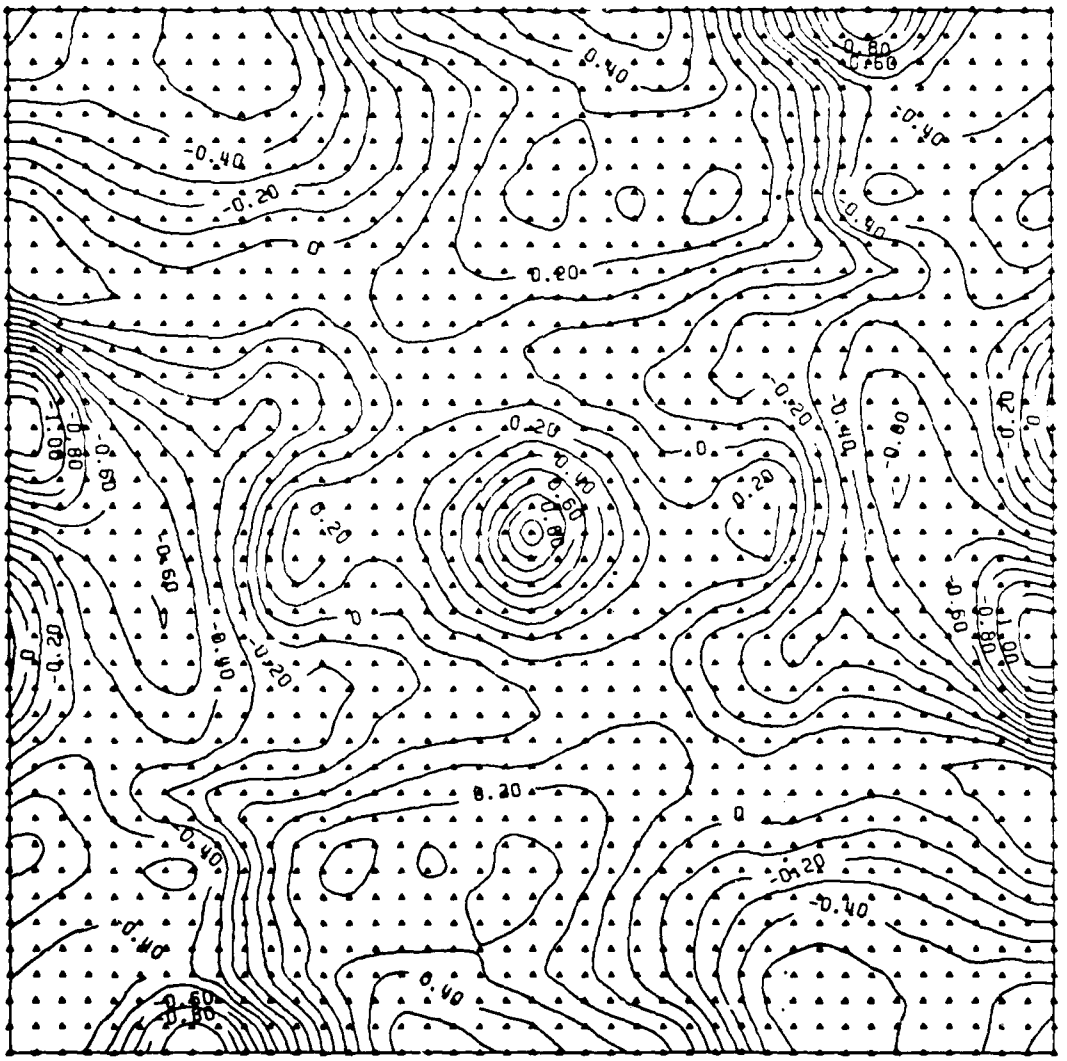

TWO-DIMENSIONAL AUTOCORRELATION FUNCTION
FOR: JAN80 TSP GRIDDED DATA **********
SURFACE REPRESENTATION USING 41X41 GRID

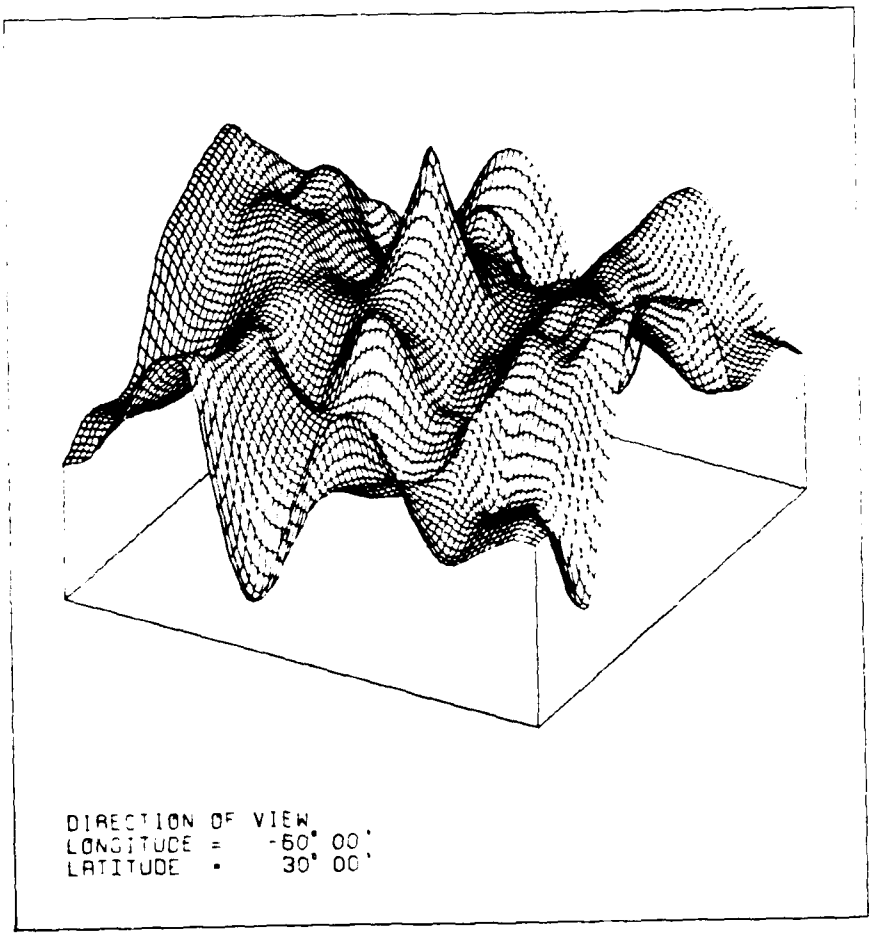

TWO-DIMENSIONAL AUTOCORRELATION FUNCTION
FOR: FEBBO TSP GRIDDED DATA ▪▪▪▪▪▪▪▪▪▪▪▪
ISARITHMS IN CORRELATION UNITS ▪ 41X41 ▪

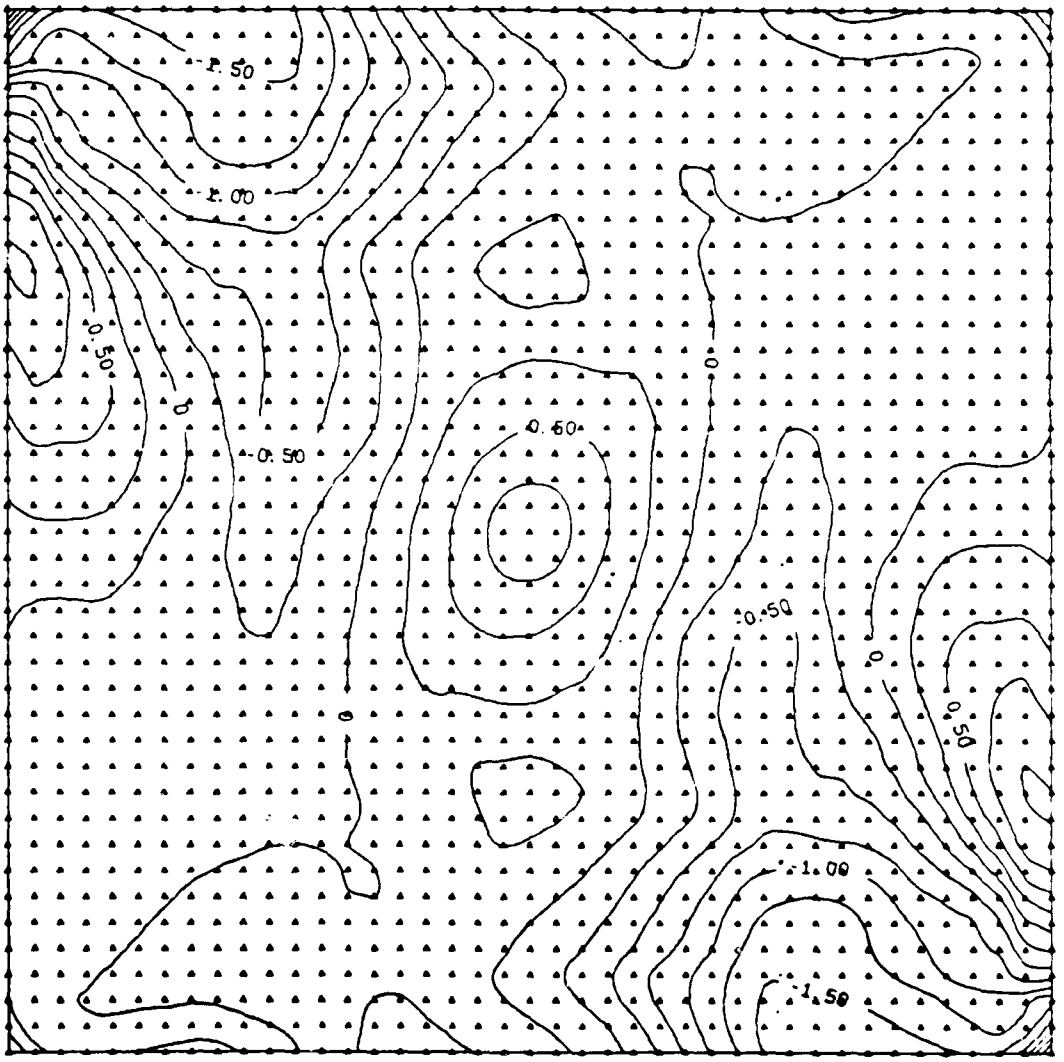

TWO-DIMENSIONAL AUTOCORRELATION FUNCTION
FOR FEB80 TSP GRIDDED DATA .....
SURFACE REPRESENTATION USING 41X41 GRID

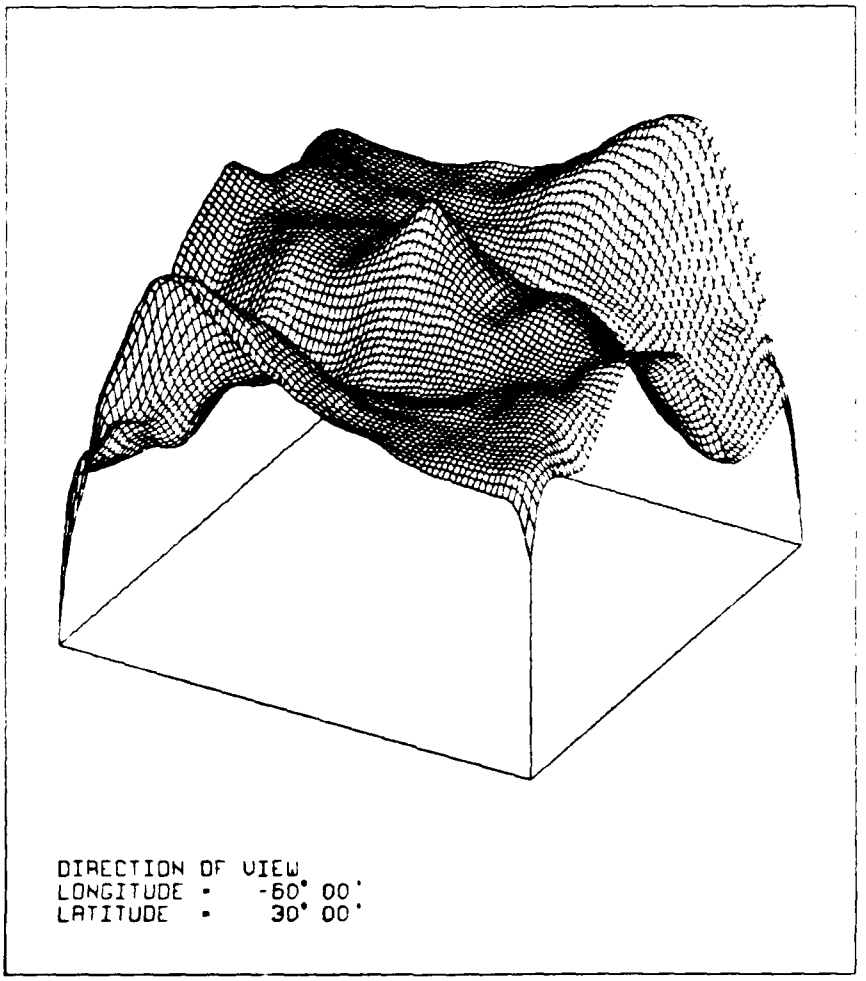

TWO-DIMENSIONAL AUTOCORRELATION FUNCTION
FOR MARBO TSP GRIDDED DATA
ISARITHMS IN CORRELATION UNITS * 41X41 *

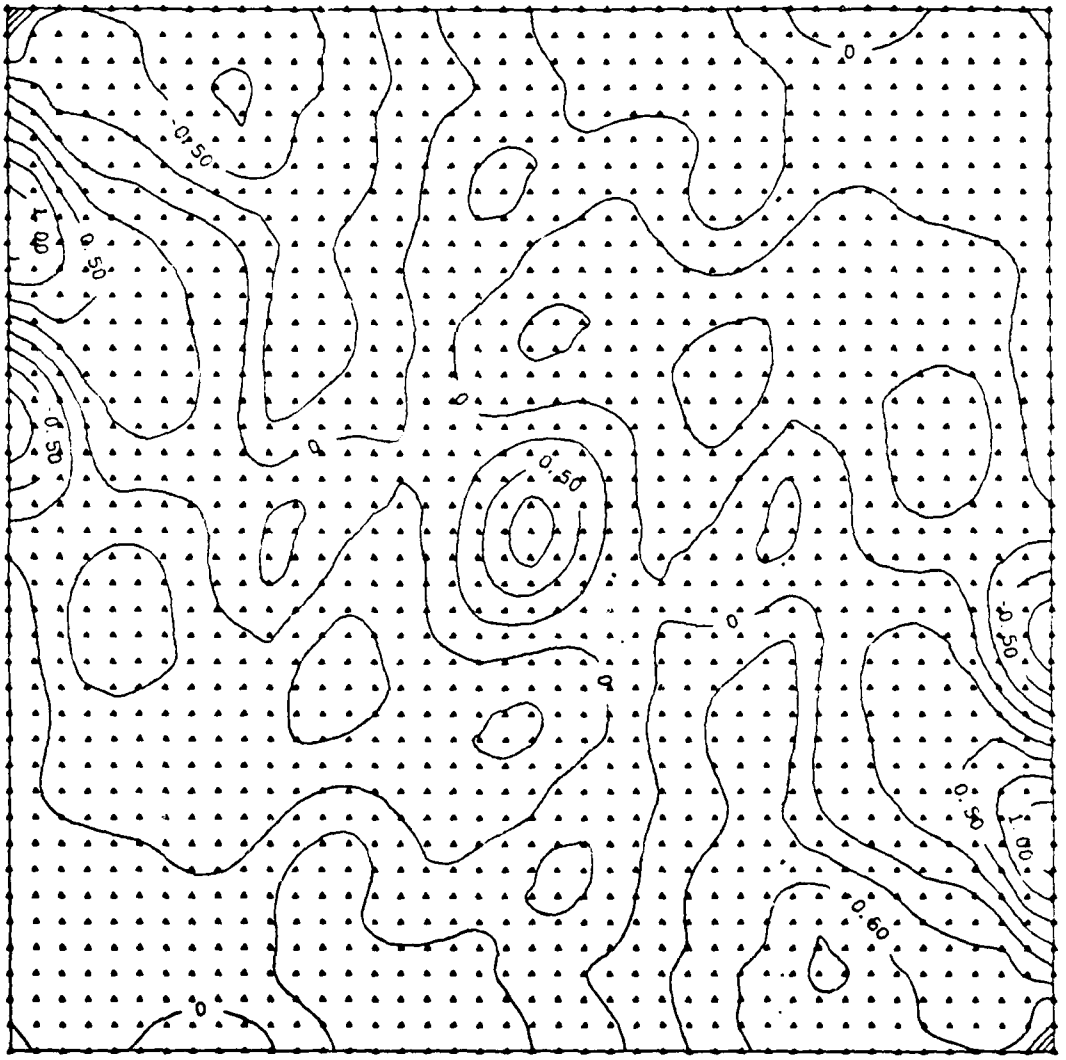

TWO-DIMENSIONAL AUTOCORRELATION FUNCTION
FOR MAR80 TSP GRIDDED DATA ••••••••••••
SURFACE REPRESENTATION USING 41X41 GRID

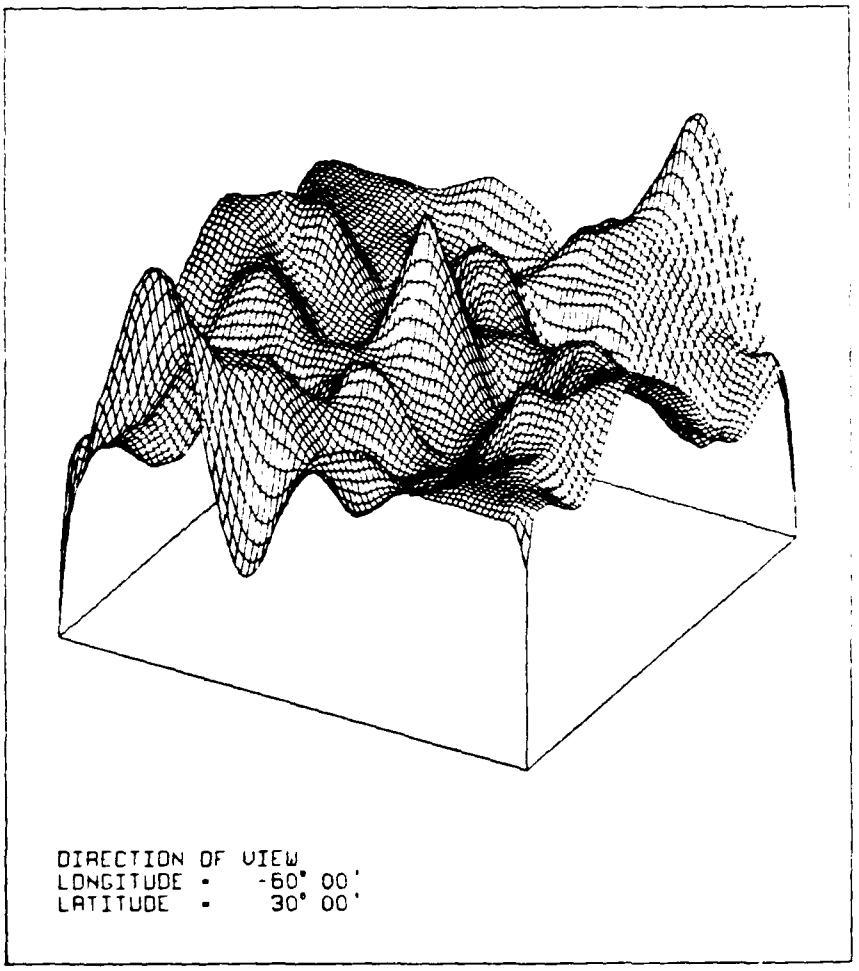

TWO-DIMENSIONAL AUTOCORRELATION FUNCTION
FOR APR80 TSP GRIDDED DATA ••••••••••••
ISORITHMS IN CORRELATION UNITS • 41X41 •

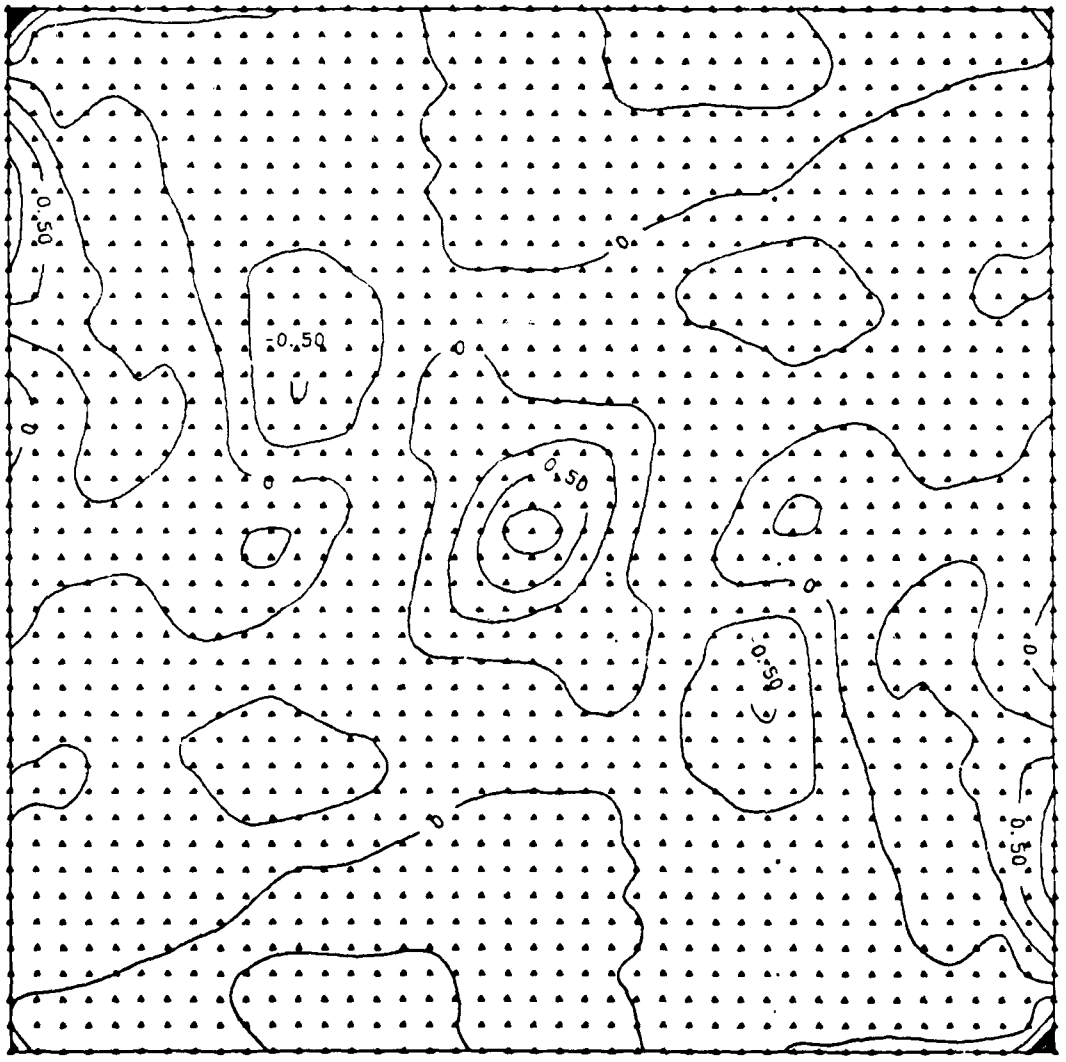

TWO-DIMENSIONAL AUTOCORRELATION FUNCTION
FOR APRBO TSP GRIDDED DATA ••••••••••••
SURFACE REPRESENTATION USING 41X41 GRID

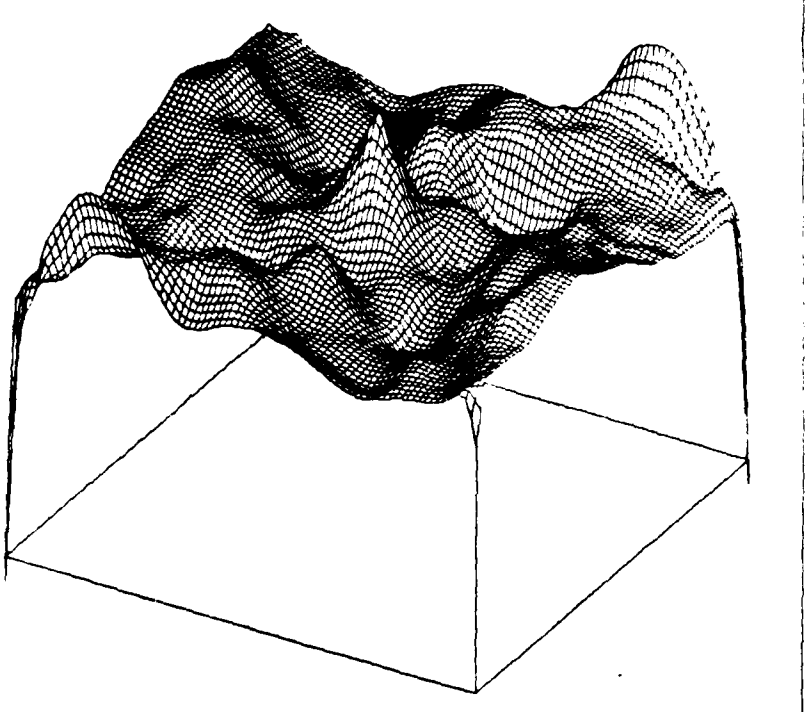

DIRECTION OF VIEW
LONGITUDE - -60° 00'
LATITUDE - 30° 00'

TWO-DIMENSIONAL AUTOCORRELATION FUNCTION
FOR· MAY80 TSP GRIDDED DATA ▪▪▪▪▪▪▪▪▪▪▪▪
ISARITHMS IN CORRELATION UNITS ▪ 41X41 ▪

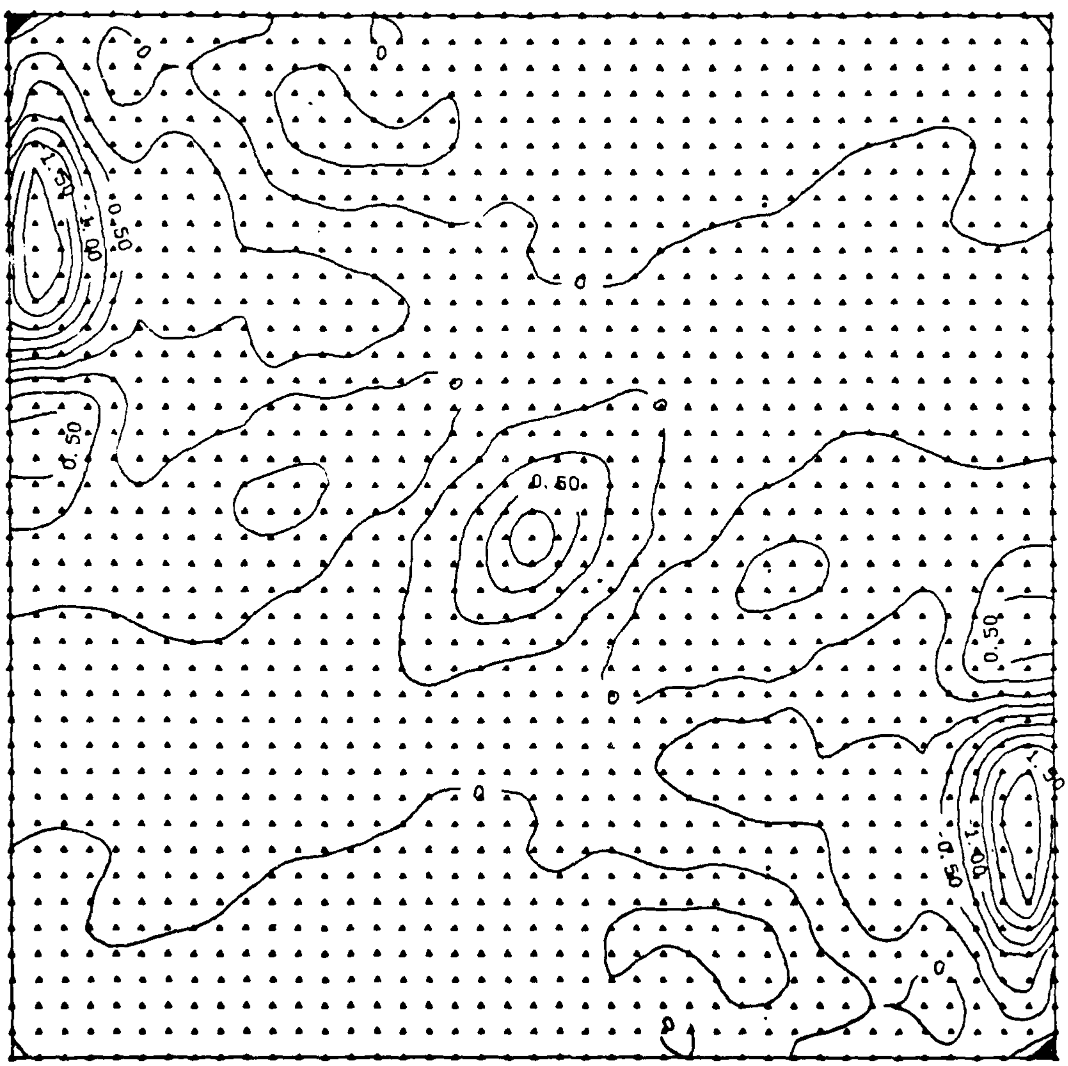

TWO-DIMENSIONAL AUTOCORRELATION FUNCTION
FOR MAY80 TSP GRIDDED DATA ••••••••••••
SURFACE REPRESENTATION USING 41X41 GRID

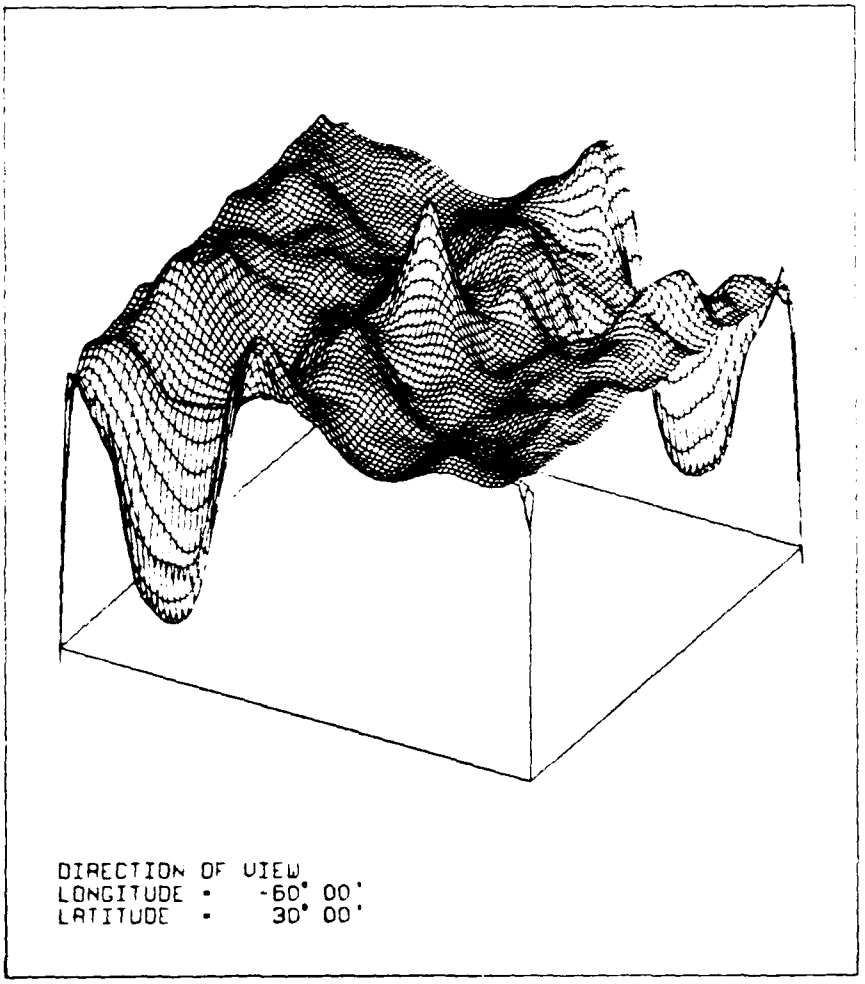

TWO-DIMENSIONAL AUTOCORRELATION FUNCTION
FOR• JUNBO TSP GRIDDED DATA ▪▪▪▪▪▪▪▪▪▪▪▪
ISARITHMS IN CORRELATION UNITS ▪ 41X41 ▪

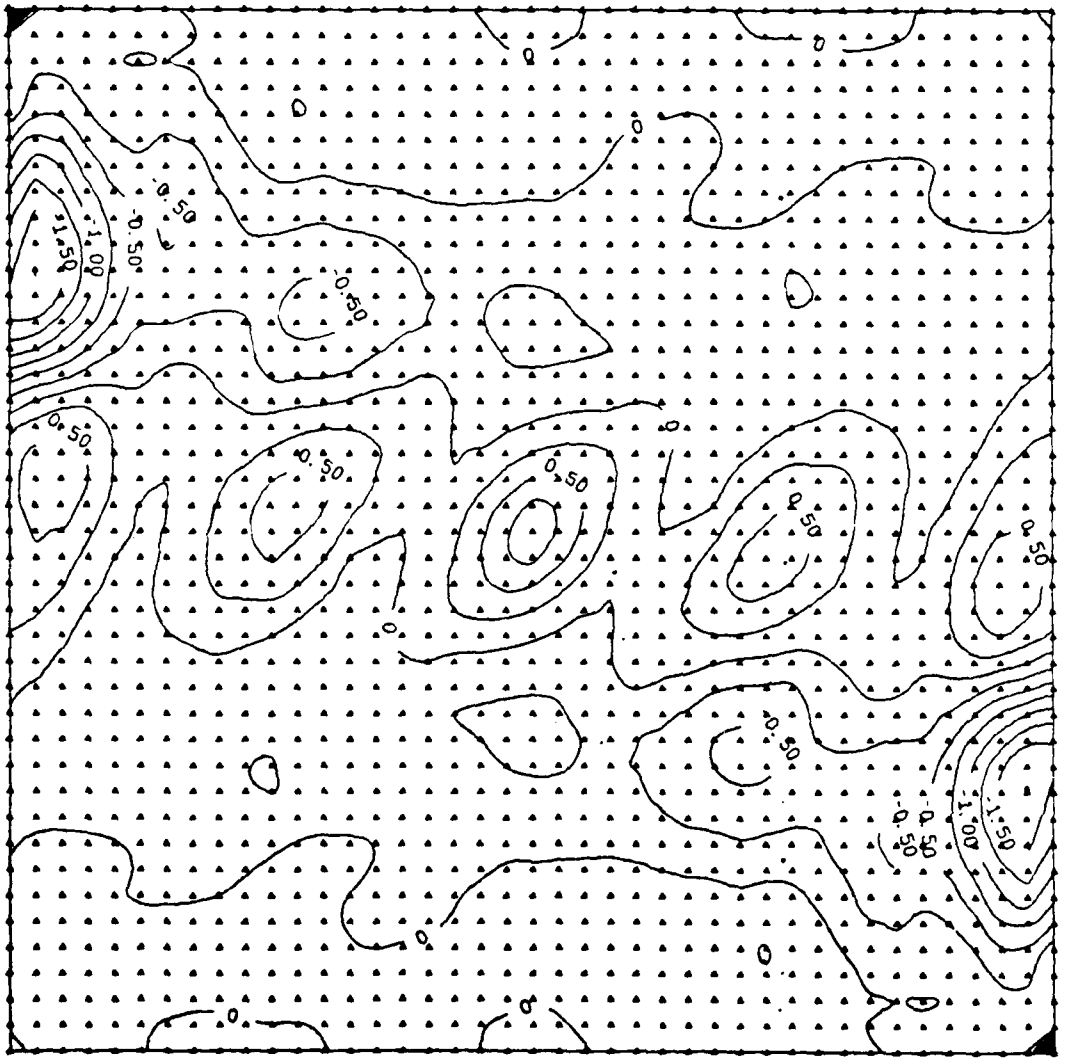

TWO-DIMENSIONAL AUTOCORRELATION FUNCTION
FOR: JUNBO TSP GRIDDED DATA ••••••••••••
SURFACE REPRESENTATION USING 41X41 GRID

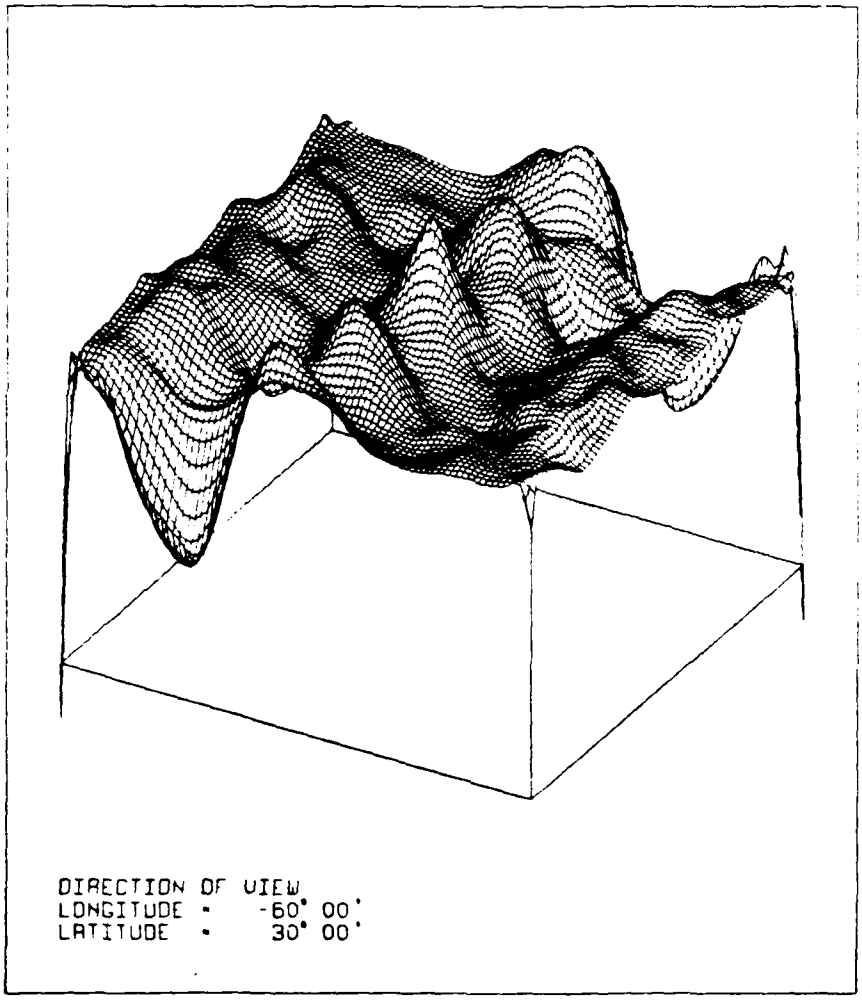

TWO-DIMENSIONAL AUTOCORRELATION FUNCTION
FOR: JUL80 TSP GRIDDED DATA ************
ISARITHMS IN CORRELATION UNITS * 41X41 *

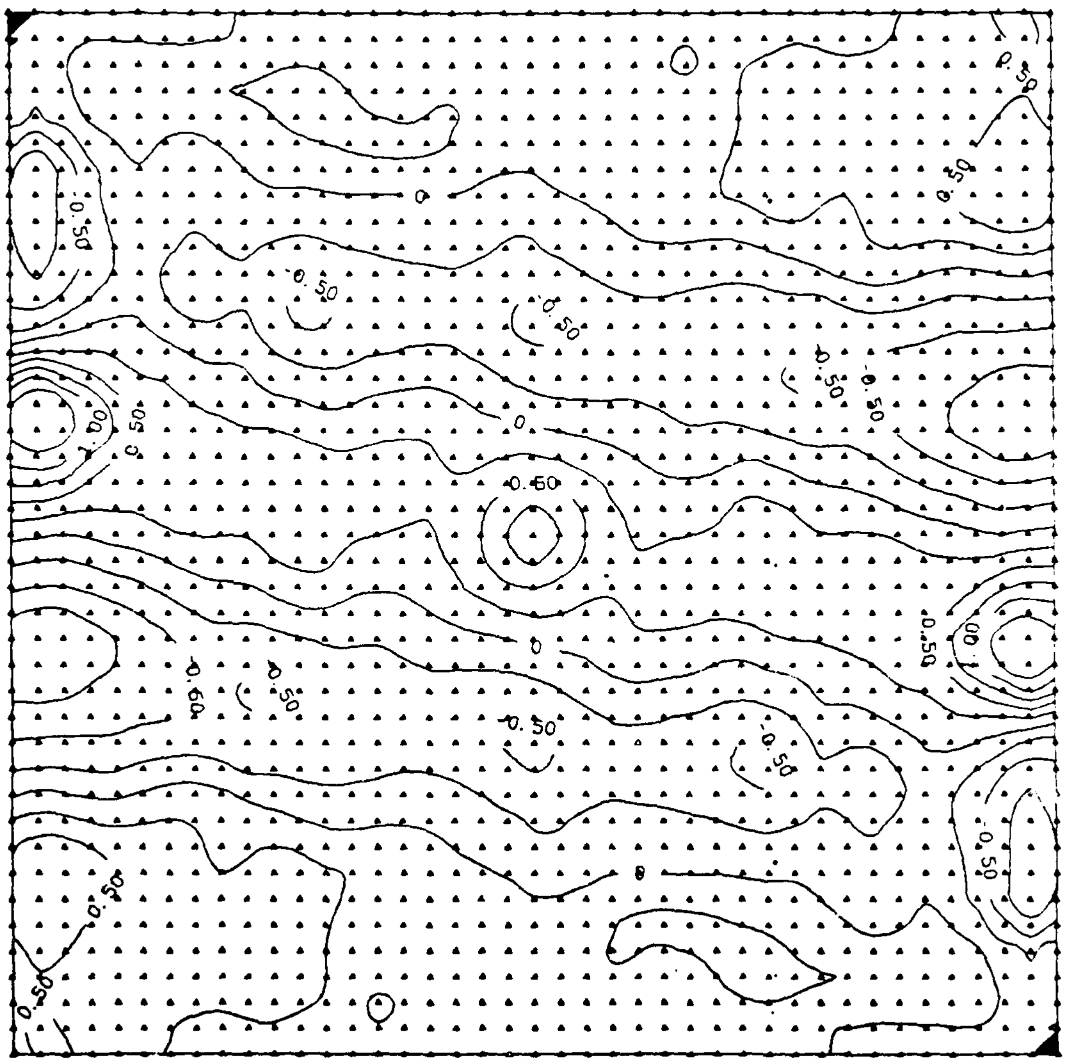

TWO-DIMENSIONAL AUTOCORRELATION FUNCTION
FOR: JUL80 TSP GRIDDED DATA ••••••••••••
SURFACE REPRESENTATION USING 41X41 GRID

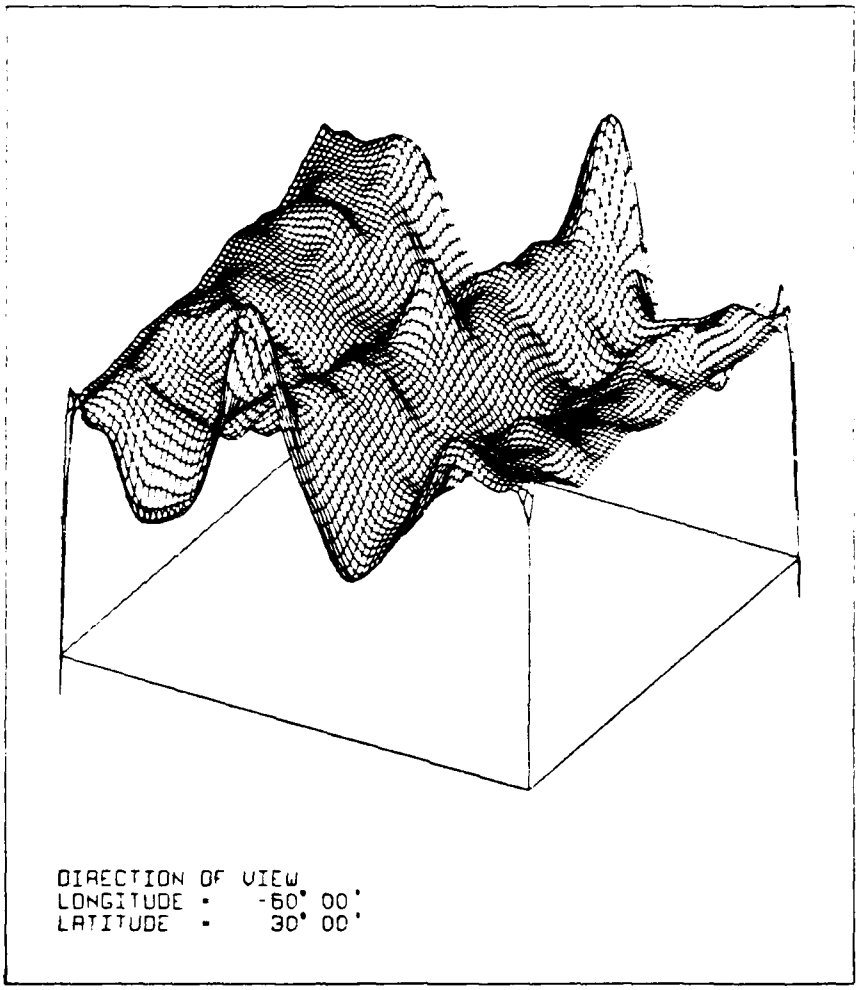

TWO-DIMENSIONAL AUTOCORRELATION FUNCTION
FOR AUG80 TSP GRIDDED DATA ••••••••••••
ISARITHMS IN CORRELATION UNITS • 41X41 •

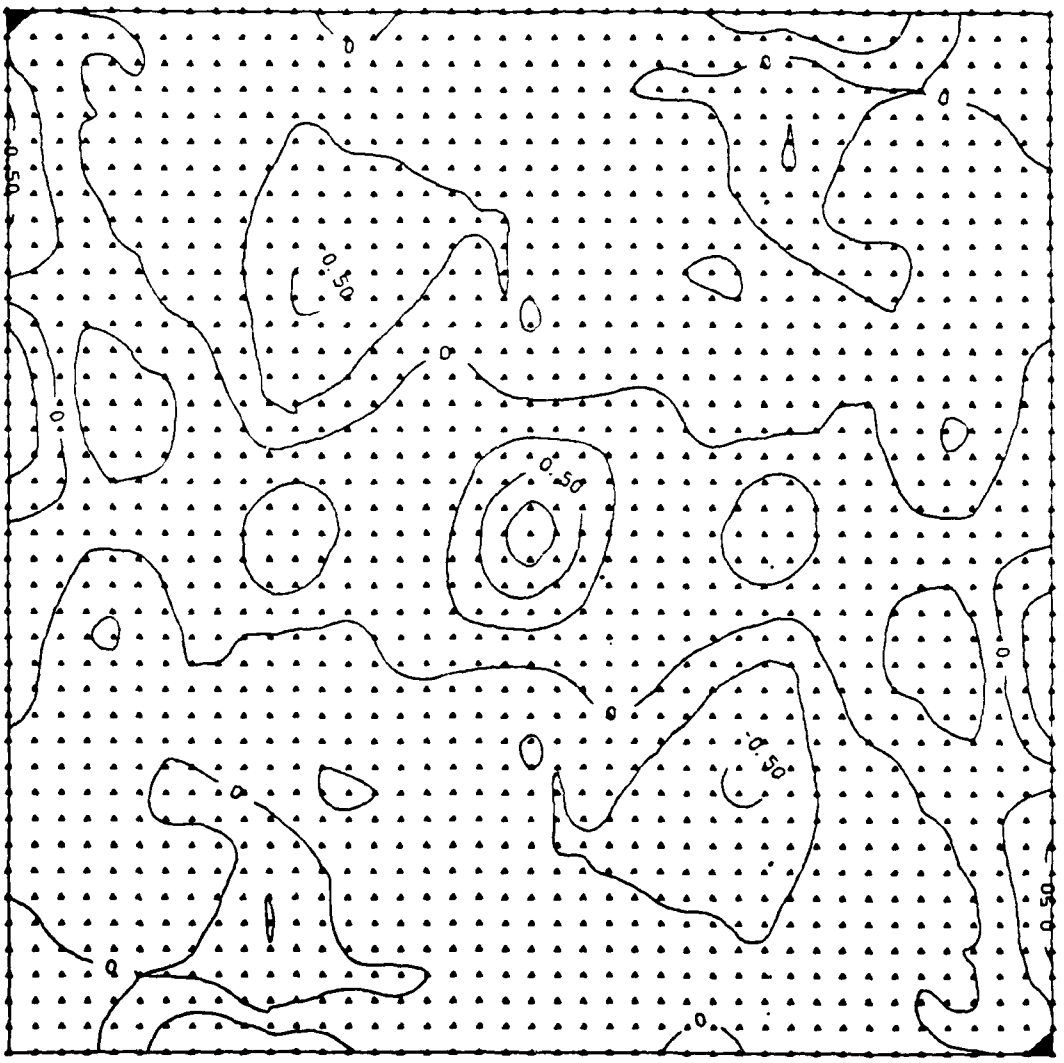

TWO-DIMENSIONAL AUTOCORRELATION FUNCTION
FOR: AUG80 TSP GRIDDED DATA ••••••••••••
SURFACE REPRESENTATION USING 41×41 GRID

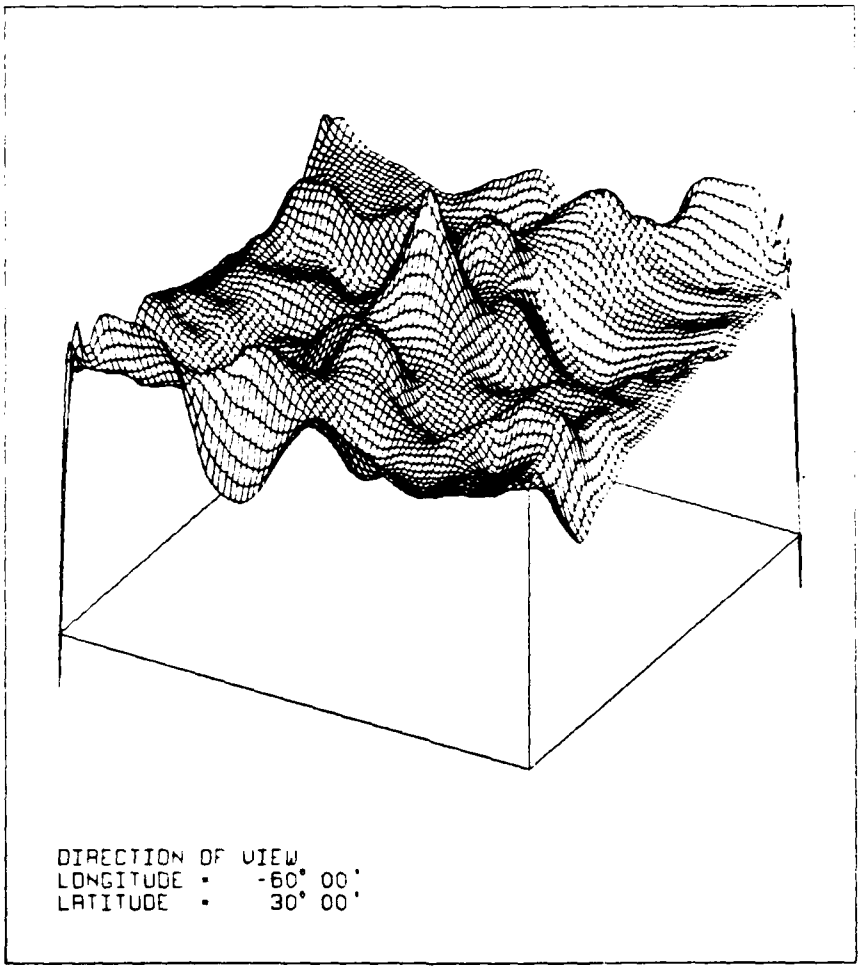

TWO-DIMENSIONAL AUTOCORRELATION FUNCTION
FOR: SEP80 TSP GRIDDED DATA ▪▪▪▪▪▪▪▪▪▪▪▪
ISARITHMS IN CORRELATION UNITS ▪ 41X41 ▪

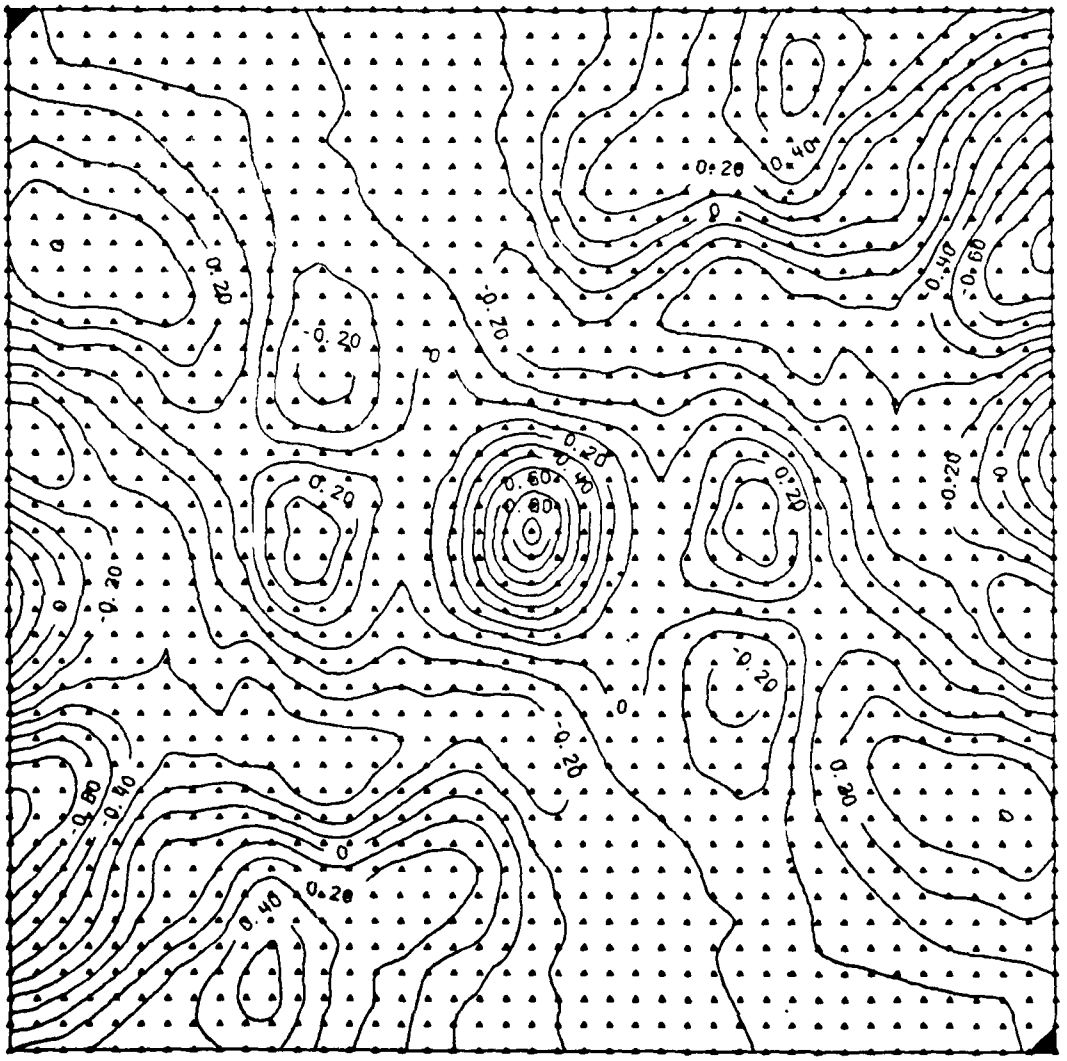

TWO-DIMENSIONAL AUTOCORRELATION FUNCTION
FOR SEPBO TSP GRIDDED DATA ....
SURFACE REPRESENTATION USING 41X41 GRID

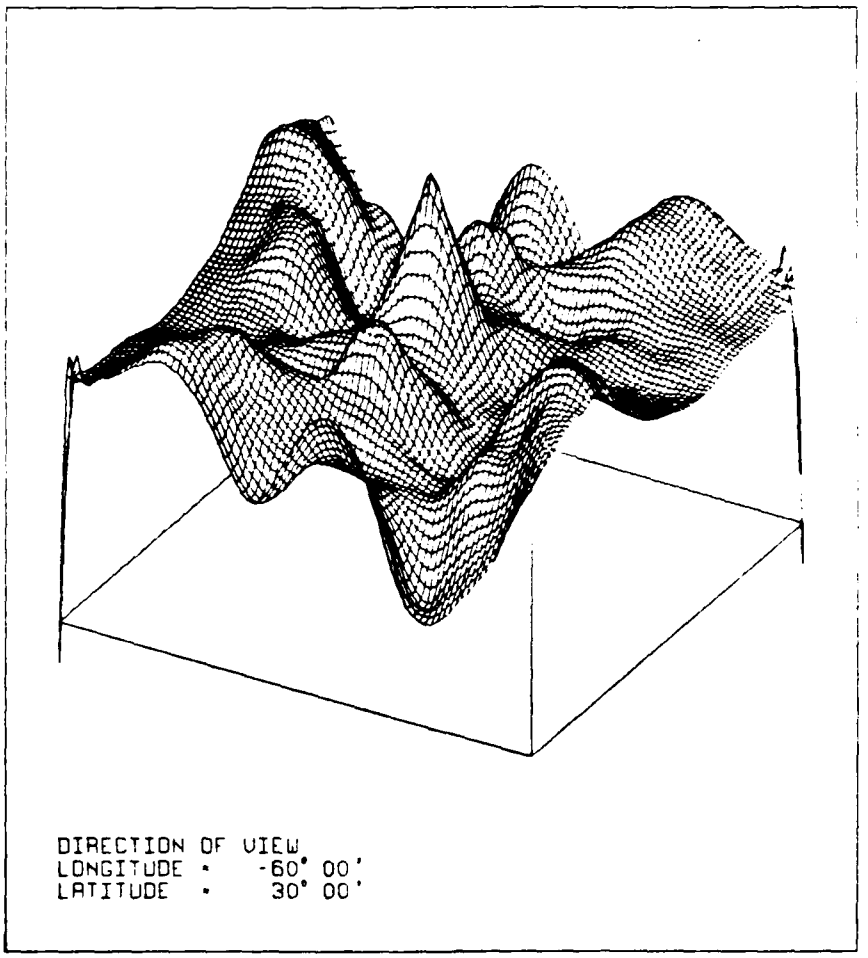

TWO-DIMENSIONAL AUTOCORRELATION FUNCTION
FOR OCT80 TSP GRIDDED DATA
ISARITHMS IN CORRELATION UNITS • 41X41 •

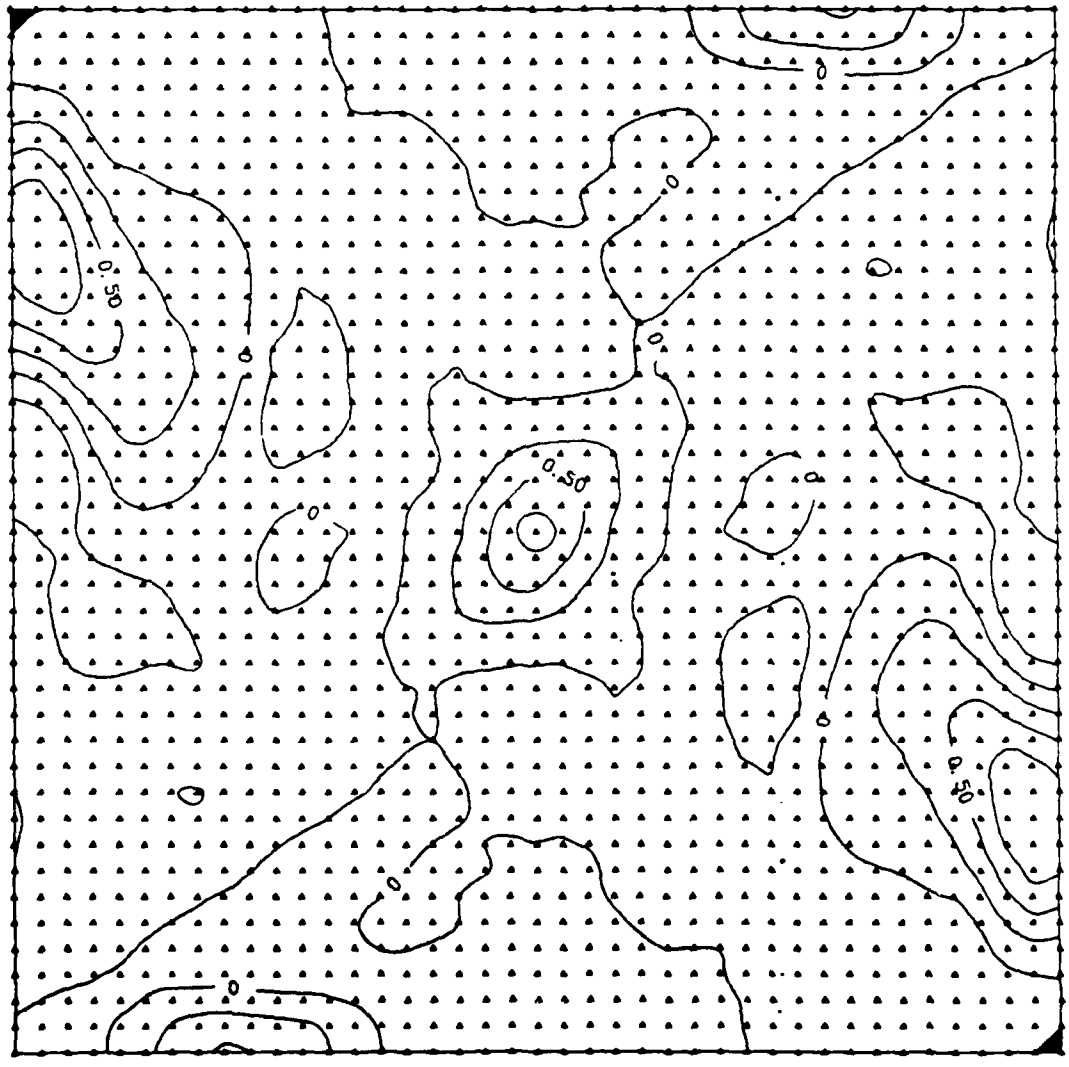

TWO-DIMENSIONAL AUTOCORRELATION FUNCTION
FOR: OCT80 TSP GRIDDED DATA ••••••••••••
SURFACE REPRESENTATION USING 41X41 GRID

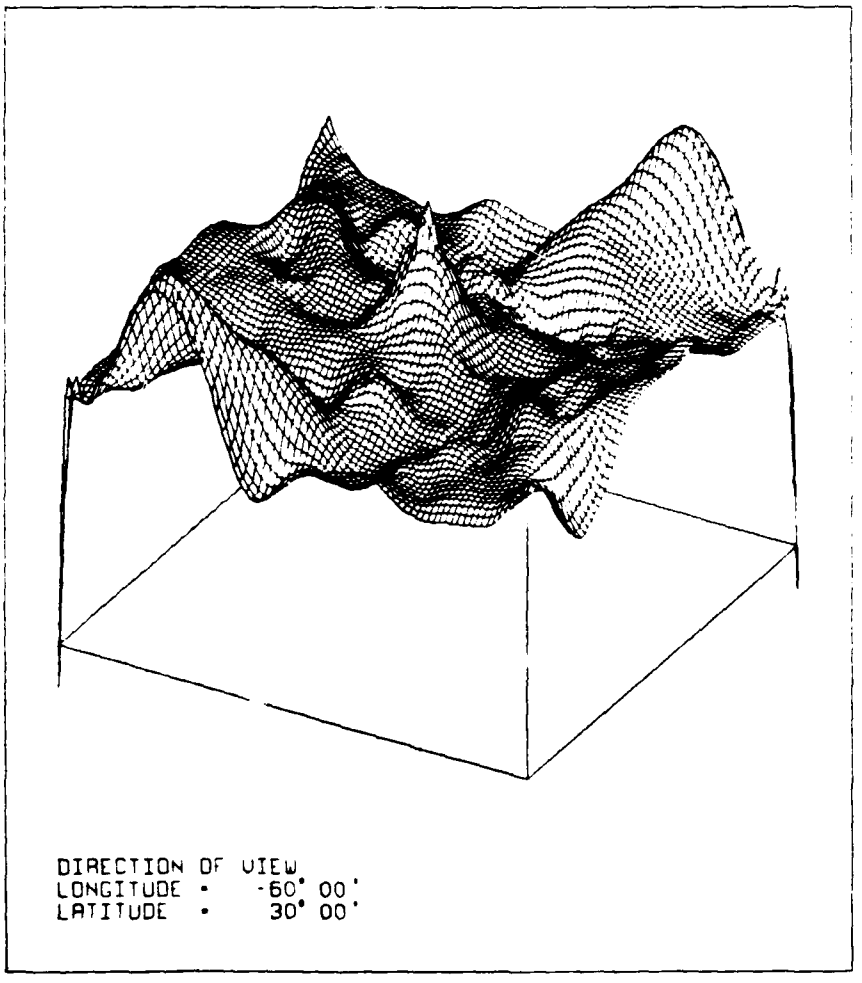

TWO-DIMENSIONAL AUTOCORRELATION FUNCTION
FOR NOVBO TSP GRIDDED DATA ▪▪▪▪▪▪▪▪▪▪▪▪
ISARITHMS IN CORRELATION UNITS ▪ 41X41 ▪

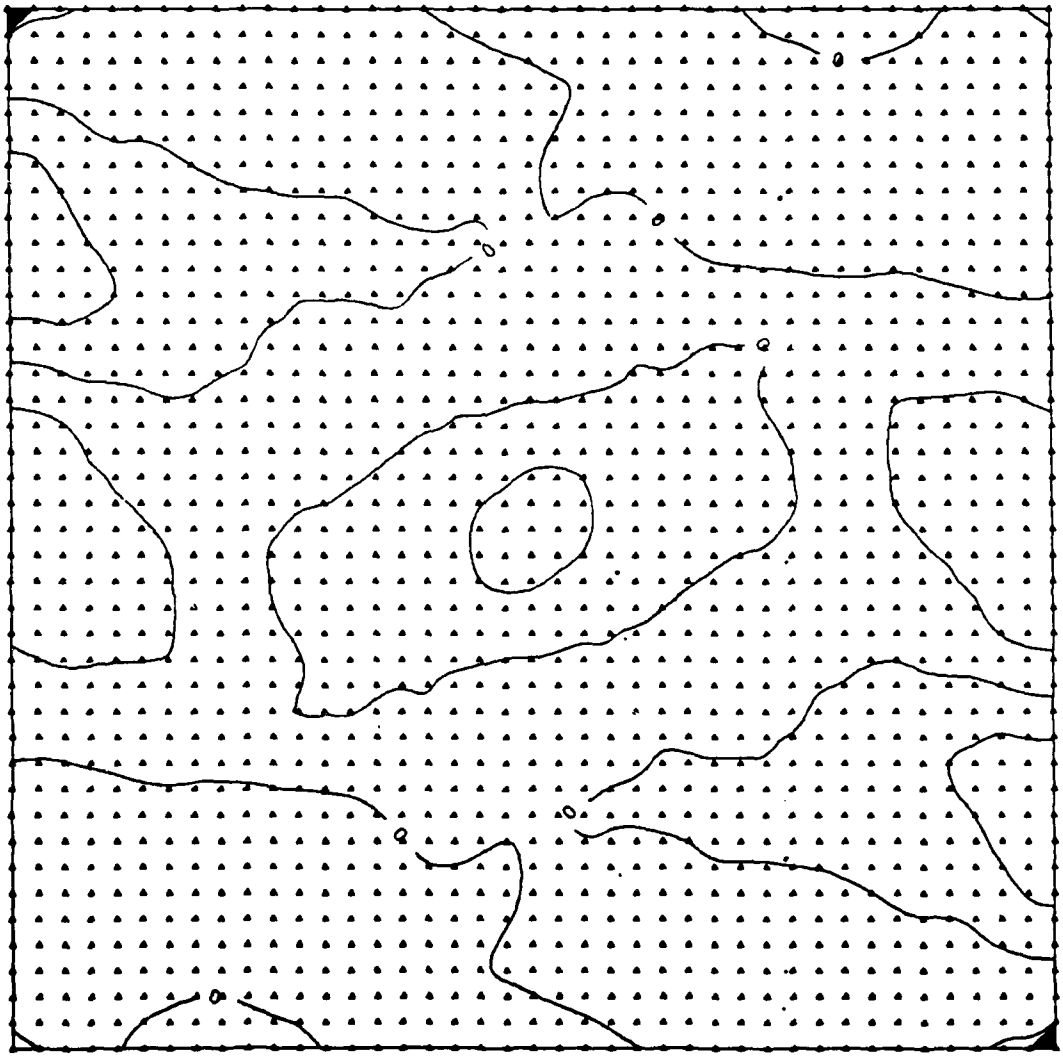

TWO-DIMENSIONAL AUTOCORRELATION FUNCTION
FOR: NOVBO TSP GRIDDED DATA ....
SURFACE REPRESENTATION USING 41X41 GRID

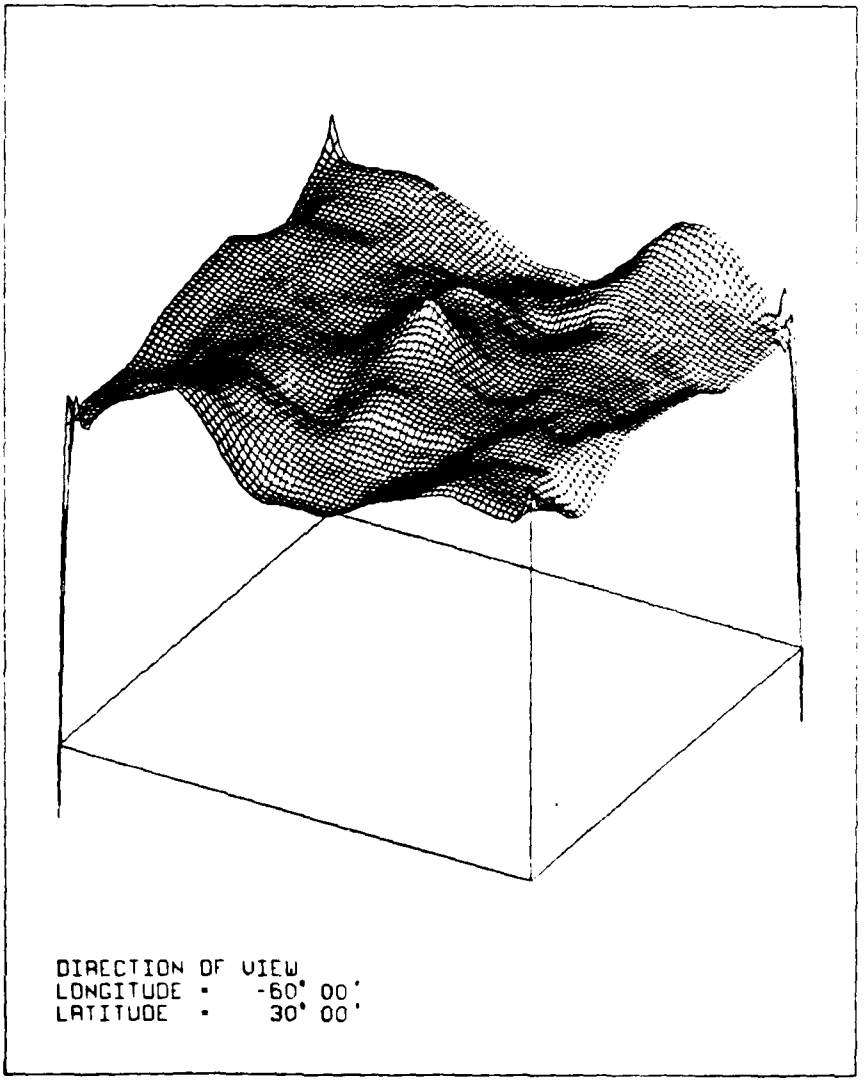

TWO-DIMENSIONAL AUTOCORRELATION FUNCTION
FOR DEC80 TSP GRIDDED DATA ▪▪▪▪▪▪▪▪▪▪▪▪
ISARITHMS IN CORRELATION UNITS ▪ 41X41 ▪

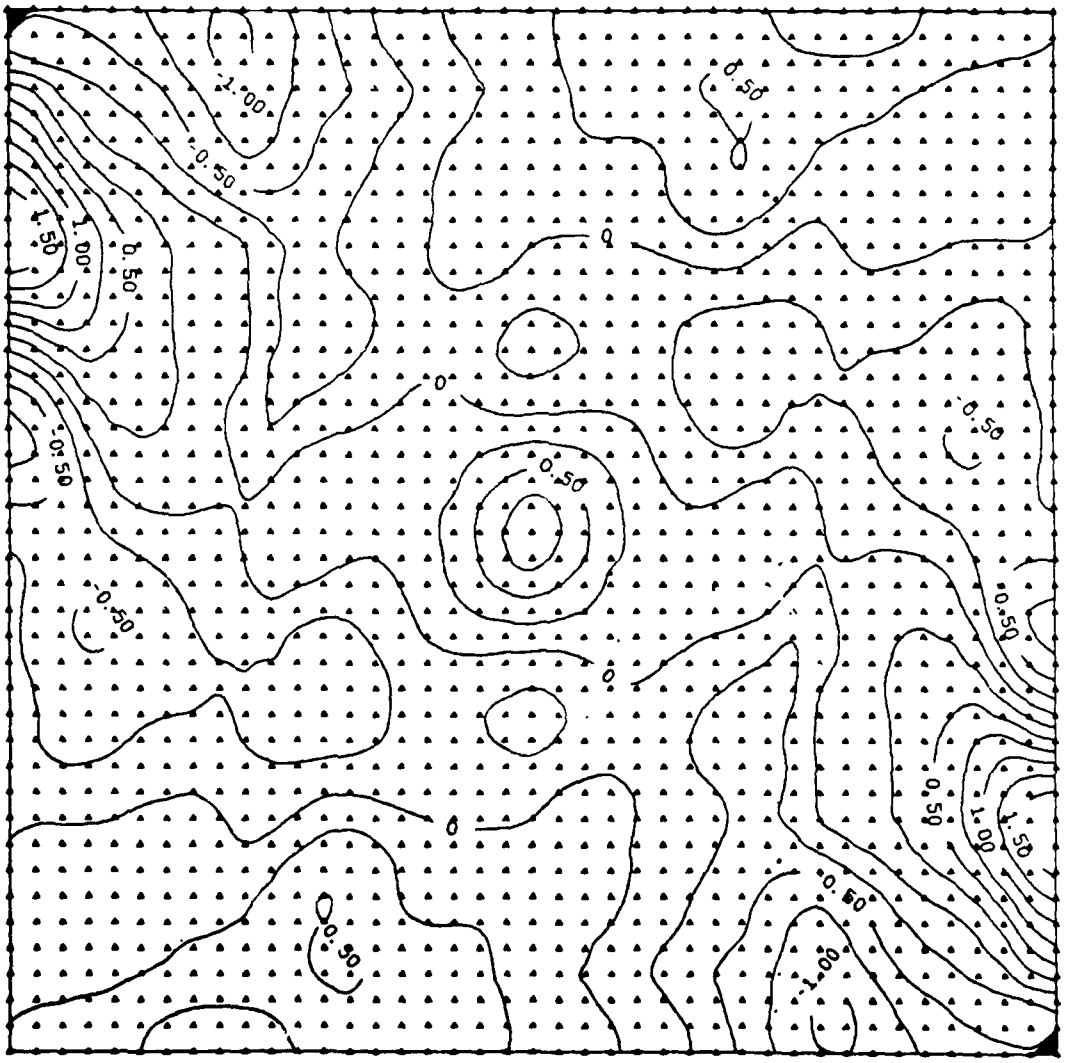

TWO-DIMENSIONAL AUTOCORRELATION FUNCTION
FOR DEC80 TSP GRIDDED DATA .....
SURFACE REPRESENTATION USING 41x41 GRID

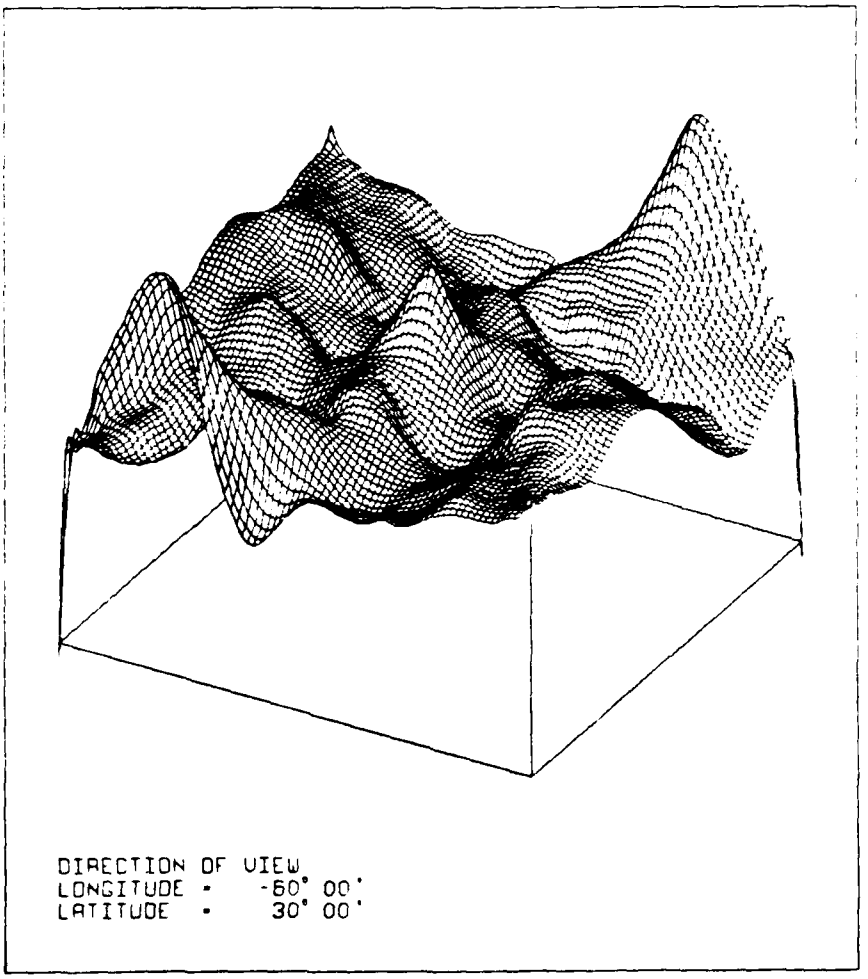

BIBLIOGRAPHY

Agterberg, F. P. Geomathematics. Amsterdam: Elsevier Publishing Company, 1974.

Cliff, A. D., Haggett, P., Ord, J., Basset, K. A. and Davies, R. E. Elements of Spatial Structure. Cambridge: Cambridge University Press, 1975.

Cliff, A. D. and Ord, J. K. Spatial Process Models and Applications. London: Pion limited, 1981.

Clark, Isobel Practical Geostistics. London: Applied Science Publishers Limited, 1979.

Davis, John C. Statistics and Data Analysis in Geology. New York: John Wiley and Sons, 1973.

Faddeev, D. K. and Faddeeva, V. N. Computational Methods of Linear Algebra. San Francisco: W. H. Freeman and Company Inc. , 1963.

Graybill, Franklin A. An Introduction to Linear Statistical Models Volume I. New York: McGraw-Hill Book Company Inc., 1961.

Graybill, Franklin A. and Krumbein, W. C. An Introduction to Statistical Models in Geology. New York: McGraw-Hill Book Company Inc., 1965.

Helava, U. V. Instruments and Methods for Digital Terrain Model Data Collection. Proceedings of the Digital Terrain Models Symposium, Virginia: American Society of Photogrammetry, 1978.

Kratky, Vladmir Image Transformation in Satellite Mapping. in Commonwealth Survey Officers Conference 1975 paper No. K.4, 1975.

Loon, Joseph C. Cartographic Generalization of Digitial Terrain Models. Ph.D. disseration The Ohio State University. Department of Geodetic Science. Columbus, 1978.

Merriam, D. F. and Sneath, P. H. A Quantitative Comparison of Contour Maps. Journal of Geophysical Research, 71, 1105-15., 1966.

Morrison, Joel L. Method-Produced Error in Isarithmic Mapping. Washington D. C.: American Congress of Surveying and Mapping Technical Monograph No. CA-5, 1971.

Norbeck, Stig and Bystedt, Bengt Computer Cartography. Lund: Studentlitteratur, 1972.

Ohio Enviromental Protection Agency Ohio Air Quality - 1979. Air Quality and Analysis Section, Office of Air Pollution Central Ohio EPA, 1979.

Puecker, Thomas K. Computer Cartography. Association of American Cartographers, Resource Paper No. 17, 1972.

Robinson, A. H. and Bryson, R. A. Correspondence of Geographical Distributions. Annals of the Association of American Geographers, December, 379-91, 1957.

Robinson, A. H., Sale, R., and Morrison, J. Elements of Cartography Fourth Edition. New York: John Wiley and Son, 1978.

Royal, A., Clark, I., Brooker, P. I., Parker, H., Journel, A. Rendu, J. M., Sadefur, R., and Mousset-Jones, P. Geostatistics. New York: McGraw-Hill Inc., 1980.

Saulnier, L. W. The design and Implementation of the Cartographic Data Base for the Defense Mapping Agency. Commission III : Computer Assisted Cartography. The Netherlands: International Association of Cartographers, 1979.

Sunkel, Hans General Surface Representation Module Designed for Geodesy. Reports of the Department of Geodetic Science Report No. 292 The Ohio State University Columbus: 1980.

Sunkel, Hans The Estimation of Free-Air Anomalies. Reports of the Department of Geodetic Science Report No. 315, The Ohio State University, Columbus: 1981.

Tesche, T. W. and Bergstrom, R. W. Use of Digitial Terrain Models in Meterological and Air Quality Modeling. Proceedings of the Digital Terrain Models Symposium, Virginia: American Society of Photogrammetry, 1978.

Unwin, D. J. Numerical Errors in a Familiar Technique: A Case Study of Polynomial Trend Surface Analysis. Geographical Analysis, Vol 7, April, 1975.

Uotila, Urho A. Statistical Test as Guidelines in Analysis of Adjustment of Control Nets. Surveying and Mapping, March, 1975.

Uotila, Urho A. Introduction to Adjustment Computations with Matrices. Department of Geodetic Science, The Ohio State University, Columbus, 1967.


ATE
LME